

REMOVAL OF COPPER(II) AND LEAD(II) FROM SOILS BY
POLY(AMIDOAMINE) DENDRIMERS AND REDUCTIVE
IMMOBILIZATION OF CHROMIUM(VI) BY
STABILIZED ZERO-VALENT IRON
NANOPARTICLES

Except where reference is made to the work of others, the work described in this dissertation is my own or was done in the collaboration with my advisory committee. This dissertation does not include proprietary or classified information.

Yinhui Xu

Certificate of approval:

Mark O. Barnett
Associate Professor
Civil Engineering

Dongye Zhao, Chair
Associate Professor
Civil Engineering

T. Prabhakar Clement
Associate Professor
Civil Engineering

Zhongyang Cheng
Assistant Professor
Materials Engineering

Jacob H. Dane
Professor
Agronomy and Soils

Stephen L. McFarland
Acting Dean
Graduate School

REMOVAL OF COPPER(II) AND LEAD(II) FROM SOILS BY
POLY(AMIDOAMINE) DENDRIMERS AND REDUCTIVE
IMMOBILIZATION OF CHROMIUM(VI) BY
STABILIZED ZERO-VALENT IRON
NANOPARTICLES

Yinhui Xu

A Dissertation

Submitted to

the Graduate Faculty of

Auburn University

in Partial Fulfillment of the

Requirements for the

Degree of

Doctor of Philosophy

Auburn, Alabama
August 7, 2006

REMOVAL OF COPPER(II) AND LEAD(II) FROM SOILS BY
POLY(AMIDOAMINE) DENDRIMERS AND REDUCTIVE
IMMOBILIZATION OF CHROMIUM(VI) BY
STABILIZED ZERO-VALENT IRON
NANOPARTICLES

Yinhui Xu

Permission is granted to Auburn University to make copies of this thesis at its discretion, upon request of individuals or institutions and at their expense. The author reserves all publication rights.

Signature of Author

Date of Graduation

VITA

Yinhui (Lucida) Xu, daughter of Jinsong Xu and Chuanfeng Yao, was born in the city of Tai-An, Shandong, China. She received a B.S. and an M.S. in Environmental Engineering in 1999 and 2002, respectively, both from Donghua University in Shanghai, China. After a brief seven months of employment with the DuPont Fibers Ltd. in Shanghai, she ventured to cross the Ocean to pursue her Ph.D. degree at Auburn University in Fall 2002. During the four years stay at Auburn, She feels so blessed and fortunate to have harvested a great deal both personally and academically. She was married to Baojian Guo in 2003, and then became the happiest Mom of their lovely daughter Lucy Y. Guo a year later. She produced five papers in prominent journals such as ES&T, JEE, I&EC Res., and Water Res., and three publications/presentations at various national/international conferences. She feels humbled and honored to be selected as a recipient of five eminent awards including the CH2M HILL Fellowship Award (2004), AWEA Outstanding Graduate Student Scholarship Award (2006), AWWA AL-MS Outstanding Graduate Student Scholarship Award (2006), AU Outstanding International Student Award (2006), and ACS Geochemistry Symposium's Outstanding Student Paper Award (2006).

DISSERTATION ABSTRACT

REMOVAL OF COPPER(II) AND LEAD(II) FROM SOILS BY
POLY(AMIDOAMINE) DENDRIMERS AND REDUCTIVE
IMMOBILIZATION OF CHROMIUM(VI) BY
STABILIZED ZERO-VALENT IRON
NANOPARTICLES

Yinhui Xu

Doctor of Philosophy, August 7, 2006
(M. S. Donghua University, China, 2002)
(B. S. Donghua University, China, 1999)

237 Typed Pages

Directed by Dongye Zhao

This research investigated the feasibility of using poly(amidoamine) PAMAM dendrimers for removal of copper(II) and lead(II) from soils, and using a new class of stabilized zero-valent iron (ZVI) nanoparticles for reductive immobilization of chromium (VI) in contaminated soils. PAMAM dendrimers ranging from generation (G) 1.0 to 4.5 and with $-NH_2$, $-COO^-$, and $-OH^-$ terminal groups were tested for extraction of copper(II) and lead(II) from a sandy loam soil, a clay soil, and a sandy clay loam. A series of fixed-bed column experiments were conducted to study the effects of dendrimer dosage, generation number, functional groups, pH, ionic strength, and soil type on the removal efficiency. It was found that more than 90% of the preloaded copper (II) was removed by

~66-bed volumes a dendrimer solution containing 0.10% (w/w) of a generation 4.5 dendrimer with –COOH terminal groups and at pH 6.0. Approximately 92% of the initially sorbed lead (II) was removed by ~ 120 bed volumes containing 0.3% (w/w) of a generation 1.5 dendrimer with –COONa terminal groups at pH 4.0. The spent dendrimers were recovered through nanofiltration and then regenerated with 2 N hydrochloric acid. The recovered dendrimers were then reused and showed comparable metal removal effectiveness to that of fresh dendrimers.

An ion-exchange based approach was developed to determine the apparent stability constants of the Cu(II)- or Pb(II)-dendrimer complexes. The method was derived by modifying the traditional Schubert ion exchange method, but offered a number of advantages, including the application of a non-linear reference isotherm and extension of the classical approach from mono-nuclear to poly-nuclear complexes.

To simulate the dynamic metal removal process by dendrimers, a two-site model was formulated. The model envisions the soil sorption sites as two distinguished fractions: one with a fast desorption rate and the other with a slow desorption rate. The model was able to not only simulate the elution histories of lead and copper by various dendrimers, but also prove promising to predict the metal elution histories under various conditions such as initial metal concentration in soil, dendrimer dosage, and solution pH.

An innovative *in situ* technology for reductive immobilization of Cr(VI) was tested. A new class of stabilized zero-valent iron (ZVI) nanoparticles was prepared using sodium carboxymethyl cellulose (CMC) as a stabilizer. Batch and column experimental results revealed that the ZVI nanoparticles could effectively reduce Cr(VI) to Cr(III), and reduce the Cr leachability by ~90%.

ACKNOWLEDGEMENTS

I would like to express my sincere appreciation to my advisor, Dr. Dongye Zhao, for his supervision, guidance, support, and patience throughout my Ph.D. studies. The experience of working with him over the last four years in Auburn leaves me wonderful memories to appreciate for the rest of my life.

I want to thank my committee members, Dr. Barnett, Dr. Clement, Dr. Cheng, and Dr. Dane, and my dissertation outside reader Dr. Yucheng Feng for providing unconditional support and valuable suggestions during the studies. I feel fortunate that I met them and had a chance to work with them.

I would also like to express my love and gratitude to my husband for his endurance, infinite support, and loving care. I wish to thank my daughter for bringing me happiness and joy in the last one and half years. Finally, I wish to thank my parents and other family members for their support. It is their constant encouragement that made this dissertation possible.

Style manual or journal used Auburn University manuals and guides for the
preparation of theses and dissertations: Organizing the manuscript – publication format

Computer software used Microsoft Word & Excel 2002; EndNote 8.0; SigmaPlot 8.0;
and Compaq Visual Fortran 6.

T

ABLE OF CONTENTS

LIST OF TABLES	xiv
LIST OF FIGURES	xvi
CHAPTER 1 . GENERAL INTRODUCTION.....	1
1.1 Soil Contamination by Heavy Metals.....	1
1.2 Current Remediation Methods for Heavy Metal Contaminated Soils.....	2
1.2.1 Isolation, containment, solidification, and stabilization.....	3
1.2.2 Thermal method	3
1.2.3 Electrokinetic remediation.....	4
1.2.4 Bioremediation.....	4
1.2.5 Soil flushing and soil washing	4
1.3 Nano-Technology in Environmental Clean-up	5
1.3.1 Nanosorbents and nanocatalysts.....	6
1.3.2 Poly(amidoamine) PAMAM dendrimers.....	7
1.3.3 Zero-Valent Iron (ZVI) nanoparticles	11
1.4 Objectives of This Research.....	11
1.5 Organization of This Dissertation	12
CHAPTER 2 . REMOVAL OF COPPER FROM CONTAMINATED SOIL BY USE OF POLY(AMIDOAMINE) DENDRIMERS.....	14
2.1 Introduction	14

2.2 Materials and Procedures	17
2.3 Results and Discussion	25
2.3.1 Titration curves of dendrimers	25
2.3.2 Copper affinity of dendrimers	25
2.3.3 Copper binding capacity of dendrimers	29
2.3.4 Copper sorption / desorption isotherms for the soil	31
2.3.5 Cu removal at various dendrimer concentrations	31
2.3.6 Effects of pH	38
2.3.7 Effects of terminal group type	41
2.3.8 Effects of dendrimer generation	44
2.3.9 Effects of ionic strength	46
2.3.10 Effect on copper speciation in soil	48
2.3.11 Recovery and reuse of spent dendrimers	50
 CHAPTER 3 . REMOVAL OF LEAD FROM CONTAMINATED SOILS USING POLY(AMIDOAMINE) DENDRIMERS	
3.1 Introduction	52
3.2 Materials and Methods	56
3.3 Results and Discussion	63
3.3.1 Sorption and desorption of lead by soils	63
3.3.2 Lead removal at various dendrimer concentrations	66
3.3.3 Lead removal using dendrimers of different terminal functional groups	71
3.3.4 Effect of dendrimer generation	73
3.3.5 Effect of pH	75

3.3.6 Impact of dendrimer treatment on Pb ²⁺ speciation and leachability	79
3.3.7 Dendrimer retention by soil and recovery of spent dendrimers	81
3.4 Summary and Conclusions.....	85
CHAPTER 4 . A REVISED ION EXCHANGE METHOD FOR ESTIMATION	
OF CONDITIONAL STABILITY CONSTANTS OF METAL-DENDRIMER	
COMPLEXES	87
4.1 Introduction.....	87
4.2 Materials and Methods.....	91
4.3 Model Formulation.....	96
4.3 Results and Discussion	99
4.3.1 Resin selection	99
4.3.2 Metal sorption isotherms	101
4.3.3 Complexation of Cu ²⁺ with G1.0-NH ₂ at pH 5.0 and 7.0.....	104
4.3.4 Complexation of Cu ²⁺ with dendrimers of various generations	106
4.3.5 Complexation of Pb ²⁺ with G1.0-NH ₂ and G1.5-COONa.....	109
4.4 Summary and Conclusions.....	112
CHAPTER 5 . MODELING THE ELUTION HISTORIES OF COPPER AND	
LEAD FROM A CONTAMINATED SOIL TREATED BY POLY(AMIDOAMINE)	
(PAMAM) DENDRIMERS.....	114
5.1 Introduction.....	114
5.2 Experiment	117
5.2.1 Materials	117
5.2.2 Experiment setup.....	117

5.3 Model.....	120
5.3.1 Model formulation.....	120
5.3.2 Parameter estimation	124
5.4 Results and Discussion	125
5.4.1 Simulating Cu ²⁺ /Pb ²⁺ transport	125
5.4.2 Predicting the Cu ²⁺ /Pb ²⁺ elution histories.....	132
5.5 Summary and Conclusions.....	142
CHAPTER 6 . REDUCTIVE IMMOBILIZATION OF CHROMATE IN WATER	
AND SOIL BY STABILIZED IRON NANOPARTICLES.....	
6.1. Introduction	144
6.2 Materials and Methods.....	147
6.3 Results and Discussion	151
6.3.1 Reduction of Cr(VI) in water by Fe nanoparticles	151
6.3.2 Reduction of Cr(VI) sorbed in soil.....	155
6.3.3 Reductive immobilization of Cr(VI) in soil: column tests	160
6.4 Summary and Conclusions.....	165
CHAPTER 7 . CONCLUSIONS AND SUGGESTIONS FOR FUTURE	
RESEARCH.....	
7.1 Summary and Conclusions.....	167
7.2 Suggestions for Future Work	170
REFERENCES.....	173
APPENDIX A FORTRAN CODE FOR TRACER TEST	201
APPENDIX B IMPLICIT METHOD FOR ONE-SITE MODEL	203

APPENDIX C IMPLICIT METHOD FOR GAMMA-DISTRIBUTION MODEL.....	207
APPENDIX D IMPLICIT METHOD FOR TWO-SITE MODEL.....	211
APPENDIX E RUNGE-KUTTA METHOD FOR BATCH METAL RELEASE WITH TWO-SITE MODEL	215

LIST OF TABLES

Table 2-1. Salient Properties of Dendrimers Used in the Copper Removal Study.....	19
Table 2-2. Compositions of a Loamy Sand Soil Used in Copper Removal Study.	20
Table 2-3. Reagents and Conditions Used in the Sequential Extraction.....	24
Table 2-4. Copper Distribution between a Chelating Ion Exchange Resin (DOW 3N) and Water with or without Dendrimer.	28
Table 2-5. Best-fitted Langmuir Model Parameters and R ² Values for the Three Dendrimers and a Loamy Sand Soil.....	33
Table 2-6. Copper Removal and Effluent pH under Various Experimental Conditions...37	
Table 2-7. Copper Speciation in Original and Dendrimer-Treated Soil.	49
Table 3-1. Salient Properties of Dendrimers Used for Lead Removal.....	57
Table 3-2. Major Compositions of Soils Used for Lead Removal.....	58
Table 3-3. Best-Fitted Freundlich Model Parameters and R ² Values for the Two Soils. .65	
Table 3-4. Lead Removal and Effluent pH Following Various Treatments of Three Soils.....	70
Table 3-5. Recovery of Spent Dendrimers and Pb ²⁺ in the Spent Dendrimer Eluent.....	84
Table 4-1. Salient Properties of Dendrimers Used in the Lead Removal Study.	92
Table 4-2. Important Properties of the Ion Exchange Resins.	94
Table 4-3. Percentage of Dendrimer Loss from the Aqueous Phase under Various Conditions (data given as mean of duplicates ± standard deviation).....	100

Table 4-4. Best-fitted Langmuir Model Parameters and R^2 values for Cu^{2+} and Pb^{2+}	103
Table 4-5. Conditional Stability Constant K_c and Cu^{2+} -to-Dendrimer Molar Ratio n for Complexes Cu^{2+} Bound with Various Generations of Dendrimers.	108
Table 5-1. General Experimental Conditions Used in Cu^{2+} and Pb^{2+} Column Experiments.	119
Table 5-2. Best Fitted Parameters of the Two Sites Model under Various Experimental Conditions.	127
Table 5-3. Values of Molar Proton/Metal Exchange Ration (b) Determined from Batch Experiments and by Eq. (5-21) and the Resultant Desorption Coefficient (K_d).	140

LIST OF FIGURES

Figure 1-1. Formation of G0.0 dendrimer with EDA core and -NH ₂ terminal groups.	8
Figure 1-2. 2-D structures of a G2.0 dendrimer with EDA core and -NH ₂ terminal groups.....	9
Figure 2-1. Titration curves for three dendrimers and DI water.....	27
Figure 2-2. Equilibrium binding of copper by three dendrimers.	32
Figure 2-3. Copper sorption and desorption isotherms with an Alabama sandy loam soil.....	35
Figure 2-4. Copper elution histories during two separate column runs using 0.040% and 0.10% of G4.5-COOH at pH 6.0.....	36
Figure 2-5. Copper elution histories during separate extraction runs using 0.040% G4.5-COOH at pH=7.0, 6.0 and 5.0 and with DI water at pH=6.0 and 5.0.	39
Figure 2-6. Copper elution histories during separate column runs using G4.5-COOH, G4.0-NH ₂ and G4.0-OH based on equal equivalent terminal groups as 0.040% of G4.5-COOH at pH=6.0.	43
Figure 2-7. Copper elution histories using dendrimers of various generations: (a) G1.5-COOH and G4.5-COOH based on equal equivalent terminal groups as 0.010% G4.5-COOH at pH=7.0; and (b) G1.0-NH ₂ and G4.0-NH ₂ based on equal equivalent terminal groups as 0.040% G4.0-NH ₂	45

Figure 2-8. Copper elution histories during two separate column runs using 0.040% of G4.5-COOH and in the absence or presence of other ubiquitous ions, equivalent to a total ionic strength of 0.8 mM.	47
Figure 2-9. Comparing copper elution histories using 0.040% of virgin and recovered G4.0-NH ₂ at pH=6.0.	51
Figure 3-1. Sorption and desorption isotherms of Pb ²⁺ with (a) loamy sand soil and (b) sandy clay loam #1. Data are given as mean of duplicates, and errors refer to standard error (Symbols: experimental data; Lines: model simulations). .	64
Figure 3-2. Lead elution histories during extraction using various concentrations of G1.0-NH ₂ for (a) sandy clay loam #1, and (b) loamy sand soil.	68
Figure 3-3. Lead elution histories from a field Pb contaminated soil (sandy clay loam #2) with 0.3% G1.0-NH ₂ at pH 4.0 and 5.0.	69
Figure 3-4. Elution histories of lead from a loamy sand soil with G1.0-NH ₂ or G1.5-COONa at an influent dendrimer concentration of 0.3% and pH 5.0.	72
Figure 3-5. Elution histories of lead from a loamy sand soil using 0.1% G1.0-NH ₂ and G4.0-NH ₂ at pH 5.0.	74
Figure 3-6. Elution histories of lead from a loamy sand soil with 0.3% of G1.5-COONa at pH 4.0 or 5.0.	76
Figure 3-7. Lead sorption edges for the sandy and clay soils.	77
Figure 3-8. Operationally defined speciation of Pb ²⁺ in: (a) untreated soil, and (b) dendrimer treated soil. All data are given as mean of duplicates. (Acronyms: EXC, Exchangeable lead; CARB, Carbonate-bound lead;	

ERO, Pb^{2+} to easily reducible oxides; SOM, Pb^{2+} to soil organic matter; AmoFe, Pb^{2+} to amorphous iron oxides; and RES, residual Pb^{2+}).	80
Figure 3-9. Dendrimer breakthrough curves in the loamy sand and sandy clay loam #1.	83
Figure 4-1. Sorption isotherms IRC-50 in the absence of dendrimer: (a) Cu^{2+} and (b) Pb^{2+} (data plotted as mean of duplicates, errors refer to standard deviations).	102
Figure 4-2. Determination of the conditional stability constant and the molar ratio of Cu^{2+} -to-dendrimer of Cu^{2+} -G1.0-NH ₂ complexes: (a) pH 5.0; (b) pH 7.0.	105
Figure 4-3. Determination of the conditional stability constant and the Pb^{2+} -to-dendrimer molar ratio of Pb^{2+} -dendrimer complexes: (a). Pb-G1.0-NH ₂ , and (b). Pb-G1.5-COONa (data plotted as mean of duplicates, errors indicate standard deviation).	110
Figure 5-1. Experimentally observed and model-simulated elution histories of Cu^{2+} from a soil treated with 0.1% of G4.5-COOH. (Influent pH = 6.0; Initial Cu in soil = 30mg/kg).	126
Figure 5-2. Experimentally observed and model-simulated elution histories of Pb^{2+} from a soil treated with 0.1% of G1.0-NH ₂ . (Influent pH = 5.0; Initial Pb in soil = 590 mg/kg).	129
Figure 5-3. Experimentally observed and model-simulated elution histories of Cu^{2+} from a soil treated with 0.04% of G4.0-NH ₂ . (Influent pH = 6.0; Initial Cu in soil = 30 mg/kg).	131

Figure 5-4. Observed and model-predicted Cu ²⁺ elution histories from a soil treated with 0.04% of G4.0-NH ₂ . (Influent pH = 6.0; Initial Cu in soil = 12 mg/k).....	133
Figure 5-5. Observed and model-predicted Cu ²⁺ elution histories from a soil treated by 0.04% of G4.5-COOH and under otherwise identical conditions as in Figure 5-1. (Model parameters were derived from Figure 5-1).	135
Figure 5-6. Observed and model-predicted Cu ²⁺ elution histories from a soil treated by 0.1% of G4.0-NH ₂ and under otherwise identical conditions as in Figure 3. (Model parameters were derived from Figure 5-3).	136
Figure 5-7. Observed and model-simulated Cu ²⁺ desorption kinetics in a batch reactor and in the presence of 0.04% of G4.5-COOH at pH 5.0, 6.0, and 7.0, respectively.....	139
Figure 5-8. Observed and model-predicted Cu ²⁺ elution histories from a soil treated by 0.04% of G4.5-COOH and at pH 5.0 (a) and 7.0 (b). Model parameters are listed in Table 5-3.....	141
Figure 6-1. Reduction of Cr(VI) in water by CMC-stabilized Fe nanoparticles. NaCMC = 0.2% (w/w); Fe = 0.08 g/L; initial Cr = 33.6 mg/L (inset: Cr(VI) removal within the first 4 hours fitted with the first-order reaction model; Symbols: experimental data, Lines: model fitting. Data given as means of duplicates and errors refer to standard deviation).....	153
Figure 6-2. Cr(VI) reduction by NZVI with different Fe(0) dose and with DIW, CMC, or NaBH ₄	156

Figure 6-3. Leaching of Cr from contaminated soil using 0.08 g/L ZVI nanopartilces or DI water in batch test.....	157
Figure 6-4. Cr(VI) desorption from contaminated soil by nanoscale Fe(0) or DI water at pH 9.0, 7.0, and 5.0.....	159
Figure 6-5. Cr elution histories during two separate column runs using NZVI or DIW at pH 5.60 ((a) total Cr; (b) Cr(VI); insets: Cr elution histories after 1.9 BVs).....	161
Figure 6-6. Cr elution histories during two separate column runs with one or two beds using NZVI at pH 5.60.....	164

CHAPTER 1. GENERAL INTRODUCTION

1.1 Soil Contamination by Heavy Metals

Modern industries have immensely improved the living standard of human being. However, they also pose serious adverse impacts on our living environment. One of the most common environmental issues is soil contamination by heavy metals. Although trace amounts of heavy metals are essential to human body, they are toxic or lethal when they become excessive. The sources of heavy metals include mining and smelting, electroplating, painting, fuel production, and fertilizer and pesticide application (Alkorta et al. 2004). Heavy metals in soil don't degrade naturally and they pose significant risks on human and environmental health. Among all the heavy metals, cadmium(Cd), copper(Cu), lead(Pb), mercury(Hg), nickel(Ni), and zinc(Zn) are listed the most hazardous and included on the list of priority pollutants of the US Environmental Protection Agency (EPA) (Cameron 1992). This research focuses on the remediation of copper, lead, and chromium contaminated soils.

Copper is relatively abundant in the crust of the earth. The copper amount present in soil is dependent on the parent rock type, distance from natural ore bodies and/or manmade air emission sources. The natural level of copper in soil is 2 to 100 mg/kg (Mulligan et al. 2001). In the past years, copper is the mostly produced metal compared to cadmium, lead, and zinc (Mulligan et al. 2001). The increased copper concentration in

soil is due to the copper application in fertilizers, building materials, rayon manufacture, pesticide sprays, agricultural and municipal wastes, and industrial emissions (Cameron 1992). Both humans and animals need some amounts of copper in their diets, but very high concentrations of copper can be toxic and cause adverse effects. The most common symptoms of copper toxicity are injury to red blood cells, injury to lungs, as well as damage to liver and pancreatic functions.

Lead has been classified as a probable human carcinogen in Group B₁ by US EPA. It is highly toxic even at very low concentrations. Usually, lead comes to the soil from air after burning of wastes and fossil fuels. Other sources of lead in soil include landfills, pesticide, paints, and military and police firing range (Mulligan et al. 2001). The divalent form Pb²⁺ is the most common species and it is capable of replacing calcium, strontium, and potassium in soils. The mobility of lead in soil is low and it is hard to remove lead from soil once it is introduced into the soil matrix (Mulligan et al. 2001).

After lead, chromium is the second most common inorganic groundwater contaminant in the United States (Kavanaugh 1994b). Chromium enters the environment primarily through its widespread application in industry such as tanning, metallurgy, and plating (Ginder-Vogel et al. 2005). Cr(VI) is a known mutagen, teratogen, and carcinogen. It usually exists in the form of anion (CrO₄²⁻ or Cr₂O₇²⁻) with high water solubility and mobility.

1.2 Current Remediation Methods for Heavy Metal Contaminated Soils

There are two major types of remediation strategies for the metal contaminated soils (Rampley and Ogden 1998b). The first is to confine the metals in the soil including

capping, excavation and off-site disposal, and solidification and stabilization, but the utilization of the land is then restricted. Because these methods deplete natural resources, and are not environmentally benign, they are increasingly discouraged by regulators. The second type is to remove metals from the contaminated soils. Compared to the first type, the second is sounder since it can provide a clean closure to a site. Some examples of the remediation technologies are discussed briefly in the following sections.

1.2.1 Isolation, containment, solidification, and stabilization

In this method, contaminants are isolated and contained to prevent further movement. Steel, cement, bentonite, and grout walls are used as physical barriers for this purpose. As required by US EPA, the permeability of the waste should be reduced to less than 1×10^{-7} m/s. Consequently, solidification/stabilization is usually applied after isolation and containment. Solidification is a physical process while stabilization involves chemical reaction to reduce the mobility of contaminants.

1.2.2 Thermal method

In this method, soil is heated to a very high temperature, 200-700 °C, to evaporate the contaminants. It was an *ex situ* method and mainly for remediation of soils contaminated with non-biodegradable organic pollutants (Koning et al. 2005). It can be effectively used for mercury since it is easily evaporated at high temperature. The vapor is then captured and Hg recovered (Kucharski et al. 2005; Kunkel et al. 2004). Other metals such as gold or platinum can also be recovered by this method, even at very low concentration (Mulligan et al. 2001).

1.2.3 Electrokinetic remediation

By passing a low intensity electric current between a cathode and an anode imbedded in the contaminated soil, ions are transported between the electrodes (Brewster et al. 1995). It has been successfully used to remove Mn, Cr, Ni, and Cd from contaminated soils (Al-Hamdan and Reddy 2006; Pazos et al. 2006). The main advantage of this method is that it is very effective for soils with low permeability (Kaya and Yukselen 2005).

1.2.4 Bioremediation

Biochemical process involves utilizing living organisms to reduce or eliminate the contaminants accumulated in the soil. Biotechnology has been used *in situ* for the treatment of soil contaminated by uranium, copper, zinc, and cadmium (Groudev et al. 2004). In a recent review paper, Gadd (Gadd 2005) discussed the major interactions of microorganisms with metals. Generally, the predominant organisms used are bacteria, fungi, algae, plankton, protozoa, and plants. Using plants for the purpose of remediation is known as phytoremediation (Alkorta et al. 2004). A Chinese brake fern has been reported very effective in accumulating arsenic (Ma et al. 2001; Tu et al. 2002; Zhang et al. 2002). It is a cost-effective, non-intrusive, and aesthetically pleasing technology. The main disadvantage of it is that it needs longer time compared to other methods (Mulligan et al. 2001).

1.2.5 Soil flushing and soil washing

Soil flushing/washing uses water with or without additives to solubilize the

contaminants. The efficiency of the flushing depends on the hydraulic conductivity and the solubility of pollutants. Water alone usually requires a very long time to clean the site and it is not very effective. Therefore, additives are usually needed to enhance the extraction efficiency. There are usually four ways to mobilize the metal in soils (Pickering 1986): (1) change the pH, (2) change the solution ionic strength, (3) change the REDOX potential, and (4) form complexes by using chelating agents. In practice, chelating soil washing and acid washing are the two most prevalent methods (Di Palma et al. 2005; Khodadoust et al. 2004; Khodadoust et al. 2005). The key advantage of this method is that less handling of soil is required.

1.3 Nano-Technology in Environmental Clean-up

Using materials and structures within nanoscale dimensions ranging from 1 to 100 nanometers (nm) is broadly defined as nanotechnology. It includes nanoparticles, nanolayers, and nanotubes. Nanoparticles are defined as a collection of tens to thousands of atoms measuring only about 1-100 nm in diameter (Masciangioli and Zhang 2003). US EPA greatly supports the research in nanotechnology in the following application area: remediation, sensor, treatment, green nanotechnology, and green energy (<http://es.epa.gov/ncer/nano/research/index.html>, accessed Feb. 2006). It is reported that approximately 80 consumer products, and over 600 raw materials, intermediate components and industrial equipment items are involved in nanotechnology (EPA Draft Nanotechnology White Paper – External Review Draft, <http://es.epa.gov/ncer/nano/publications/whitepaper12022005.pdf>, accessed Feb. 2006).

1.3.1 Nanosorbents and nanocatalysts

Research on application of nanotechnology has been primarily conducted in the field of environment remediation and end-of-pipe treatment. Nanoscale adsorbents can offer two major advantages: large surfaces and flexibility of being functionalized with chemical groups toward target compounds (Savage and Diallo 2005). An inexpensively synthesized zeolite NaP1 has been used as an effective ion exchanger to remove heavy metals from acid mine wastewaters (Moreno et al. 2001). It was also successfully applied to remove Cr(III), Ni(II), Cd(II), Zn(II), and Cu(II) from metal electroplating wastewater (Alvarez-Ayuso et al. 2003). Multiwalled carbon nanotubes have been reported for their large sorption capacities for Pb(II), Cu(II), and Cd(II) (Li et al. 2003). It was found that the metal ion sorption capacity of multiwalled carbon nanotubes were 3-4 times greater than that of granular activated carbon or the activated carbon powder (Li et al. 2003). In another research conducted by Li et al. (Li et al. 2004), multiwalled carbon nanotubes showed great potential to trap volatile organic compounds (VOC) from environmental samples. The application of carbon nanotube was also investigated by Peng et al. (Peng et al. 2004). They developed a novel sorbent, ceria supported on carbon nanotubes (CeO₂-CNTs), for the removal of arsenate from water. This sorbent has a surface area of 189 m²/g. The used sorbent could be easily regenerated by 0.1 M NaOH with a recovering efficiency of 94%. The prospect of using carbon nanotubes for air and water pollution control has appeared to be promising. Nanotubes have been suggested as a superior sorbent for dioxins (Long and Yang 2001).

As nanocatalyst, titanium dioxide (TiO₂) nanoparticle has attracted wide interest for water purification in the last decades (Adesina 2004). It greatly enhanced the removal

of total organic carbon (TOC) from waters contaminated by organic wastes (Chitose et al. 2003). TiO₂ nanoparticles have also been successfully used in the removal of toxic metals such as Cr(VI), Ag(I), and Pt(II) in aqueous solutions under UV light (Kabra et al. 2004). A synthesized N-doped TiO₂ has been developed to photodegrade methylene blue under visible light (Adesina 2004; Asahi et al. 2001). Bae and Choi (Bae and Choi 2003) modified TiO₂ by ruthenium-complex sensitizer and Pt deposits, which drastically enhanced the degradation rate of trichloroacetate and carbon tetrachloride in aqueous solutions under visible light.

1.3.2 Poly(amidoamine) PAMAM dendrimers

PAMAM dendrimers were first synthesized by Donald A. Tomalia at the DOW Chemical company in the early 1980's. Dendrimers are highly branched polymers consisting of three structural components: a core, interior branches, and terminal groups (Tomalia 1993; Tomalia et al. 1990). The ethylene diamine core dendrimers with –NH₂ terminal groups are made by alternating sequential reaction between ethylene diamine (EDA) and methylacrylate (MA). This reaction produces a methylester intermediate defined as a half generation (*G n.5*). The addition of ethylene diamine via an amidation reaction produces a product with primary amine terminations and is termed a whole generation. **Figure 1-1** describes the formation of a generation 0 (G0.0) dendrimer (information supplied by Aldrich technical service, 2002). **Figure 1-2** is the structure of a G2.0 with primary amine terminal groups (Cakara et al. 2003). The hydroxyl terminated dendrimers are prepared with the same approach, except that ethanol amine is used for the last step rather than EDA.

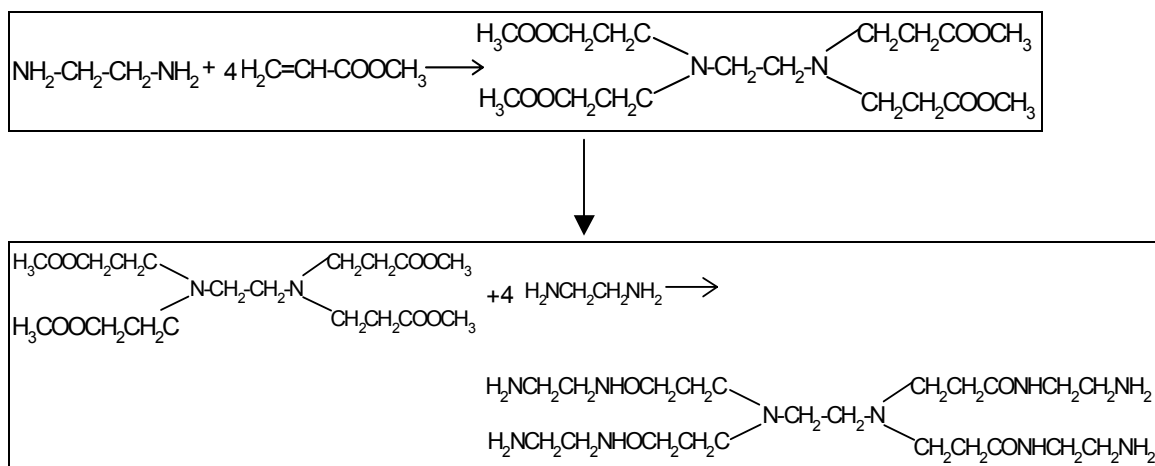


Figure 1-1. Formation of G0.0 dendrimer with EDA core and -NH₂ terminal groups.

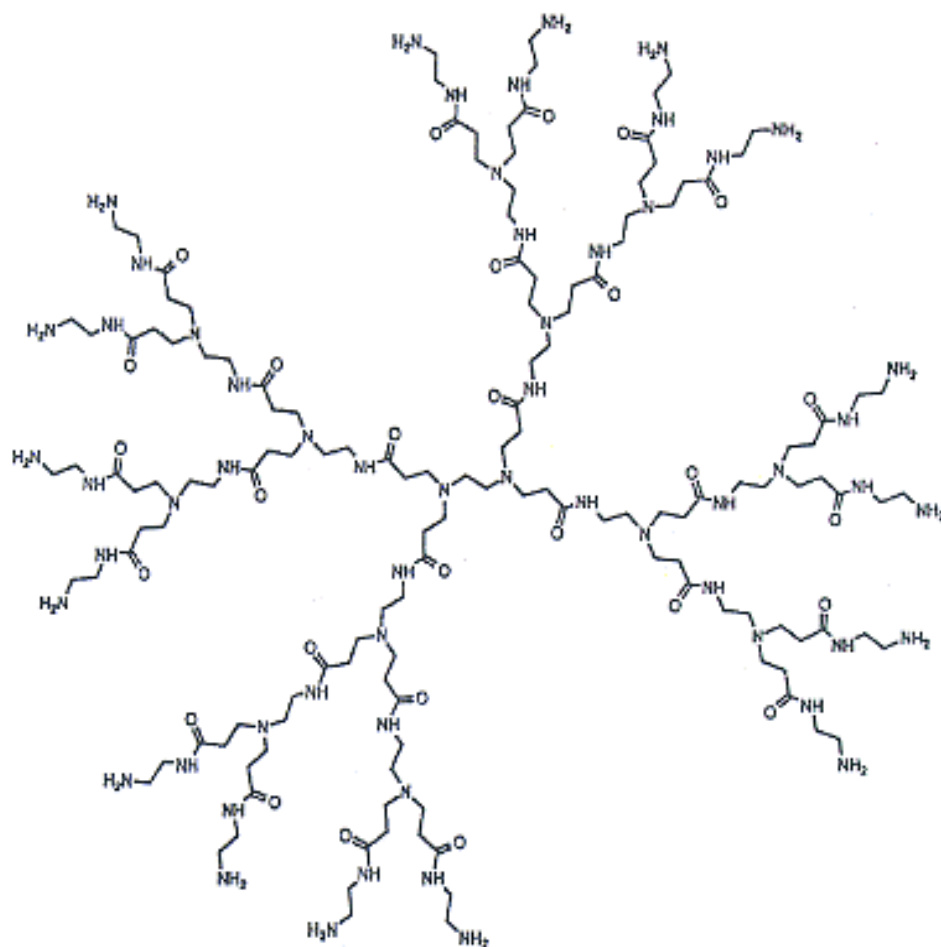


Figure 1-2. 2-D structures of a G2.0 dendrimer with EDA core and -NH₂ terminal groups.

Because of their unique properties such as nanoscale features, controlled size, and flexibility of modifying the terminal functional groups, PAMAM dendrimers have attracted much attention as advanced materials for a variety of applications. They have been studied for uses in catalysis (Kriesel and Tilley 2001), gene vectors (Haensler and Szoka 1993; Kukowska-Latallo et al. 1996), drug delivery (Yoo et al. 1999), and stabilizing nanoparticles such as Pt, Ag, Pd, and Cu (Balogh et al. 2001; Chechik and Crooks 2000; Crooks et al. 2001; Ottaviani et al. 2002; Zhao and Crooks 1999a; Zhao et al. 1998; Zhao and Crooks 1999c).

Because of the large amount of nitrogen atoms and the functional terminal groups (-NH₂, -COO, or -OH), PAMAM dendrimers have the potential application as metal complexing agents. Diallo et al. (Diallo et al. 1999; Diallo et al. 2004) applied dendrimers to removal of Cu(II) from aqueous phase. They found that an EDA core generation 8 (G8.0) dendrimer with -NH₂ terminal groups could bind with 153 ± 20 Cu(II) ions. They applied extended X-ray absorption fine structure (EXAFS) spectroscopy to probe the structures of Cu(II) complexes with G3.0~G5.0 EDA core dendrimers with -NH₂ terminal groups in aqueous phase at pH 7.0, and reported that the Cu(II) binding with the dendrimers involved both the tertiary amine and the terminal groups and the extent of binding was affected by the protonation of the functional groups.

The nanoscale dendritic chelating agents have also been used in the polymer-supported ultrafiltration (PSUF). In another study conducted by Diallo et al. (Diallo et al. 2005), dendrimers were used for enhanced ultrafiltration (DEUF) to recover Cu(II) from aqueous solutions. The Cu(II) binding capacities of the PAMAM dendrimers are much larger and more sensitive to solution pH than those of linear polymers with amine groups.

Separation of Cu(II)-dendrimer complexes could be efficiently achieved by UF membrane with the appropriate molecular weight cut-off (MWCO). They found that the EDA core dendrimers with $-NH_2$ terminal groups had very low tendency to foul the commercially available Ultracel Amicon YM generated cellulose (RC) and PB Biomax polyethersulfone (PES) membranes.

1.3.3 Zero-Valent Iron (ZVI) nanoparticles

ZVI nanoparticles have larger surface area and reactivity than Fe(0) particles (Nurmi et al. 2005; Zhang 2003) and has been found effective for the detoxification of organic contaminants such as polychlorinated biphenyls (PCB), or trichloroethene (TCE) (He and Zhao 2005b; Wang and Zhang 1997). It is reported that the surface area-normalized rate constant for degradation of PCBs by NZVI is 10-100 times higher than those commercially available iron particles (Wang and Zhang 1997). Using NZVI to reduce TCE essentially eliminates all the undesirable byproducts such as dichloroethylenes and vinyl chloride (Elliott and Zhang 2001; Wang and Zhang 1997). In a review paper, Zhang (Zhang 2003) summarized the synthesis, characterization, and applications of ZVI nanoparticles and the bimetallic Fe-Pd nanoparticles in environmental remediation.

1.4 Objectives of This Research

The overall goal of this research is to investigate the feasibility of applying reactive nanoparticles in the *in situ* remediation of soils contaminated with heavy metals such as Cu(II), Pb(II), or Cr(VI). The specific objectives of this research are to:

1. Investigate the feasibility of using PAMAM dendrimers as nanoscale chelating agents to remove Cu(II) or Pb(II) from contaminated soils through fixed-bed column experiments. The effect of dendrimer generation number, type of terminal functional groups, dendrimer dose, pH, ionic strength, or type of soils on the removal effectiveness will be determined.
2. Develop a method by revising the traditional ion-exchange (IX)-based approach to estimate the conditional stability constants of metal-dendrimer complexes. The metal binding capacity of dendrimer can also be estimated by this method.
3. Develop a numerical model to simulate and predict the dendrimers-facilitated metal elution histories from soils.
4. Test the effectiveness of using stabilized nanoscale zero-valent iron to reduce and immobilize Cr(VI) in contaminated soil. The ZVI nanoparticles are stabilized by carboxymethyl cellulose (CMC) to avoid agglomeration. The removal efficiency and the soil mobility of the stabilized ZVI nanoparticles will be investigated through a series of batch and column experiments.

1.5 Organization of This Dissertation

Except Chapter 1 (General Introduction) and Chapter 7 (Conclusions and Suggestions for Future Research), each chapter of this dissertation is formatted in a standalone journal paper. Chapters 2 and 3 present the results on Cu(II) and Pb(II) removal by dendrimers under various conditions, respectively. Chapter 4 introduces a modified method to determine the conditional stability constant of Cu- and Pb-dendrimer complexes. Chapter 5 shows a numerical model developed to simulate and predict the

metal elution histories from soils treated by dendrimers. Chapter 6 discusses the application of stabilized ZVI nanoparticles for the reduction and immobilization of Cr(VI) from contaminated soils.

CHAPTER 2. REMOVAL OF COPPER FROM CONTAMINATED SOIL BY USE OF POLY(AMIDOAMINE) DENDRIMERS

This chapter characterizes poly(amidoamine) (PAMAM) dendrimers of various generations and terminal functional groups for removal of copper(II) from a sandy soil. Effects of dendrimer dose, generation number, pH, terminal functional groups, and ionic strength on the removal efficiency were investigated through a series of column tests. The feasibility of recovering and reusing the spent dendrimer was also investigated.

2.1 Introduction

Contamination of soils and groundwater by heavy metals such as lead, cadmium, and copper has been a major concern at hundreds of contaminated sites, many of which are included in the National Priorities List (NPL) (Mulligan et al. 2001). Due to the associated adverse health effects, a number of stringent regulations have been established to limit levels of toxic metals in the environment. However, clean-up of metal contaminated sites remains a highly challenging and costly business. To a great extent, current practices still rely on conventional remediation strategies such as excavation, off-site disposal and capping (Lo and Yang 1999; Rampley and Ogden 1998b). These processes are often extremely costly and environmentally disruptive. For instance, the estimated cost for excavating a 60 cm deep soil and subsequent off-site disposal is ~U.S. \$ 730/m² (Berti and Cunningham 1997). To achieve “permanent treatment to the

maximum extent practicable” as proposed by U.S. EPA (Dienemann et al. 1992), in-situ flushing of metal-contaminated soil has received increasing attention (Allen and Chen 1993; Furukawa and Tokunaga 2004; Kim et al. 2000; Lim et al. 2004b; Lo and Yang 1999; Rampley and Ogden 1998b; Van Benschoten et al. 1994). Typically, metals are desorbed from soil by introducing an extracting agent into the contaminated soil.

Chelating agents and acids have been the most commonly employed agents for this purpose (Allen and Chen 1993; Lo and Yang 1999). However, soil washing by acids often causes changes in soil physical and chemical properties and produces large amounts of metal-laden wastewater (Lo and Yang 1999). To minimize the environmental disturbance, various chelating agents have been tested in lieu of acids. Chelating agents studied thus far include pyridine-2,6-dicarboxylic acid (Macauley and Hong 1995), N-iminodiacetic acid (Hong et al. 1993), nitrilotriacetic acid (NTA) (Elliott and Brown 1989), and ethylenediamine tetraacetic acid (EDTA) (Allen and Chen 1993; Elliott and Brown 1989; Hong et al. 1999; Lo and Yang 1999; Van Benschoten et al. 1994), of which EDTA has received the most attention for its ability to form strong complexes with transition metals. However, EDTA flushing generates large volumes of metal- and EDTA-laden wastewater, which requires costly additional treatment or disposal.

Although desirable, it is extremely difficult to recover spent EDTA from groundwater.

Poly(amidoamine) (PAMAM) dendrimers are a new class of nanoscale materials that can function as water-soluble chelators. These highly branched macromolecular compounds consist of three key structural components: a core, interior repeating units and terminal functional groups (Hedden and Bauer 2003; Ottaviani et al. 1996).

Typically, PAMAM macromolecules are synthesized by repeatedly attaching

amidoamine monomers in radially branched layers, termed generations, to a starting ammonia core (Ottaviani et al. 1997). Dendrimers terminated with amine or hydroxyl groups are called full generation dendrimers (designated as Gn.0, where n is an integer), whereas those with carboxylate groups are termed half-generation dendrimers (Gn.5). Dendrimers are potentially valuable for a number of applications including drug delivery, gene therapy, chemical sensing and catalyst preparation (Chen et al. 2000; Zhao and Crooks 1999a; Zhou et al. 2001). Owing to their unique architectural and functional flexibility, the solubility of dendrimers in water as well as in organic solvents can be well manipulated.

The environmental application of PAMAM dendrimers was first explored in 1999 for removal of copper ions from water (Diallo et al. 1999). It was reported that a G8.0 dendrimer with $-NH_2$ terminal groups was able to bind up ~ 153 Cu^{2+} ions (Diallo et al. 1999). Later, Rether et al. (Rether and Schuster 2003) studied selective separation and recovery of heavy metals such as Co^{2+} , Cu^{2+} , Hg^{2+} , Ni^{2+} , Pb^{2+} , and Zn^{2+} from water using PAMAM dendrimers modified with N-benzoylthiourea, and Kovvali and Sirkar (Kovvali and Sirkar 2001) prepared an immobilized liquid membrane by immersing the porous polymer film in pure dendrimer for selectively separating CO_2 from other gases. However, application of dendrimers to soil remediation has remained unexplored thus far, although researchers have studied a water-soluble chelator termed Metaset-Z for removal of lead from soil (Rampley and Ogden 1998b).

The overall objective of this chapter was to test the technical feasibility of using dendrimers as a recoverable extracting agent for in-situ removal of heavy metals sorbed in soil. Copper was used as the model metal contaminant for its extensive environmental

impacts as well as its strong Lewis acid characteristics. The specific goals of this research were to: 1) characterize representative dendrimers that can act as nanoscale chelators for removing Cu^{2+} from a contaminated sandy soil; 2) determine the effects of dendrimer generation, concentration, terminal functional groups, ionic strength, and pH on the removal efficiency; and 3) explore the feasibility of recovering and reusing spent dendrimers.

2.2 Materials and Procedures

Five dendrimers were studied for Cu(II) removal, including G4.5-COOH, G4.0-NH₂, G4.0-OH, G1.5-COOH, and G1.0-NH₂ (G# indicates generation number; -COOH, -NH₂ and -OH refer to respective terminal groups). They were purchased from Aldrich Chemical Co., Milwaukee, WI, USA, as stock solutions (5.0~40%) in methyl alcohol solution (Note: throughout the dissertation, concentration of dendrimers is given as percent by weight unless indicated otherwise). **Table 2-1** provides salient properties of these dendrimers (dendritech; dendritech; Tomalia et al. 1990; Zhao et al. 1998).

A loamy sand soil obtained from a local farm in Auburn, AL, USA was used throughout for this study. Before use, raw soil was sieved using a standard sieve of 2 mm openings and then rinsed using deionized water (DI water) to remove any dissolved solids. **Table 2-2** presents primary compositions of the soil. Mineral analysis was conducted following the EPA Method 3050B. NH₄-N was determined following the method of microscale determination of inorganic N in water and soil extracts (Sims et al. 1995). Organic nitrogen and organic carbon were analyzed following the Dumas method and using a LECO CN-2000 combustion unit (LECO Corp., Joseph, MI, USA) at 1050°C. The organic matter (OM) content was estimated by multiplying the organic

carbon content by an empirical factor of 1.72, as recommended by the Auburn University Soil Testing Laboratory. Copper was then loaded to the soil by equilibrating 4L solution of 4 mg/L Cu^{2+} with 400g air-dried soil in a batch reactor at pH 6.5, which resulted in a 30 mg/kg (dry soil) copper concentration in the soil. The Cu-loaded soil was air-dried and stored for the subsequent tests. EPA method 3050B was followed to analyze Cu in the soil before and after dendrimer treatment.

Titration of various dendrimers was conducted by adding 0.1 N HCl to 50 mL dendrimer solution at a volume increment of 20~200 μL . The initial pH of dendrimer solutions was adjusted to around 11.0. During titration, each solution was continuously stirred using a magnetic stirring plate and pH was measured using an Orion EA940 pH meter. Dendrimer concentrations were: 0.04% for G4.5-COOH, 0.04% for G4.0-OH, and 0.04% and 0.1% for G4.0-NH₂.

To demonstrate the metal extracting power of dendrimers, copper distribution coefficient between a Cu^{2+} -selective ion exchange resin and water was measured in the presence or absence of dendrimers. The resin, referred to as DOW 3N, is a chelating resin containing bis-picolyamine functional groups in free-base form and with a bead size ranging from 0.3 to 1.2 mm (Zhao and SenGupta 2000). DOW 3N was purchased from Aldrich Chemical Co., Milwaukee, USA. First, 0.004 g DOW 3N was added into parallel vials, each containing 20 mL of 4 mg/L Cu^{2+} solution at pH 7.0. Setting aside two of the vials as blanks (no dendrimers), each of the remaining vials then received 0.0025 g of a dendrimer (duplicates were used for each dendrimer). All vials were shaken for two days to equilibrate. Then, copper concentration in the solution phase was analyzed with a

Table 2-1. Salient Properties of Dendrimers Used in the Copper Removal Study.

Dendrimer	Core Type	Molecular Weight	Measured Hydrodynamic Diameter (nm)	# of terminal Groups	pKa	
					Interior N	Terminal Groups
G4.5-CCOOH	Ethylene diamine	26,258	5	128	Not available	Not available
G1.5-COOH*	Ethylene diamine	2,935	2	16	Not available	Not available
G4.0-NH₂	Ethylene diamine	14,215	4.5	64	6.65, 6.85	9.2, 10.29
G1.0-NH₂	Ethylene diamine	1,430	2.2	8	(3.55~6.70), 3.86	6.85, 9.00
G4.0-OH	Ethylene diamine	14,279	4.5	64	6.3	Not available

* The terminal groups were originally in the sodium form.

Table 2-2. Compositions of a Loamy Sand Soil Used in Copper Removal Study.

Minerals (mg/kg)										Sand%	Silt%	Clay%	Organic matter %	pH
Ca	K	Mg	P	Cu	Fe	Mn	Al	Pb	Na	84	10	6	0.43	5.5
240	199	222	136	6.9	1,921	65	5,447	16.9	143					

flame atomic-absorption spectrophotometer (AAS) (Varian 220FS). At equilibrium, pH in all vials was in the range of 6.6~6.9.

Copper sorption isotherms were constructed for three dendrimers (G4.5-COOH, G4.0-NH₂, and G4.0-OH) through batch tests using 20 mL glass vials with Teflon-lined caps. Each vial contained 15 mL of solution with an initial Cu²⁺ concentration ranging from 0.5 to 15 mg/L. Following addition of 0.0008 g dendrimer to each vial, the initial solution pH was adjusted to 6.5 for all vials. The vials were then shaken in an incubator at room temperature for 48 hours. Then dendrimers were separated from water through ultrafiltration using a Macrosep Centrifugal device containing a membrane with a molecular weight cut-off (MWCO) of 10K, purchased from Pall Life Sciences, Ann Arbor, MI, USA. Copper concentration in the filtrate was analyzed. Metal uptake was calculated by comparing initial and final concentrations of metal in the aqueous phase.

Copper sorption and desorption isotherms were also measured for the soil tested by batch tests. One gram soil was equilibrated with 20 mL of solution containing Cu²⁺ ranging from 0 to 10 mg/L and at a constant pH of 6.0 (pH was adjusted intermittently). Duplicates were used for all isotherm points (10 replicates were prepared for the point of the highest concentration for subsequent desorption isotherm tests). The mixtures were shaken for 7 days at room temperature in an incubator and then centrifuged at 2000 rpm. The supernatant was analyzed for Cu²⁺ using AAS, and copper uptake by the soil was then calculated. For the subsequent desorption isotherm tests, 200 mL soil-amended solution was also prepared by mixing soil and DI water at the same soil:solution ratio as in the sorption tests. Desorption isotherm tests were then initiated by replacing an aliquot (2~18 mL) of the supernatant in the 10 replicate vials using the same amount of soil-

amended solution. The mixture was then re-equilibrated for another week and centrifuged to obtain the desorption isotherm. Separate kinetic tests indicate that sorption equilibrium of Cu^{2+} by the soil was reached within one day.

Effects of dendrimer concentration, generation number, pH, ionic strength and terminal functional groups on copper removal were investigated through a series of fixed-bed column tests. Similar experimental method was also employed by other researchers (Kim et al. 2000; Rampley and Ogden 1998b; Roy et al. 1995). The column test set-up included an HPLC pump, a glass column (1 cm in inner diameter, Omnifit, Cambridge, England) and a fraction collector (Eldex Laboratories, Napa, CA, USA). In all tests, the volume of the soil bed was ~ 3.14 mL. About 0.5 cm (height) of glass wool was placed on the bottom to support the soil bed. In all cases, the empty bed contact time (EBCT) was 17 min and superficial liquid velocity (SLV) 3.8×10^{-5} m/s. Before a dendrimer was introduced, ~ 14 bed volumes (BVs) of DI water at a pH equal to that of the subsequent dendrimer solution were passed through the soil bed to obtain a stable base line. Following introduction of a dendrimer solution, copper elution history was monitored for ~ 66 BVs in each column run.

A commonly used sequential extraction procedure (Han et al. 2001) was employed to determine the operationally defined copper speciation in the soil before and after dendrimer treatment, where ~ 66 BVs of a G4.0-NH₂ (0.040%, pH=6.0) were used to treat 4.5 g of soil in a fixed-bed. Seven operationally defined copper species in the soil phase were analyzed, including (in the order of ascending affinity to the soil): exchangeable copper (EXC), copper bound to carbonate (CARB), copper bound to easily reducible oxides (ERO), copper bound to soil organic matter (SOM), copper bound to

amorphous iron oxides (AmoFe), copper bound to crystalline iron oxides (CryFe), and residual copper (RES). **Table 2-3** provides the extraction conditions used for extracting each form of the Pb^{2+} species. In all cases, the ratio of solution-to-soil was kept at 25 (mL):1 (g).

Possible dendrimer retention by the soil bed in the column was determined by comparing the influent and effluent dendrimer concentrations. Two dendrimers (G4.0-NH₂ and G4.5-COOH) were tested in this regard. About 66 BVs of a solution containing 0.040% of a dendrimer and at pH 6.0 were passed through the soil bed under identical hydrodynamic conditions as in other column runs. Dendrimer concentration in the effluent was measured as total organic carbon (TOC) using a UV-persulfate TOC analyzer (Phoenix 8000), and compared with that in the influent. A parallel test was carried out with DI water only, which indicated no TOC leakage from the soil.

Recovery of a spent dendrimer (G4.0-NH₂) was probed by nano-filtering the spent dendrimer solution using a Macrosep Centrifugal device containing an Omega membrane with an MWCO of 1K (Pall Life Science, Ann Arbor, MI, USA). Measurement of TOC before and after membrane filtration indicated that ~72% of the dendrimer was recovered through the nanofiltration in two consecutive runs. The retained dendrimer was then regenerated with 100 mL of 2N HCl for 24 hours. After removal of the acid, ~28% of fresh dendrimer was added in the recovered dendrimer to compensate the mass loss, and then the mixture was reused for another cycle of soil extraction run.

Table 2-3. Reagents and Conditions Used in the Sequential Extraction.

Step	Pb²⁺ Species	Extraction methods and conditions
1	EXC	25 mL of 1 M NH ₄ NO ₃ , pH =7.0 (adjusted by NH ₄ OH) , 25 °C, 30 min
2	CARB	25 mL of 1 M NaOAc-HOAc, pH=5.0, 25 °C, 6 hr
3	ERO	25 mL of 0.1 M NH ₂ OH•HCl + 0.01 M HCl solution, 25 °C, 30 min
4	SOM	3 mL of 0.01 M HNO ₃ and 5 mL of 30% H ₂ O ₂ , water bath 80 °C, 2 h 2 mL of H ₂ O ₂ , 80 °C, 1 hr 15 mL of 1 M NH ₄ NO ₃ , 10 min
5	AmoFe	25 mL of 0.2 M oxalate buffer solution (0.2 M (NH ₄) ₂ C ₂ O ₄ -0.2 M H ₂ C ₂ O ₄ , pH=3.25), 25 °C, 4 hr
6	CryFe	25 mL of 0.04 M NH ₂ OH•HCl in a 25% acetic solution, water bath 97-100 °C, 3 hr
7	RES	25 mL of 4 M HNO ₃ , water bath 80 °C, 16 hr

2.3 Results and Discussion

2.3.1 Titration curves of dendrimers

Dendrimers are rich in nitrogen donor atoms. Consequently, dendrimers are expected to behave as a polyprotic base (Ottaviani et al. 1996) and will protonate or deprotonate as solution pH varies. **Figure 2-1** shows titration curves for the three dendrimers as well as for DI water. It is evident that the low concentrations of a dendrimer increased the pH buffer capacity of water considerably. At the same dendrimer concentration of 0.04%, the pH buffer capacity appears to follow the sequence of G4.0-NH₂ > G4.5-COOH > G4.0-OH. Similar observations were also reported by others for dendrimers with -NH₂ and -COOH terminal groups (Ottaviani et al. 1996). For all three dendrimers, the titration curves do not appear to exhibit a distinctive inflection point (especially in the pH range of 4.0-8.0), suggesting that the protonation of the dendrimers is rather gradual during the acid titration. In other words, there exists no distinctive point of zero charge (PZC) in the typical groundwater pH range, and a minor change in solution pH will not markedly impact the sorption behaviors of the dendrimers.

2.3.2 Copper affinity of dendrimers

To test the copper extracting power of the dendrimers, equilibrium distribution of copper between a copper-selective ion exchange resin (DOW 3N) and solution was compared with or without a dendrimer. The distribution coefficient K_d is defined as the ratio of copper concentration in a dendrimer, q (mg/g), to that in water, C_e (mg/L), at equilibrium, namely

$$K_d = \frac{q}{C_e} \quad (2-1)$$

where q was calculated by mass balance:

$$q = \frac{(C_0 - C_e) \times V}{M} \quad (2-2)$$

where C_0 is the initial Cu^{2+} concentration (mg/L), V the volume of solution (L), and M the mass of the ion exchange resin (g). **Table 2-4** gives K_d values in the presence or absence of one of the five dendrimers. The presence of the dendrimers reduced K_d by a factor of 17~31, indicating the strong copper affinity of these dendrimers.

An examination of copper binding to DOW 3N and the dendrimers may help understand the experimental observations. Each functional group of DOW 3N contains one tertiary amine, and two pyridine N donor atoms (Henry et al. 2004). Consequently, Cu^{2+} is taken up through Lewis acid-base interaction between Cu^{2+} and the nitrogen donor atoms. On the other hand, the dendrimers may be envisioned as multi-functional, multi-dentate ligands, which contain interior N and O donor atoms inside the macromolecules as well as terminal functional groups such as $-\text{COOH}$, $-\text{OH}$ and NH_2 . Consequently, uptake of Cu^{2+} by dendrimers are facilitated by the following mechanisms (Diallo et al. 2004; Ottaviani et al. 1994; Ottaviani et al. 1997; Zeng and Zimmerman 1997; Zhou et al. 2001): 1) complexation with terminal donor atoms; 2) complexation with interior donor atoms; 3) ion-pairing (electrostatic interactions) with charged terminal groups; and 4) other non-specific interactions such as physical encapsulation in the interior cavities, interactions with trapped counter ions and/or water molecules. In the presence of a strong competing sorbent such as DOW 3N, stronger specific interactions such as Lewis acid-base interaction and electrostatic interactions between Cu^{2+} and the terminal groups (and

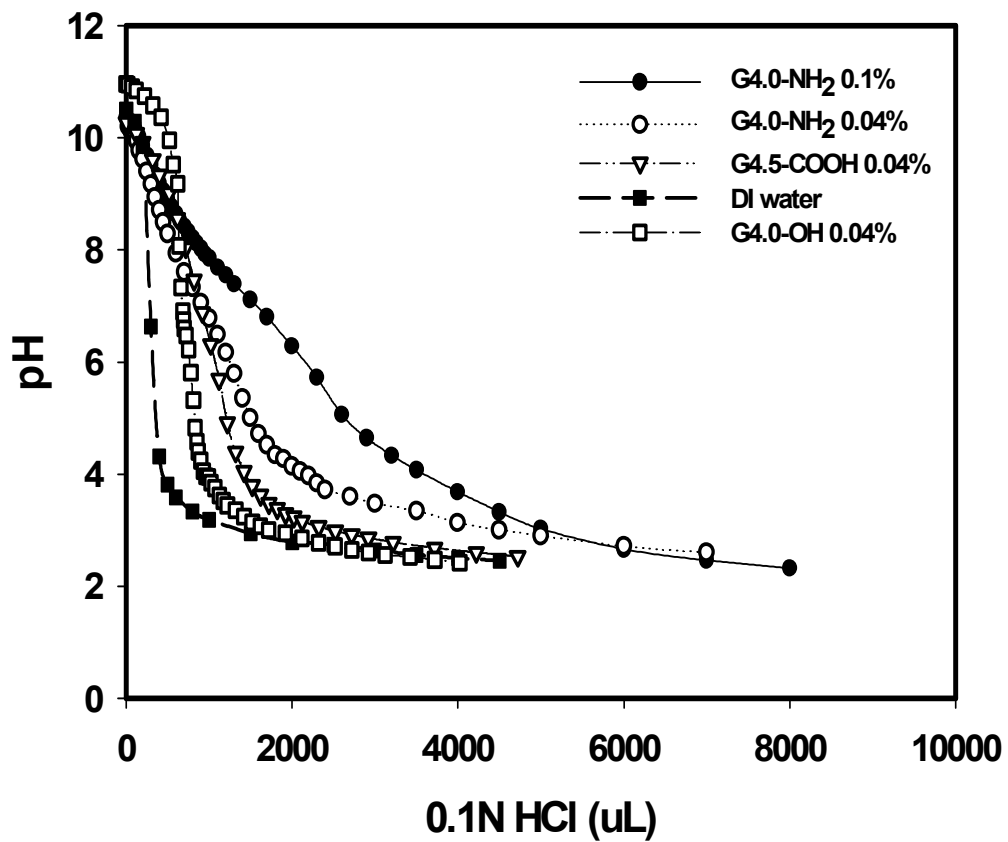


Figure 2-1. Titration curves for three dendrimers and DI water.

Table 2-4. Copper Distribution between a Chelating Ion Exchange Resin (DOW 3N) and Water with or without Dendrimer.

		K_d ((mg/g)/(mg/L))	Standard Deviation
Without Dendrimer		16	0.26
With Dendrimer	G4.0-OH	0.89	0.03
	G4.0-NH ₂	0.74	0.07
	G4.5-COOH	0.84	0.03
	G1.0-NH ₂	0.51	0.08
	G1.5-COOH	0.93	0.05

possibly some of the interior donor atoms) of the dendrimers are the primary mechanisms in the competitive uptake of Cu^{2+} by dendrimers. For example, in the uptake of Cu^{2+} by G4.5-COOH, one Cu^{2+} ion can form four coordination bonds with two neighboring -COOH groups and two adjacent N donor atoms (Ottaviani et al. 1994). In addition, electrostatic interactions between Cu^{2+} and the fixed COO^- groups are also operative, which further enhances the affinity. In addition, the higher density of functional sites in a dendrimer molecule may also strengthen its Cu^{2+} binding ability.

2.3.3 Copper binding capacity of dendrimers

In all batch isotherm tests, the equilibrium pH was maintained at ~ 6.30 and there was no metal precipitation under the experimental conditions. **Figure 2-2** shows equilibrium copper binding isotherms for three dendrimers: G4.5-COOH, G4.0-NH₂ and G4.0-OH. On a weight basis, G4.0-NH₂ appears to possess the highest capacity in the tested copper concentration range. The three dendrimers share the same interior structure, each containing 62 interior tertiary nitrogen donor atoms per molecule. However, while a G4.0-NH₂ molecule possess 64 terminal primary N-donor atoms, a G4.0-OH molecule holds 64 -OH groups, and a G4.5-COOH contains 128 -COOH groups (**Table 2-1**). Also note that the number of terminal groups per gram dendrimer is almost the same for the three dendrimers, i.e., 2.9×10^{21} for G4.5-COOH and 2.7×10^{21} for G4.0-NH₂ and for G4.0-OH. Since nitrogen is a stronger Lewis base than oxygen in -OH or -COOH groups, stronger Lewis acid-base interaction would be expected between G4.0-NH₂ and Cu^{2+} . For all cases, electrostatic interactions or ion pairing between Cu^{2+} and terminal functional groups are likely to be concurrently operative. The degree of

electrostatic interactions will depend on the degree of dissociation of the terminal groups. It was reported that for dendrimers with -NH_2 terminal groups, both the exterior primary amino groups and the interior tertiary nitrogen atoms are capable of binding with copper from the aqueous phase (Diallo et al. 1999). Since many OH groups in G4.0-OH may remain undissociated at the equilibrium pH, ion pairing may not be the predominant copper-binding mechanism, thus the interior nitrogen atoms are likely to be important copper binding sites (Zhao et al. 1998; Zhou et al. 2001). It was reported that each Cu^{2+} ion may coordinate with about 4 interior nitrogen atoms (Diallo et al. 1999; Zhao et al. 1998). G4.5-COOH has twice as many terminal groups as other two dendrimers on a per-molecule basis. At the solution pH of 6.30, the -COOH groups may be partially dissociated. Consequently, copper binding may be attributed to interactions with both interior tertiary nitrogen atoms and a fraction of -COOH groups (Roma-Luciw et al. 2000). The lower copper binding with G4.5-COOH compared to G4.0-NH₂ in the low concentration range (**Figure 2-2**) is likely due to the more tightly packed structure, which may hinder the interior copper binding capacity (Diallo et al. 1999).

The classic Langmuir isotherm model was employed to interpret the equilibrium binding of copper. The model takes the form,

$$q = \frac{bQC}{1 + bC} \quad (2-3)$$

where q is the equilibrium Cu^{2+} concentration in dendrimer (mg/g); C is the corresponding aqueous- phase concentration (mg/L); b is the Langmuir affinity coefficient (L/mg); and Q is Langmuir maximum capacity (mg/g). Values of b and Q were determined by non-linear curve fitting of eqn (2-3) to the respective equilibrium

binding data. **Table 2-5** gives the best-fitted model parameters and values of coefficient of determination (R^2) for the three dendrimers. The parameters indicate that G4.0-NH₂ holds a higher affinity (b) over G4.5-COOH, but the total Langmuir capacity (Q) of G4.5-COOH is greater. Namely, at high copper concentrations, more protons in the –COOH groups will be replaced by Cu²⁺. The best fitted lines are also shown in **Figure 2-2**.

2.3.4 Copper sorption / desorption isotherms for the soil

Figure 2-3 presents the copper sorption and desorption isotherms obtained using the soil tested. Each point in the plot represents the mean value of duplicates, and the standard deviation never exceeds 4.3%. The equilibrium pH was 5.4±0.2 for all points. The sorption branch was fitted with the Langmuir isotherm model (eqn (2-3)), and the resultant model parameters are given in **Table 2-5**. The desorption branch exhibited an extreme case of sorption hysteresis. The nearly flat desorption isotherm suggests that copper bound in the soil is hardly water-soluble.

2.3.5 Cu removal at various dendrimer concentrations

Figure 2-4 shows copper elution histories during two separate column elution tests using G4.5-COOH at pH 6.0 and at dendrimer concentrations of 0.040% and 0.10%, respectively. When only DI water at the same pH was passed through the soil bed (< ~14 BVs), copper concentration in the effluent was nearly zero, indicating that DI water alone did not remove any appreciable amounts of copper. In contrast, immediately (~3 BVs) after dendrimer was introduced, an abrupt increase in the effluent copper concentration

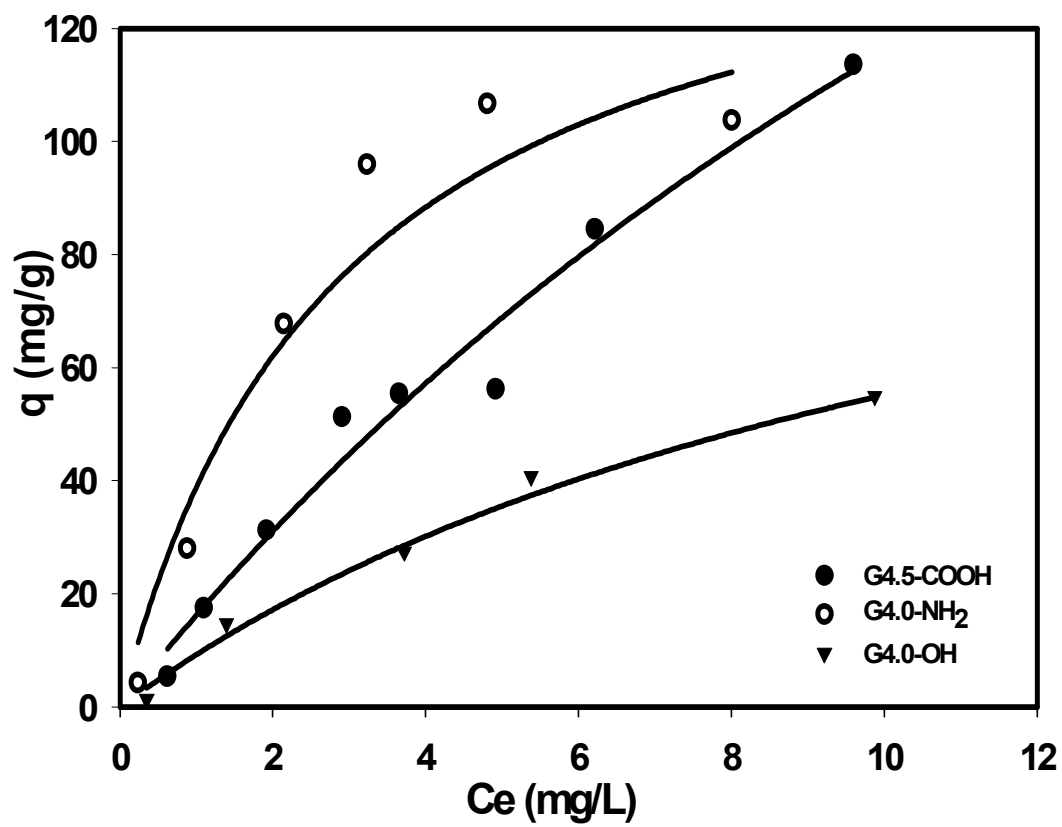


Figure 2-2. Equilibrium binding of copper by three dendrimers.

Table 2-5. Best-fitted Langmuir Model Parameters and R² Values for the Three Dendrimers and a Loamy Sand Soil.

	b (L/mg)	Q (mg/g)	R²
G4.0-NH₂	0.382 ± 0.161 ^{a)}	152 ± 26.8	0.945
G4.5-COOH	0.047 ± 0.023	363 ± 137	0.973
G4.0-OH	0.093 ± 0.029	116 ± 19.1	0.990
Soil	0.141 ± 0.036	0.729 ± 0.156	0.993

^{a)} All errors refer to standard errors.

was observed. The sharp chromatographic peaks confirm the strong complexing ability of the dendrimer with Cu^{2+} , and the relatively small tailing of the peaks suggests that mass transfer of the dendrimer in the soil is reasonably fast. Mass balance calculation reveals that ~57% and ~90% of the initially sorbed Cu^{2+} was removed within ~66 BVs of G4.5-COOH at 0.040% and 0.10%, respectively. Similar copper elution profiles were observed when G4.5-COOH was used at 0.010% and 0.040%, respectively, and at pH 6.0. **Table 2-6** gives the respective copper removal rates under a variety of experimental conditions.

Unlike in homogeneous (water-only) systems, where copper molecules can freely disperse in water and thus are able to utilize both interior and terminal binding capacity of a dendrimer molecule, removal of soil-sorbed Cu^{2+} by dendrimers is essentially a “go-and-get” process. While the current knowledge on dendrimer diffusion in aqueous solutions and on the interactions between dendrimers and solid surfaces is very limited, it appears that the following four steps are needed for a pre-sorbed Cu^{2+} ion to be removed by a dendrimer molecule: 1) mass transfer of Cu-free dendrimer molecules from the bulk aqueous phase to the water-soil interface, 2) colliding and binding of dendrimers with Cu^{2+} sorbed at the soil surface, 3) desorption of dendrimer- Cu^{2+} complexes from the soil surface, and 4) diffusion of copper-laden dendrimer molecules back into water. Because of the rather dense and rigid globular end layer of G4.0 or G4.5 dendrimers (Diallo et al. 1999; Ottaviani et al. 1997), only surface or near-surface groups (including the terminal functional groups and some near-surface tertiary amines) of a dendrimer molecule can physically come in contact with Cu^{2+} ions sitting on the soil surface. Therefore, the efficiency of copper removal from soil will depend on both the affinity and number of collisions between sorbed Cu^{2+} ions and the surface groups of dendrimers. The higher

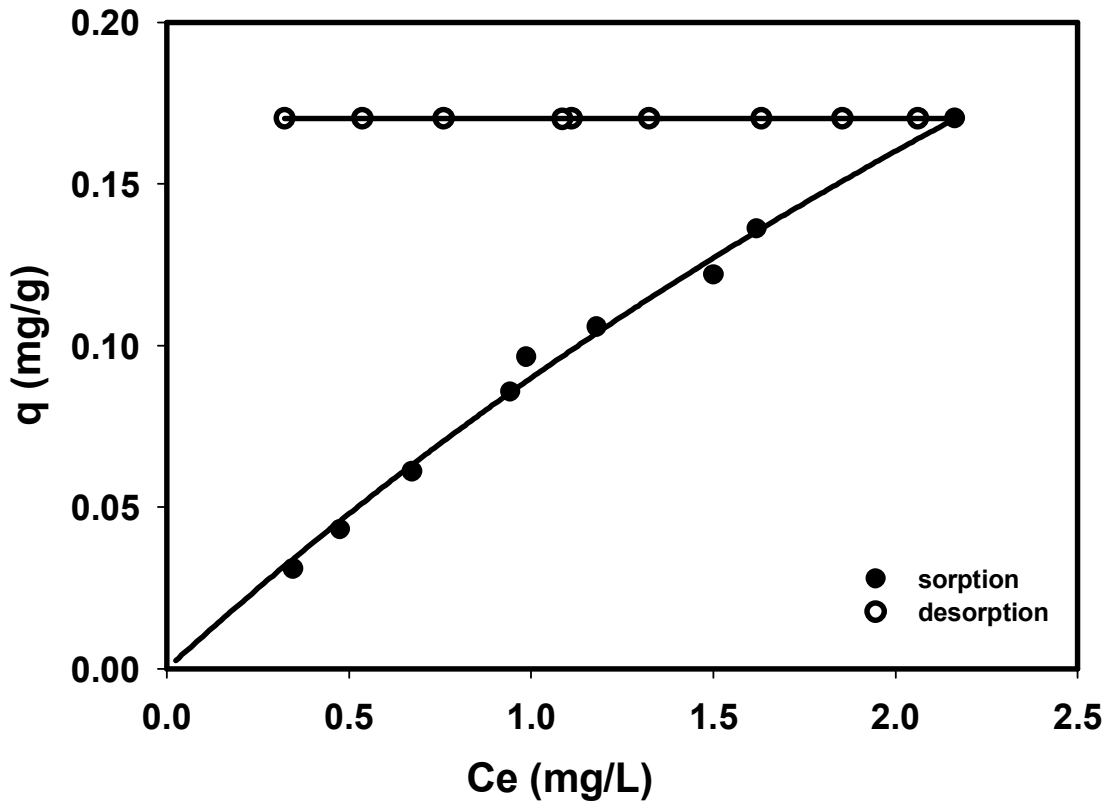


Figure 2-3. Copper sorption and desorption isotherms with an Alabama sandy loam soil.

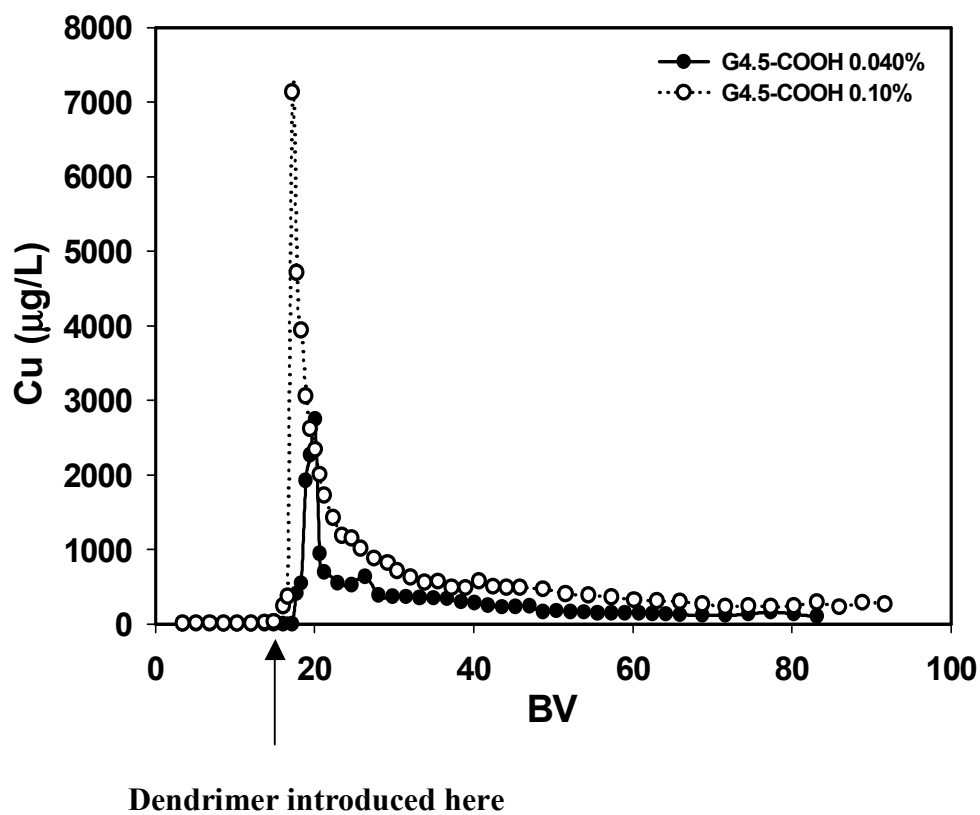


Figure 2-4. Copper elution histories during two separate column runs using 0.040% and 0.10% of G4.5-COOH at pH 6.0.

Table 2-6. Copper Removal and Effluent pH under Various Experimental Conditions.

Dendrimer	Concentration (w/w)	Bed Volumes	Influent pH	Effluent pH	Copper Removal
G4.5-COOH	0.040%	66	7.0	6.7~7.0	52%
G4.5-COOH	0.010%	66	7.0	6.7	35%
G4.5-COOH	0.10%	66	6.0	6.0~6.1	90%
G4.5-COOH	0.040%	66	6.0	6.4	57%
G4.5-COOH	0.040%	66	5.0	5.6~5.7	77%
G4.5-COOH (with $I=0.008M$)	0.040%	66	6.0	6.6~6.7	66%
G1.5-COOH	0.0089%	66	7.0	6.6~6.7	57%
G4.0-NH₂	0.042%	66	6.0	5.9	54%
G4.0-NH₂ (72% recovered)	0.040%	66	6.0	5.9	51%
G1.0-NH₂	0.035%	66	6.0	6.3~6.5	73%
G4.0-OH	0.043%	66	6.0	6.1~6.3	51%

dendrimer concentration provides more collisions, resulting in more removal. Utilization of the interior capacity of dendrimers will require further mass transfer of sorbed Cu^{2+} inside the dendrimer macromolecule, which is likely much slower (Ottaviani et al. 1994; Ottaviani et al. 1997).

Measurement of the effluent dendrimer concentration (as TOC) indicated that <2.1% of the G4.5-COOH dendrimer introduced was retained during the course of the operation. This minimal dendrimer retention is in accord with the observation that breakthrough of Cu^{2+} took place almost immediately after dendrimers were introduced (Note that the slight lag in breakthrough was attributed to the ~3 BVs of headspace water in the column). Upon rinsing using <4 BVs DI water, >98% of the soil-retained dendrimer was removed, suggesting that only physical forces are involved.

2.3.6 Effects of pH

Figure 2-5 shows that G4.5-COOH at 0.040% removed 52%, 57%, and 77% of pre-sorbed copper at a solution pH of 7.0, 6.0 and 5.0, respectively (**Table 2-6**). Namely, the dendrimer removed 25% more copper when the pH was lowered from 7.0 to 5.0. For comparison, **Figure 2-5** also includes Cu^{2+} elution histories obtained using only DI water at pH=6.0 and 5.0, respectively. Evidently, DI water can not remove any appreciable amounts of copper at the pH tested.

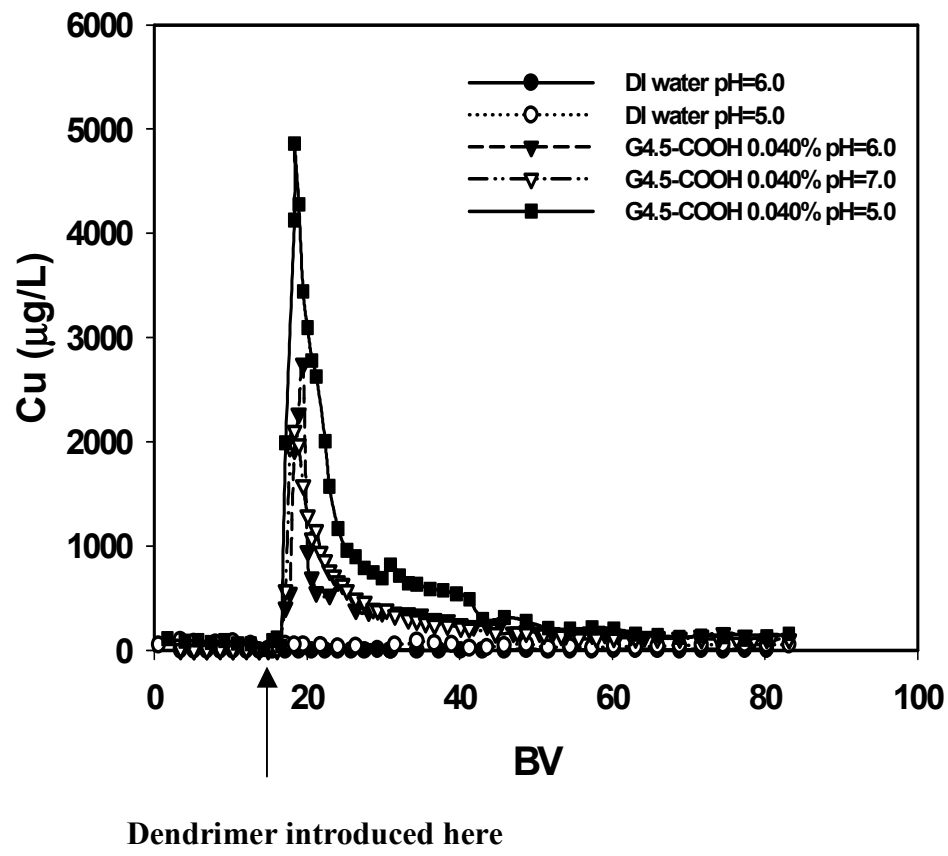


Figure 2-5. Copper elution histories during separate extraction runs using 0.040% G4.5-COOH at pH=7.0, 6.0 and 5.0 and with DI water at pH=6.0 and 5.0.

Solution pH can affect both availability of Cu^{2+} in soil and sorption capacity of dendrimers. In general, sorption of Cu^{2+} to soil is characterized by a so-called ‘adsorption edge’, i.e. Cu^{2+} uptake can change drastically within a narrow pH range (<2 pH units) (Dzombak and Morel 1990). For various hydrous ferric oxides (HFO), the $\Delta\text{pH}_{10-90\%}$ (the pH range corresponding to Cu^{2+} uptake from 10% to 90%) has been reported in the range of 4.2-6.0 (Dzombak and Morel 1990), which also applies to the soil tested based on our test (data not shown). Lowering pH will increase the protonation of the soil surface, which diminishes the Cu^{2+} -soil interactions and thereby favors the copper removal process. On the other hand, lowering pH also increases protonation of the weak base or weak acid sites in dendrimer molecules and thereby reduces their Cu-binding capacity. The fact that copper removal was enhanced at lower pH suggests that pH affects the soil to a greater degree than the dendrimer.

Potentiometric (acid-base) titration of various dendrimers was recently reported (Cakara et al. 2003; Diallo et al. 2004; Niu et al. 2003). In general, two classes of protonation sites were considered, including the interior tertiary amines and terminal functional groups. Ionization constants (pK_a) for select dendrimers were calculated by interpreting the titration data using various theoretical models. The reported pK_a values for G4.0- NH_2 are 6.30~6.85 for interior tertiary amines and 9.00~10.29 for terminal primary amines (Cakara et al. 2003; Diallo et al. 2004; Niu et al. 2003). The pK_a value of interior amines for the G4.0-OH dendrimer was ~6.30 (Niu et al. 2003). While further validation appears to be needed to confirm these reported values, it is generally believed that 1) protonation in the interior microenvironment takes place at a much lower pH (nearly 3 pH units) than at the dendrimer surface; 2) the pK_a value of interior amines is 1-

2 pH units lower than that of their monomeric analogues; and 3) the pK_a value of terminal groups is about the same as their monomeric analogues (Diallo et al. 2004; Niu et al. 2003). Niu et al. (Niu et al. 2003) attributed the pK_a shift between interior and terminal amines to the hydrophobic microenvironment inside dendrimers.

There appears no pK_a value available in the literature for G4.5-COOH. However, Manriquez et al. (Manriquez et al. 2003) reported that the average pK_a value was 3.79 for the terminal groups of a close analogue, G3.5-COOH. This low pK_a value suggests that at $pH > 5.0$ the terminal groups of G4.5-COOH remain largely available for binding with Cu^{2+} (Note that the effluent pH in response to the influent pH of 5.0 was actually 5.6~5.7 (**Table 2-5**)). Earlier, Ottaviani et al (Ottaviani et al. 1994) reported that strong electron paramagnetic resonance (EPR) signals were detected for complexes ($Cu-N_2O_2$) between Cu^{2+} and the terminal groups of G2.5-COOH at $pH < 4$.

2.3.7 Effects of terminal group type

As stated before, soil-sorbed Cu^{2+} ions are removed through interactions primarily with surface and/or near-surface functional groups of the dendrimer molecules. **Figure 2-6** compares copper elution histories with three dendrimers of the same core structure but different terminal groups. The concentrations of the three dendrimers are all equivalent to a solution containing 0.040% of G4.5-COOH (i.e. 0.040% for G4.5-COOH, 0.042% for G4.0-NH₂, and 0.043% for G4.0-OH) and the influent solution pH was 6.0 in all cases. Despite the known differences in copper affinity and in degrees of protonation for these terminal groups, **Table 2-6** shows that all three dendrimers removed comparable amounts of copper, ranging from 51% for G4.0-OH to 57% for G4.5-COOH.

The observed results coupled with the fact that at the prevailing pH 5.9~6.4, nearly all the terminal NH_2 or $-\text{OH}$ groups are protonated (whereas only ~50% of the internal tertiary amines remain neutral) strongly suggest that the soil-sorbed Cu^{2+} ions are extracted primarily through interactions with the internal tertiary amine groups of the dendrimers. Researchers have observed that the outer-shell tertiary N atoms can bind strongly with copper ions (Ottaviani et al. 1997).

In addition, the Cu^{2+} removal process in the fixed-bed column is likely a non-equilibrium process and it can be influenced by a number of thermodynamic and kinetic parameters such as sorption capacity, number, accessibility and reactivity of terminal groups, and particle size and mobility. Consequently, the difference in the dendrimer functional groups resulted in only modest difference in copper removal. From a practical viewpoint, the observed comparable effectiveness grants users the flexibility of selecting the cheapest dendrimer (the current market price for G4.0- NH_2 or G4.0- OH is ~58% of that for G4.5- COOH).

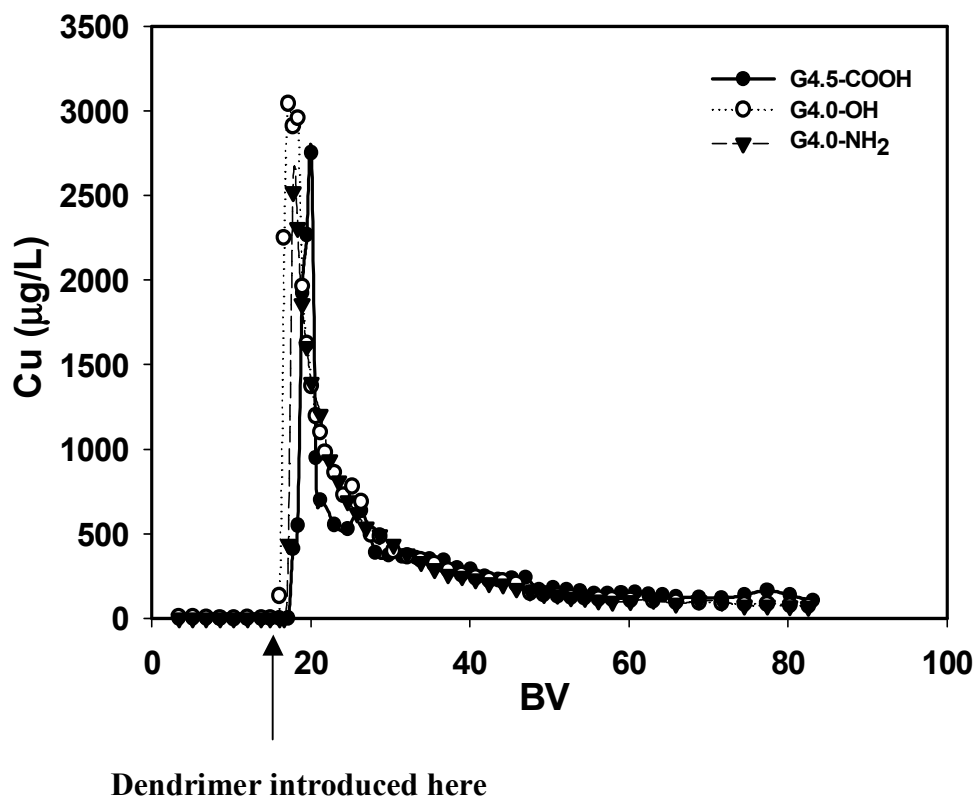


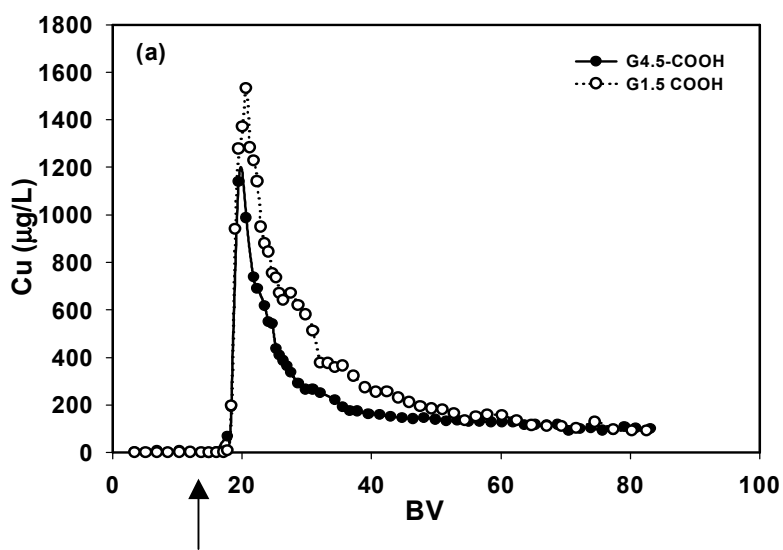
Figure 2-6. Copper elution histories during separate column runs using G4.5-COOH, G4.0-NH₂ and G4.0-OH based on equal equivalent terminal groups as 0.040% of G4.5-COOH at pH=6.0.

2.3.8 Effects of dendrimer generation

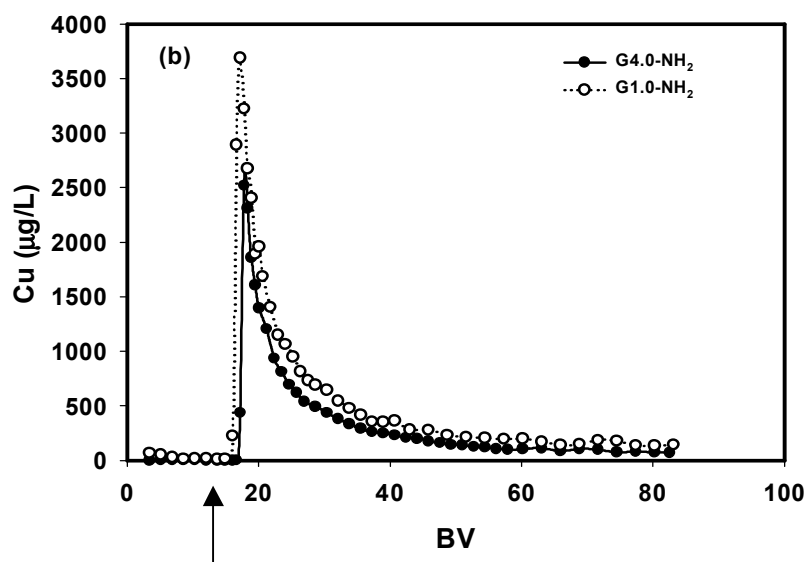
Figure 2-7 (a) shows copper removal by equal equivalent of G4.5-COOH (0.010%) and G1.5-COOH (0.0089%) at pH 7.0. **Table 2-5** indicates that G1.5-COOH removed 22% more copper than G4.5-COOH under otherwise identical conditions.

Figure 2-7 (b) compares copper removal using equal equivalent of G1.0-NH₂ (0.035%) and G4.0-NH₂ (0.04%) at pH 6.0. **Table 2-5** shows that G1.0-NH₂ removed 19% more copper than G4.0-NH₂. Evidently, dendrimers of lower generation are more effective in removing soil-sorbed Cu²⁺ than dendrimers of higher generation on an equal equivalent basis.

For each generation increment, the hydrodynamic diameter increases by ~1 nm (Tomalia et al. 1990), and the total number of Cu²⁺-binding sites (interior N-donor atoms + terminal functional groups) doubles. From a kinetic view point, the smaller the dendrimer particles, the less mass transfer resistance the particles will undergo. Taking the common notion that the intraparticle diffusivity is inversely proportional to the square of the particle radius, and given that the size of a G1.0-NH₂ molecule is about half that of a G4.0-NH₂ molecule (**Table 2-1**), the intraparticle diffusivity for G1.0-NH₂ will be four times greater. This kinetic advantage grants smaller dendrimer particles greater mobility and thus more chances to collide and interact with more Cu²⁺ ions. In addition, for a given number of terminal groups (or on an equal equivalent basis), the number of molecules for a lower generation dendrimer far exceeds that for a higher generation dendrimer. For example, one G4.0-NH₂ molecule is equivalent to 8 G1.0-NH₂ molecules, i.e. there are actually 8 times more G1.0-NH₂ molecules in the system. Consequently, the capacity for lower generation dendrimers is much better used.



Dendrimer introduced



Dendrimer introduced

Figure 2-7. Copper elution histories using dendrimers of various generations: **(a)** G1.5-COOH and G4.5-COOH based on equal equivalent terminal groups as 0.010% G4.5-COOH at pH=7.0; and **(b)** G1.0-NH₂ and G4.0-NH₂ based on equal equivalent terminal groups as 0.040% G4.0-NH₂.

Both Electron paramagnetic resonance (EPR) spectra and molecular simulation of the dendrimer morphology (Ottaviani et al. 1994) indicated that dendrimers of earlier generations (<3) display more flexible structure, allowing for easier access into the interior copper binding sites. As generation goes up (≥ 3), the exterior surface becomes tighter and the globular shape turns more rigid, resulting in much reduced accessibility of the interior sites.

2.3.9 Effects of ionic strength

Ionic strength (I) of the solution can affect both copper-soil interactions and the performance of dendrimers (e.g., protonation and ion pairing behaviors). The presence of salts can influence the surface potential and the double-layer thickness, and may compete with Cu^{2+} for binding sites. To test the overall effects, a dendrimer solution was prepared with the following compositions: G4.5-COOH = 0.040%, pH = 6.0, Na_2SO_4 = 2 meq/L, NaCl = 1 meq/L, and NaHCO_3 = 1 meq/L, which results in an ionic strength of 0.008 M (contribution from the dendrimer neglected). **Figure 2-8** shows that an increase in I from 0 to 8 mM resulted in an increase in copper removal from ~57% to ~66%. For G4.0-NH₂, Niu et al. (Niu et al. 2003) observed that pK_a of the terminal amines increased slightly (from 9.15 to 9.30) when I was raised from 29 to 129 mM (for interior tertiary amines, pK_a increased from 6.00 to 6.65 as I was raised from 15 to 115 mM). The modest increase in pK_a suggests that the change in I in **Figure 2-8** may not drastically reduce the dendrimer's copper removal capacity. The ~9% increase in copper removal shown in **Figure 2-8** is therefore ascribed to the reduced copper affinity of the soil at elevated I . Note that the presence of bicarbonate in the solution also favors the dissolution of copper.

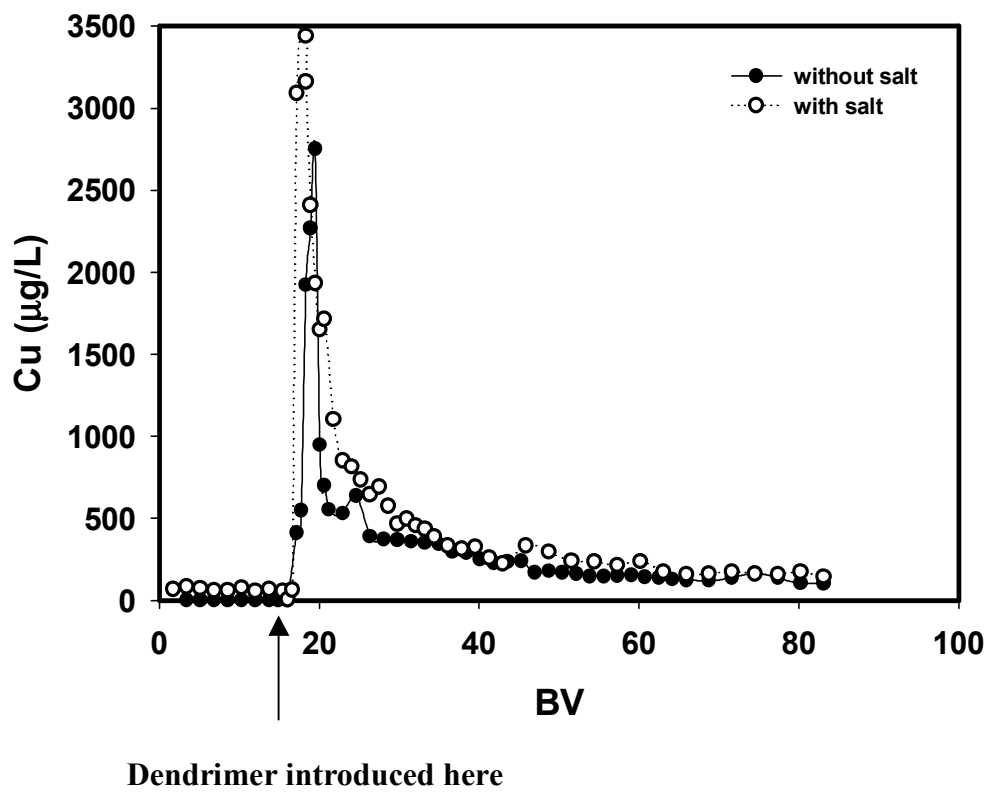


Figure 2-8. Copper elution histories during two separate column runs using 0.040% of G4.5-COOH and in the absence or presence of other ubiquitous ions, equivalent to a total ionic strength of 0.8 mM.

2.3.10 Effect on copper speciation in soil

To investigate the availabilities of the residual copper after dendrimer treatment, an operationally defined copper speciation was investigated. **Table 2-7** compares fraction of copper bound to various components of the soil before and after the dendrimer treatment. Five of the seven operationally defined copper species were detected. The availability of these species follows the sequence of EXC > CARB > ERO > SOM > CryFe. The total copper in the untreated soil was initially 30 mg/kg, which was present primarily as exchangeable (38%, or ~11 mg/kg) or carbonate-bound species (36%, or ~11 mg/kg), both being more easily available. About 22% (or 6.6 mg/kg) copper was bound with SOM. In contrast, the fraction bound with iron was only 0.47% or 0.14 mg/kg, suggesting that Fe oxides did not play a major role in binding copper to this soil. After the dendrimer treatment, the total copper in soil was reduced to 14 mg/kg, i.e. 54 % of copper was removed. The copper bound with SOM turns out to be the most predominant form, accounting for 52% of total residual copper, or 7.1 mg/kg, which is about the same as that (6.6 mg/kg) before dendrimer treatment. Copper in the exchangeable form was reduced from 11 to 2.9 mg/kg, and copper in carbonate form 11 to 2.0 mg/kg. Although the EXC form of Cu is the mostly available species, there was still some left after dendrimer treatment. The exchangeable copper was extracted with NH_4NO_3 , which is a small molecule. Compared to the macromolecule of dendrimer it could access some soil sorption sites where dendrimer could not go. Since the remaining copper after dendrimer treatment is much less mobile or less available, the extraction process using dilute dendrimers may provide a remediation alternative to comply with risk-based regulations.

Table 2-7. Copper Speciation in Original and Dendrimer-Treated Soil.

	EXC(%)	CARB(%)	ERO(%)	SOM(%)	CryFe(%)	Total Copper in Soil (mg/kg)
Original Soil	38	36	4	22	0.5	30
Treated Soil	20	14	8	52	6	14

(Acronyms: EXC = Exchangeable copper; CARB = Carbonate-bound copper; ERO = Copper bound to easily reducible oxides; SOM = Copper bound to soil organic matter; CryFe = Copper bound to crystalline iron oxides)

2.3.11 Recovery and reuse of spent dendrimers

Compared to other extracting agents such as EDTA, dendrimers possess larger and well-controlled molecule size. This advantage enables the spent dendrimers and the associated contaminant metal to be recovered using relatively simple separation processes. In addition, metal-laden dendrimers can be easily regenerated (Diallo et al. 1999; Diallo et al. 2004). Efficient regeneration of various water-soluble polymers has been achieved via chemical, electrochemical or thermal treatment (Geckeler and Volchek 1996).

To test the feasibility, ~66 BVs of spent 0.040% G4.0-NH₂ solution was collected during a copper extraction column run. TOC measurement indicated that less than 1.8% of the dendrimer was retained during the run, which can be fully washed off using <4 BVs of DI water. Upon one nanofiltration run, ~60% of the spent dendrimer was retained by the filter as indicated by the change in TOC before and after the nanofiltration. When the filtrate was re-filtered one more time, an additional ~12% was recovered, resulting in a total of ~72% of recovery in two consecutive nanofiltration runs.

It was reported that PAMAM dendrimers can be fully protonated and thereby regenerated by lowering pH to < 4.0 (Diallo et al. 1999). To test the feasibility of regenerating and reusing the recovered dendrimers, a 2 N HCl solution was used to regenerate the recovered dendrimer. Upon addition of approximately 28% of the virgin dendrimer to compensate the dendrimer loss, the mixture was reused in another extraction run. **Figure 2-9** compares the copper elution histories using virgin G4.0-NH₂ and primarily recovered G4.0-NH₂ at pH 6.0. The two elution profiles almost coincide. Copper removal was 54% and 51% by the virgin and recovered dendrimers, respectively

(Table 2-5), indicating that dendrimers may serve as a reusable extracting agent for copper removal.

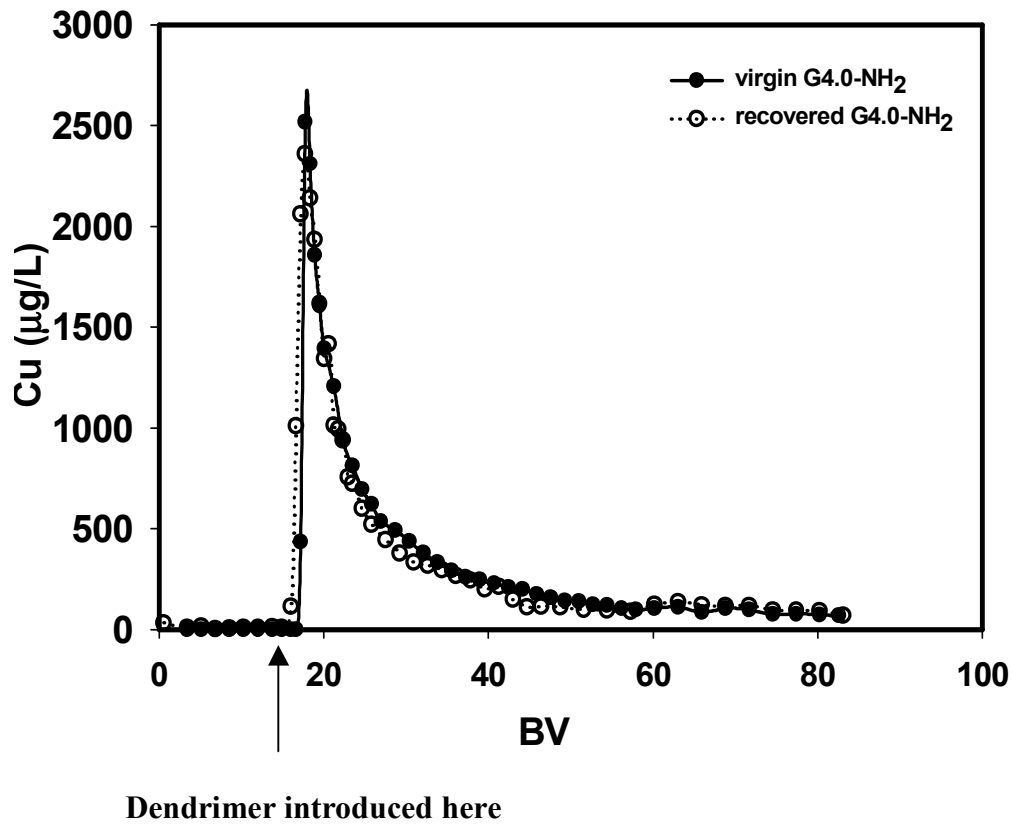


Figure 2-9. Comparing copper elution histories using 0.040% of virgin and recovered G4.0-NH₂ at pH=6.0.

CHAPTER 3. REMOVAL OF LEAD FROM CONTAMINATED SOILS USING POLY(AMIDOAMINE) DENDRIMERS

In this chapter, soil remediation using dendrimers presented in chapter 2 is extended to the removal of lead (Pb^{2+}) from three contaminated soils. Lead removal was tested in the same fixed-bed column set-up where a prescribed dendrimer solution was passed through a lead-loaded soil bed. Effects of dendrimer generation, concentration, type of the terminal groups, solution pH, and soil type were investigated.

3.1 Introduction

Toxic metals such as lead, cadmium, chromium, arsenic, zinc, copper, and mercury have been detected in over one thousand of the EPA's National Priorities List (NPL) sites (Mulligan et al. 2001). Among these contaminants, lead has been ranked the third in terms of frequency of detection on the sites (Rampley and Ogden 1998b). Due to the contamination extensiveness and the associated toxic effect of lead, there has been a consistent need for technologies to remove lead from thousands of contaminated sites in the U.S.

Among various technologies for remediation of heavy-metal contaminated soils are excavation, isolation, containment, electrokinetic separation, biochemical process, and soil washing (Mulligan et al. 2001). However, current remediation practices remain,

to a great extent, relying on excavation and subsequent landfill, which is rather costly and environmentally destructive (Berti and Cunningham 1997).

In recent years, soil washing using acids or chelating agents have received increasing interests (Allen and Chen 1993; Cline and Reed 1995; Elliott and Brown 1989; Furukawa and Tokunaga 2004; Hong et al. 1999; Kedziorek et al. 1998a; Lim et al. 2004b; Lo and Yang 1999; Macauley and Hong 1995; Peters 1999; Reed et al. 1996; Samani et al. 1998). Soil washing can be practiced either *in-situ* or *ex-situ*, and it is less environmentally disruptive compared to excavation. However, soil washing by acids often changes the soil chemistry and results in large volumes of wastewater that requires further treatment (Lo and Yang 1999). Compared to acids, chelating agents offer several key advantages, including high metal selectivity and extraction efficiency, high thermodynamic stabilities of the metal complexes formed, and less disturbance of the soil chemistry (Lim et al. 2004b).

Several chelating agents have been studied for removing lead from soils, including ethylenediaminetetraacetic acid (EDTA) (Allen and Chen 1993; Hong et al. 1999; Kedziorek et al. 1998a; Lim et al. 2004b), nitrilotriacetic acid (NTA) (Elliott and Brown 1989; Lim et al. 2004b), pyridine-2, 6-dicarboxylic acid (PDA) (Macauley and Hong 1995), and diethylenetriamine pentaacetic acid (DTPA) (Lim et al. 2004b), of these compounds, EDTA has been the most frequently cited chelating agent for its strong metal binding ability (Allen and Chen 1993; Cline and Reed 1995; Elliott and Brown 1989; Hong et al. 1999; Kedziorek et al. 1998a; Lim et al. 2004b; Lo and Yang 1999; Samani et al. 1998). The downsides with EDTA include that, although desirable, it is extremely difficult to recover spent EDTA and desorbed metals from groundwater. In addition,

there have been concerns regarding the fate and health effects of EDTA when applied in soils (Reed et al. 1996). In search for an alternative chelating agent, Rampley et al. (Rampley and Ogden 1998b) tested a chelating polymeric material, known as Metaset-Z, for removing Pb^{2+} from soils. They observed that the chelating material had low affinity for quartz and a solution with 0.5% (w/w) of Metaset-Z was able to remove 95% of Pb^{2+} from a weathered superfund soil in 12 hours of contact in a batch experiment.

In the past decade or so, tremendous progress has been achieved in the synthesis and characterization of dendrimers, especially, PAMAM dendrimers (Niu et al. 2003; Tomalia et al. 1990; Zhou et al. 2001). Because of their tunable architecture, particle size, and functionality, PAMAM dendrimers hold the promise of acting as a novel recoverable extracting agent for removing lead from soils under a range of environmental conditions. Typically, these dendritic macromolecules are synthesized by repeatedly attaching amidoamine monomers in radially branched layers, each of which corresponds to a generation (G), to a starting ammonia or amine core (Tomalia et al. 1990). Dendrimers terminated with amine or hydroxyl groups are referred to as full generation dendrimers (designated as Gn.0-NH_2 or Gn.0-OH , where n is an integer indicating the generation number), whereas those with carboxylate groups are classified as half-generation dendrimers (Gn.5-COO^-).

The environmental application of dendrimers was first explored by Diallo et al. (Diallo et al. 1999), who reported effective removal of copper from water using various generations of PAMAM dendrimers terminated with primary amine groups. Later, Rether et al. (Rether and Schuster 2003) studied selective separation and recovery of heavy metals such as Co^{2+} , Cu^{2+} , Hg^{2+} , Ni^{2+} , Pb^{2+} , and Zn^{2+} from water using PAMAM

dendrimers modified with N-benzoylthiourea, and Kovvali et al. (Kovvali 2000) prepared an immobilized liquid membrane by immersing the porous polymer film in pure dendrimer for selectively separating CO₂ from other gases. More recently, Diallo et al. (Diallo et al. 2005) observed that the PAMAM dendrimers were able to enhance removal and recovery of Cu(II) from water by ultrafiltration.

Application of dendrimers for soil remediation for removal of copper was discussed in chapter 2. The feasibility of removing and recovering copper(II) from a contaminated sandy soil using PAMAM dendrimers of amine, carboxyl and hydroxyl terminal groups was investigated. It was observed that over 90% of copper in a sandy soil was removed using ~66 bed volumes of a G4.5 dendrimer solution containing 0.10% (w/w) dendrimer at pH 6.0. It was also found that the spent dendrimer can be recovered through nanofiltration and the recovered dendrimer can be regenerated and reused.

This chapter aims to test the feasibility of using selected dendrimers as recoverable extracting agents for removal of lead (Pb²⁺) from three soils including a sandy soil, a clay soil, and a weathered field contaminated sandy clay loam soil. The specific objectives of this chapter are to: (1) investigate the effectiveness of selected dendrimers for extracting Pb²⁺ from three representative soils; (2) determine the effects of dendrimer concentrations, terminal functional groups, generation number, pH, and soil characteristics on the extracting efficiency; and to quantify the recoverability of the spent dendrimers and desorbed Pb²⁺.

3.2 Materials and Methods

This study tested three PAMAM dendrimers, including a generation 1.5 dendrimer terminated with carboxylic groups in sodium form (G1.5-COONa), a generation 1.0 dendrimer with primary amine groups (G1.0-NH₂), and a generation 4.0 dendrimer with primary amine groups (G4.0-NH₂). All dendrimers were purchased from Dendritech Inc. (Midland, MI, USA) as stock solutions methyl alcohol (19.28% for G1.5-COONa, 39.49% for G1.0-NH₂, and 26.00% for G4.0-NH₂ (Note: throughout the paper, the dendrimer is given in percent by weight unless indicated otherwise). **Table 3-1** provides salient properties of these dendrimers (Cakara et al. 2003; dendritech; Diallo et al. 2004; Leinser and Imae 2003; Li et al. 2005).

This study tested three surface (<12 cm deep) soils, including a lead-free loamy sand soil, a lead-free sandy clay loam #1, and an aged lead-contaminated sandy clay loam #2. The loamy sand soil was taken from a local farm land in Auburn, AL, USA, whereas the other two soils were obtained from a local police firing range, which has been in use since 1987. Before use, all soils were ground to pass a 2 mm standard sieve. **Table 3-2** gives major compositions of these soils. Mineral analysis was conducted following the EPA Method 3050B. NH₄-N was determined following the method of microscale determination of inorganic N in water and soil extracts (Sims et al. 1995). Organic nitrogen and organic carbon were analyzed following the Dumas method and using a LECO CN-2000 combustion unit (LECO Corp., Joseph, MI, USA) at 1050 °C. The organic matter (OM) content was estimated by multiplying the organic carbon content by an empirical factor of 1.72, as recommended by the Auburn University Soil Testing Laboratory. EPA method 3050B was followed for analyzing lead in the soil samples. The

Table 3-1. Salient Properties of Dendrimers Used for Lead Removal.

Dendrimer	Core type	Molecular Weight	Measured Hydrodynamic Diameter (nm)	Number of interior tertiary amines	Number of Terminal Groups	pKa	
						Interior N	Terminal Groups
G1.5-COONa	Ethylene diamine	2,935	2.8	14	16	Not available	Not available
G1.0-NH₂	Ethylene diamine	1,430	2.2	6	8	(3.55~6.70), 3.86	6.85, 9.00
G4.0-NH₂	Ethylene diamine	14,215	4.5	62	64	6.65, 6.85	9.2, 10.29

Table 3-2. Major Compositions of Soils Used for Lead Removal.

	Minerals (mg/kg)					Sand%	Silt%	Clay%	Organic matter%	pH
	Ca	Mg	P	Fe	Al					
Loamy sand	240	222	136	1,921	5,447	84	10	6	0.43	5.5
Sandy clay loam #1	157	943	323	12,194	21,277	-	-	-	0.50	5.1
Sandy clay loam #2	302	151	-	8,500	18.9	51	22	28	-	5.4

- Not analyzed

lead concentration in the contaminated range soil was 1600 mg/kg. For subsequent column elution tests, Pb^{2+} was pre-loaded to the two Pb-free soils by equilibrating 2 L of a solution containing 100 mg/L Pb^{2+} (initial concentration) with 100 g of an air-dried soil sample in a batch reactor at an equilibrium pH of 7.0. The pre-loading process resulted in a Pb^{2+} uptake of 590 mg/kg for the sandy soil and 965 mg/kg for the clay soil. The Pb^{2+} -loaded soil samples were then air-dried and used within three months.

Sorption isotherms of Pb^{2+} were constructed for the two Pb-free soils through batch equilibrium experiments. One gram of a dry soil was equilibrated with 20 mL of a solution containing an initial concentration of Pb^{2+} ranging from 0 to 43 mg/L in screw-capped glass vials. The soil-solution mixtures were shaken on a rotating rack at 40 rpm for seven days in an incubator at 21 °C. Solution pH was intermittently adjusted with dilute NaOH or HCl and kept at 6.0 until equilibrium was reached. All isotherm points were duplicated to assure data quality. Upon equilibrium, which was confirmed by separate kinetic tests, the vials were centrifuged at 400g for 20 minutes, and the supernatant was analyzed for Pb using a flame atomic-absorption spectrophotometer (FLAA) (Varian 220FS). Lead uptake by each soil sample was then determined through mass balance calculations.

Desorption isotherms of Pb^{2+} were constructed by first equilibrating 10 replicates of 1 g of a dry soil and 20 mL of a solution containing 43 mg/L Pb^{2+} in the same manner as described in the sorption isotherm tests. The equilibrium pH was maintained at 6.0. After the equilibrium uptake of Pb^{2+} was determined in the same manner as described above, desorption of Pb^{2+} was initiated by replacing an aliquot (2-18 mL) of the supernatant solution with the same volume of a soil-amended, Pb-free solution. The soil-

amended solution was prepared by mixing a soil with deionized water (DI water) at the same soil/solution ratio as in the sorption equilibrium tests. The use of soil-amended solution assures that the replacing solution contains the same background compositions (i.e. soil exudates) as in the solution being replaced. The diluted mixtures were then equilibrated under mixing for another 7 days. Upon centrifuging, Pb in the solution phase was analyzed using the FLAA, and Pb²⁺ in each soil sample was calculated through mass balance calculations.

The effectiveness of selected dendrimers for extracting Pb²⁺ from soils was probed in a series of column elution experiments under various operating conditions. Three soils which differ in their compositions and aging (i.e. contaminant-soil contact time), were tested and compared. The column test set-up included an Acuflow series II HPLC pump, a Plexiglass column (diameter = 1.0 cm; length = 10 cm) with adjustable headspace volume (Omnifit, Cambridge, England), and a fraction collector (Eldex Laboratories, Napa, CA, USA). In all cases, the volume of the soil packed in the column was ~1.6 mL, and the headspace volume was kept at 0.2 mL. First, the soil bed was rinsed using ~30 BVs of DI water at the same pH as in the subsequent dendrimer solution. Then, a dendrimer solution was passed through the soil column at a constant flowrate of 0.06 mL/minute, which translated to an empty bed contact time (EBCT) of 27 minutes and superficial liquid velocity (SLV) 1.27×10^{-5} m/s. Lead elution history was then followed for ~120 BVs in each column run by analyzing lead concentration in the effluent using a graphite atomic-absorption spectrophotometer (graphite AA).

A sequential extraction procedure (SEP) (Han et al. 2001) was employed to determine the operationally defined speciation of Pb²⁺ in the sandy soil before and after

the dendrimer treatment, which was carried out by passing ~120 BVs of 0.5% G1.0-NH₂ solution at pH 5.0 through a lead-loaded soil bed. According to the extraction procedure, Pb²⁺ in the soil phase was classified as seven species, including: exchangeable Pb²⁺ (EXC), Pb²⁺ bound to carbonate (CARB), Pb²⁺ to easily reducible oxides (ERO), Pb²⁺ to soil organic matter (SOM), Pb²⁺ to amorphous iron oxides (AmoFe), Pb²⁺ bound to crystalline iron oxides (CryFe), and residual Pb²⁺ (RES). **Table 2-3** provides the extraction conditions used for extracting each form of the Pb²⁺ species. In all cases, the ratio of solution-to-soil was kept at 25 (mL):1 (g).

The leachability of lead in the soils before and after the dendrimer treatment was also tested following the Toxicity Characteristic Leaching Procedure (TCLP) (EPA Method 1311). The extracting fluid was prepared by mixing 5.7 mL of glacial acetic acid and 64.3 mL of 1 N NaOH. The mixture was then diluted by adding DI water to a total solution volume of 1 L. The pH of the resultant solution (TCLP extraction fluid #1) was ~4.9. Soil samples were extracted at a solid to solution ratio of 1:20. Typically, the extraction was conducted by rotating the mixture at 30 rpm for ~19 hours. Then the mixture was centrifuged at 500g for 20 minutes. The supernatant was then acidified with 1N HNO₃ to pH less than 2.0, and analyzed for Pb²⁺.

To quantify the possible retention of dendrimers by soils, dendrimer breakthrough curves were measured as a solution of 0.1% G1.0-NH₂ was pumped through the loamy sand soil and the sandy clay loam #1, respectively. In these tests, the dendrimer was measured as total organic carbon (TOC), which was determined using a Tekmar-Dohrmann, Phoenix 8000 UV Persulfate TOC analyzer (Teledyne Tekmar, Mason, OH, USA). Following the full breakthrough, DI water was passed through each of the

dendrimer-saturated soil beds, and dendrimer elution histories were followed to quantify the recovery of retained dendrimers. In each test, a control test was carried out with a solution containing no dendrimer but with the same background compositions (pH and methanol) to correct the contribution of methanol to the total TOC and any possible TOC leaching/uptake from/by the soil.

To test the recovery of spent dendrimers and dendrimer-bound Pb^{2+} , spent G1.0-NH₂ (0.1%) and G4.0-NH₂ (0.04%) solution after the column tests were collected, and then passed, respectively, through a membrane nanofiltration unit with a molecular weight cutoff (MWCO) of 1000 (Millipore, Bedford, MA) and with a stirred cell (series 8000, Millipore, Bedford, MA). The retention/recovery of a dendrimer was then determined by comparing the TOC level in the raw solution and in the filtrate. Since the dendrimers were supplied in methanol solution, TOC resulting from methanol was deducted in the calculations based on control experiments where the same concentration of methanol (no dendrimer) was subjected to the same column and nanofiltration runs. For each dendrimer, four consecutive nanofiltration runs were carried out, and the recovery in each run was recorded. To test the regenerability of the recovered dendrimers and recoverability of the retained Pb^{2+} , the retentate was then put in contact with 50 mL 2 N HCl for 24 hours. The acid-dendrimer solution was then nano-filtered once, and the concentration of Pb^{2+} before and after the nanofiltration was compared, and mass balance for Pb^{2+} was calculated. To quantify the possible TOC leakage due to the acid treatment, TOC in the acid filtrate was also measured. All tests were carried out in duplicates.

3.3 Results and Discussion

3.3.1 Sorption and desorption of lead by soils.

Figure 3-1 shows the lead sorption and desorption isotherms for the sandy soil and clay soil, respectively, at pH 6.0. While the clay soil showed a favorable sorption isotherm, the sandy soil displayed a more linear isotherm profile. The Freundlich isotherm model (eq (3-1)) was used to interpret the experimental data,

$$q = K_F C_e^N \quad (3-1)$$

where q (mg/g) is the Pb^{2+} concentration in soil; K_F is the Freundlich capacity parameter; N is the Freundlich exponent; and C_e (mg/L) is the corresponding aqueous phase Pb^{2+} concentration. **Table 3-3** gives the best-fitted model parameters and values of the coefficient of determination (R^2). As indicated by the 5-fold difference in the K_F value, the clay soil offered a much greater Pb^{2+} sorption capacity than the sandy soil. The values of the Freundlich exponent (N) also indicated that sorption with the sandy clay loam #1 is much more non-linear than with the loamy sand soil.

Both soils exhibited clear sorption hysteresis. The nearly flat desorption branch for the clay soil indicated that sorption of Pb^{2+} is almost irreversible, i.e. the Pb^{2+} sorbed can hardly be desorbed with water at the same pH. The sorption of Pb^{2+} with the loamy sand soil appeared only slightly reversible.

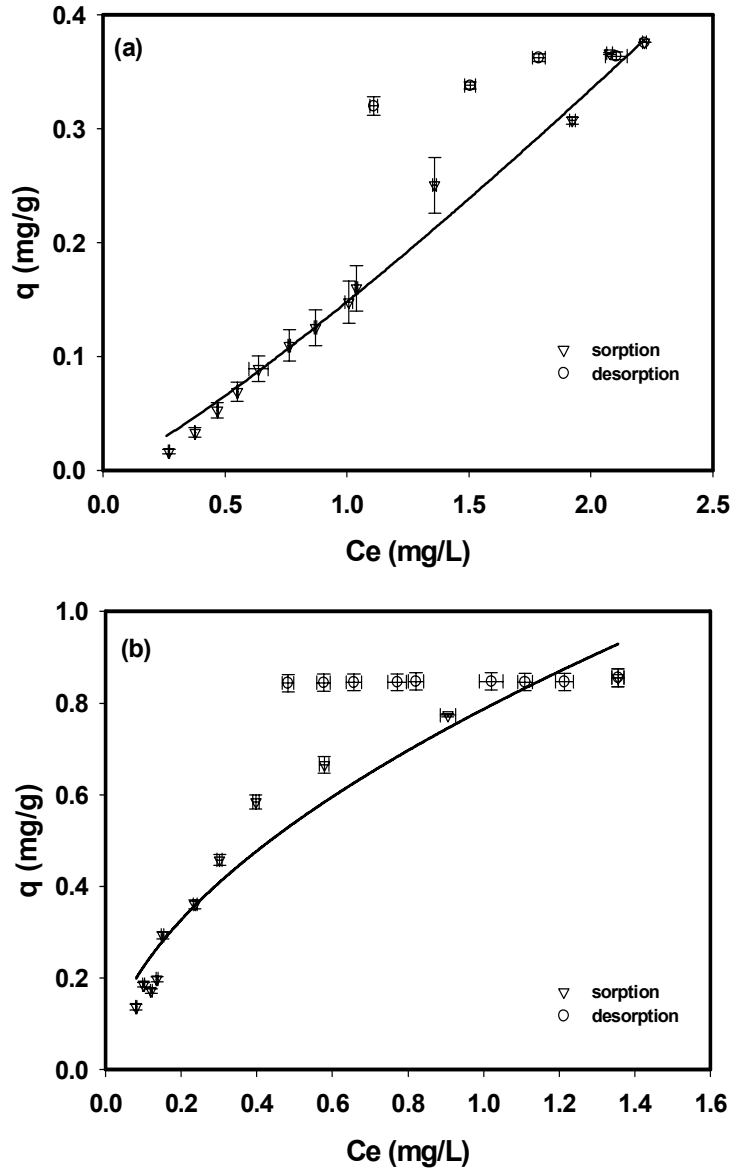


Figure 3-1. Sorption and desorption isotherms of Pb^{2+} with (a) loamy sand soil and (b) sandy clay loam #1. Data are given as mean of duplicates, and errors refer to standard error (Symbols: experimental data; Lines: model simulations).

Table 3-3. Best-Fitted Freundlich Model Parameters and R^2 Values for the Two Soils.

Soil	K_F	Standard Error	N	Standard Error	R^2
Loamy sand	0.15	0.0045	1.2	0.047	0.99
Sandy clay loam #1	0.80	0.034	0.56	0.049	0.95

3.3.2 Lead removal at various dendrimer concentrations

Elution histories of Pb^{2+} initially sorbed in the soils were followed during the fixed-bed column tests using G1.0-NH₂ at an influent concentration of 0.1%, 0.3% and 0.5%, respectively. **Figures 3-2(a)** and **2(b)** show the elution histories of Pb^{2+} for the clay and sandy soil, respectively, at various influent dendrimer concentrations and at an influent pH of 5.0. Note that before a dendrimer solution was introduced, ~30 bed volumes (BV) of DI water (pH adjusted to 5.0) were passed through the soil bed. In accord with the desorption isotherm results (**Figure 3-1**), DI water was not able to elute any significant amounts (<0.1%) of Pb^{2+} from the soils. In contrast, once the dendrimer solution was introduced, a sharp peak of Pb^{2+} in the effluent was evident in all cases.

Table 3-4 summarizes the percentage removal of Pb^{2+} after ~120 BVs of a dendrimer solution under various influent conditions. Since Pb^{2+} was pre-sorbed in the soil phase, the removal of Pb^{2+} by dendrimers may undergo a series of reaction and mass transfer steps, including 1) transport of Pb^{2+} -free dendrimer molecules from the bulk aqueous phase to the water-soil interface, 2) colliding and binding of dendrimer molecules with Pb^{2+} ions at the soil-water interface, 3) desorption of dendrimer- Pb^{2+} complexes from the soil surface, and 4) transport of Pb^{2+} -bound dendrimer molecules back into bulk water. Consequently, the Pb^{2+} extraction efficiency can be affected by both thermodynamic properties and mass transfer behaviors of dendrimers in soils. A higher dendrimer concentration would offer a greater Pb^{2+} binding capacity as well as more frequent molecular collisions, thereby may result in more Pb^{2+} removal. On the other hand, diffusion of dendrimer molecules may undergo greater mass transfer

retardation if the diffusant molecules get too crowded in more concentrated solutions. This is more likely the case for a sandy soil than for a clay soil because the pore volume in a sandy soil is smaller. Results in **Figures 3-2** and **Table 3-4** indicate that an increase in influent dendrimer concentration from 0.1% to 0.5% increased Pb^{2+} removal from 21% to 58% for the sandy soil, but from 24% to 47% for the clay soil. The mass transfer limitation on Pb^{2+} removal can be revealed by inspecting the profiles of the elution curves in **Figure 3-2b**. While the Pb^{2+} elution curve showed a sharp peak at an influent dendrimer concentration of 0.3% dendrimer solution, the elution peak at 0.5% appeared much blunted and displayed a more extensive tailing. In contrast, the diffusion retardation was not as profound for the clay soil (**Figure 3-2a**).

To probe the extraction effectiveness for aged contaminated soils, G1.0-NH₂ was tested for a weathered sandy clay loam obtained from a local police firing range, **Figure 3-3**. This soil was contaminated with high Pb^{2+} concentration up to 1600mg/kg with an estimated aging of 17 years. About 120 BVs of a 0.3% G1.0-NH₂ solution were able to remove 36% of Pb^{2+} from the aged firing range soil at pH 5.0, while 73% were removed at pH 4.0 (**Table 3-4**).

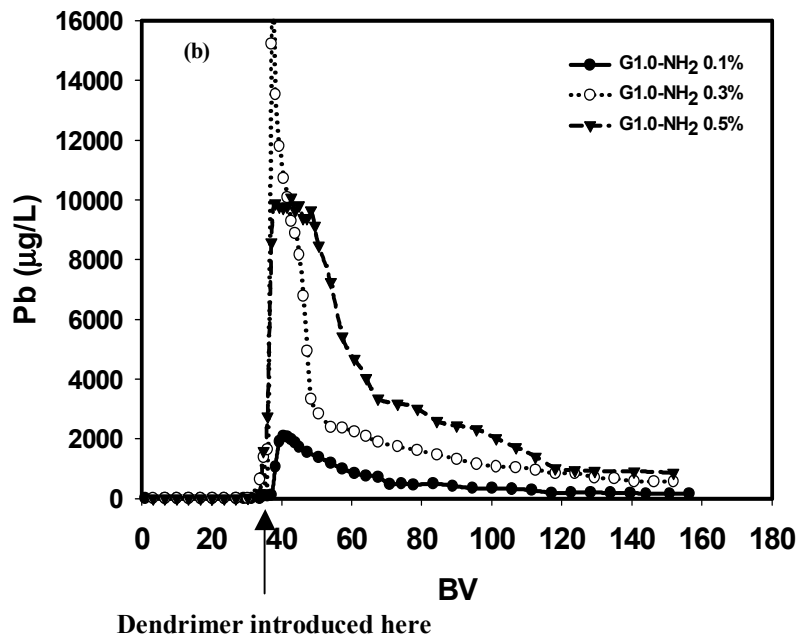
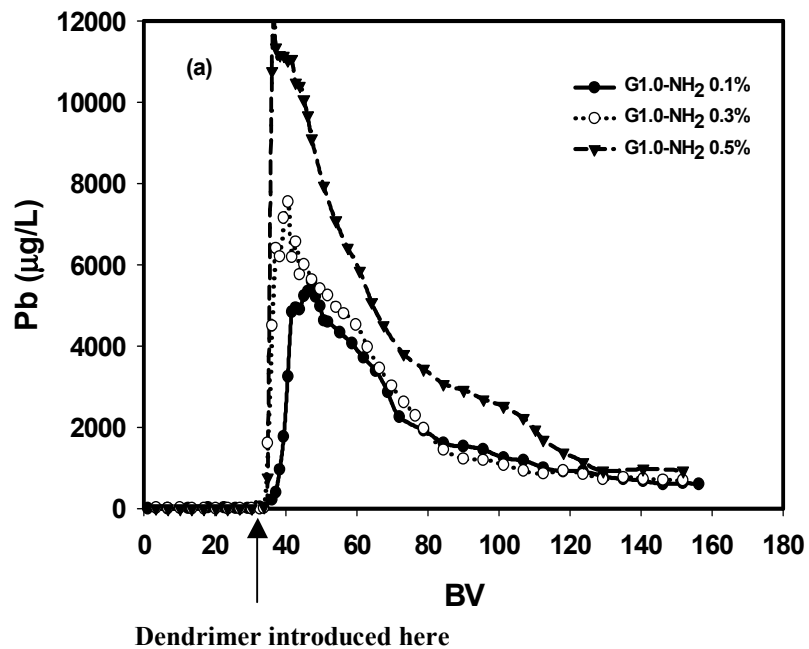


Figure 3-2. Lead elution histories during extraction using various concentrations of G1.0-NH₂ for (a) sandy clay loam #1, and (b) loamy sand soil.

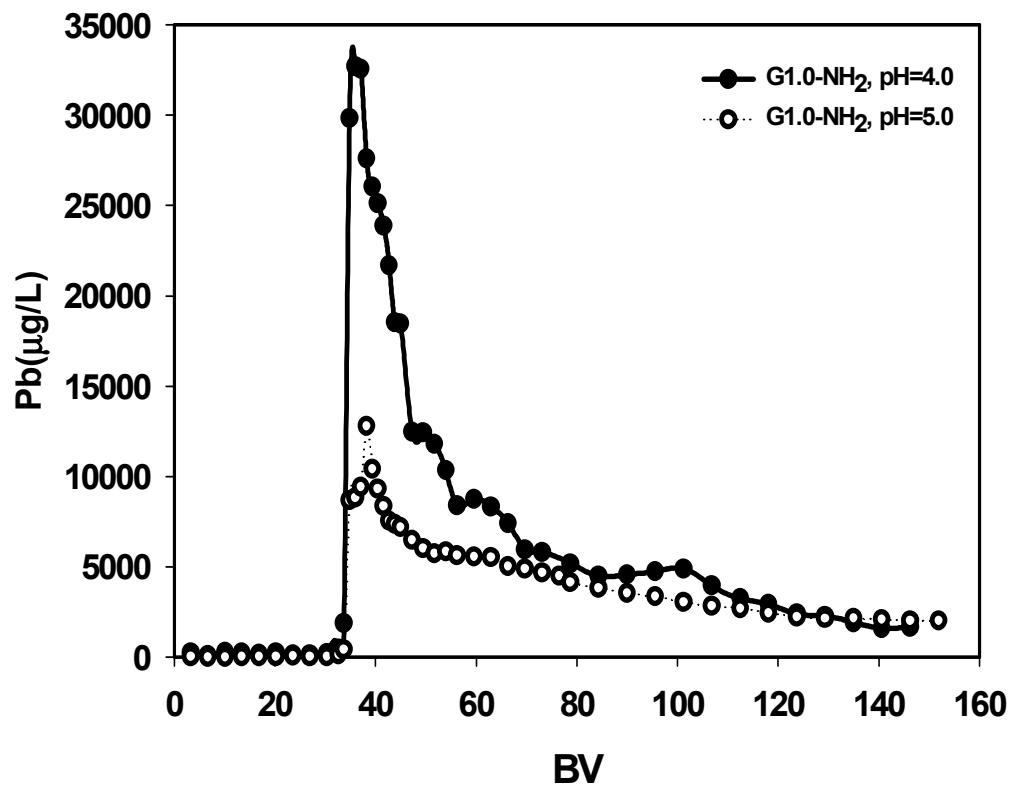


Figure 3-3. Lead elution histories from a field Pb contaminated soil (sandy clay loam #2) with 0.3% G1.0-NH₂ at pH 4.0 and 5.0.

Table 3-4. Lead Removal and Effluent pH Following Various Treatments of Three Soils.

Dendrimer	Dosage (%)	Influent pH	Soil type	Effluent pH	% Pb²⁺ removal (120 BV's)
G1.0-NH₂	0.1	5.0	Sandy	5.2	21
	0.3			5.1	48
		6.0		5.1	22
		4.5		4.5	82
	0.5	5.0		5.0	58
	0.1	5.0	Clay	5.2	24
	0.3			5.1	38
	0.5			5.3	47
	0.3		Sandy	5.1~5.2	36
		4.0	clay loam	4.1~4.2	73
G4.0-NH₂	0.1	5.0	Sandy	5.3	6.9
G1.5-COONa	0.3	5.0	Sandy	5.1	43
		4.0		4.0	92

3.3.3 Lead removal using dendrimers of different terminal functional groups

Figure 3-4 compares Pb^{2+} elution histories obtained using 0.3% of G1.0-NH₂ or G1.5-COONa at pH 5.0 for the sandy soil. As shown in **Table 3-4**, the Pb^{2+} removal for the two dendrimers, when used on the basis of equal weight, was quite comparable (48% for G1.0-NH₂ and 43% for G1.5-COONa). Note that the number of G1.0-NH₂ in the system actually doubles that of G1.5-COONa (the molecular weight of G1.0-NH₂ is about half that of G1.5-COONa, **Table 3-1**). The results in **Figure 3-4** are attributed to two factors. First, the Pb^{2+} removal by a dendrimer from soils is likely a non-equilibrium process. Therefore, the equilibrium Pb^{2+} binding capacity of the dendrimers was not fully utilized in the column desorption process due to kinetic limitations. Second, in the soil-water system, Pb^{2+} removal from soils is predominantly a “go-and-get” process, i.e. the mass transfer of dendrimer molecules plays a controlling role in the Pb^{2+} extraction efficiency. Since the G1.5-COONa is physically bulkier, its removal efficiency is diminished by its poorer mass transfer rate and accessibility of its interior binding sites. This kinetic disadvantage of G1.5-COONa is evident through the blunt peak and more profound tailing of the Pb^{2+} elution curve as shown in **Figure 3-4**.

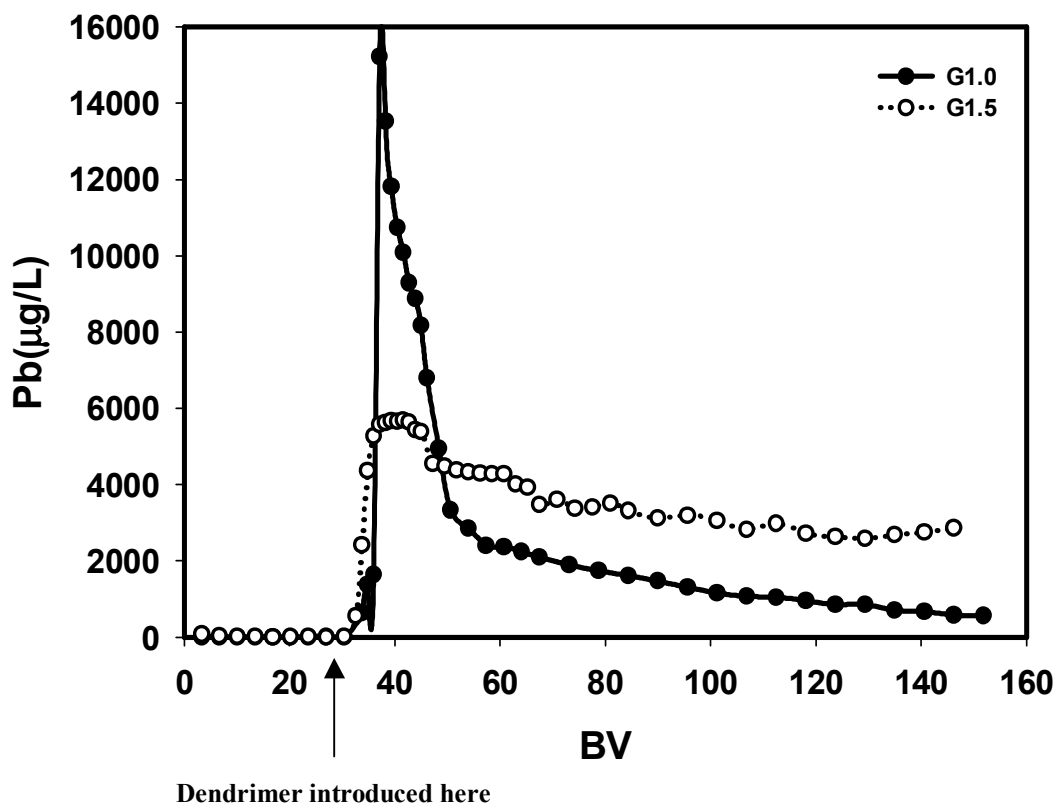


Figure 3-4. Elution histories of lead from a loamy sand soil with G1.0-NH₂ or G1.5-COONa at an influent dendrimer concentration of 0.3% and pH 5.0.

3.3.4 Effect of dendrimer generation

Figure 3-5 shows Pb^{2+} removal by G1.0-NH₂ and G4.0-NH₂ at the same concentration of 0.1% and at pH 5.0. **Table 3-4** indicates that G1.0-NH₂ removed 14% more lead than G4.0-NH₂ at the equal weight-based concentration (G1.0-NH₂ removed 21% and G4.0-NH₂ removed 6.9%), indicating that smaller dendrimer molecules are likely more powerful for Pb^{2+} removal.

For each generation increment, the hydrodynamic diameter of a dendrimer molecule increases by about 10Å (Tomalia et al. 1990), and the total number of Pb^{2+} -binding sites (interior N-donor atoms + terminal functional groups) doubles. While higher generation dendrimers possess greater binding capacity, lower generation dendrimers offer better mass transfer rates and easier accessibility to their binding sites. The size of a G1.0-NH₂ molecule is about half that of a G4.0-NH₂ molecule (**Table 3-1**), which grants the smaller dendrimer particles greater mobility and more chances to collide and interact with the sorbed Pb^{2+} ions. In addition, on the basis of equal weight, the number of G1.0-NH₂ molecules is about 10 times more than that for G4.0-NH₂ (**Table 3-1**). Furthermore, molecular simulation of the dendrimer morphology (Ottaviani et al. 1994) has indicated that the molecular structure for dendrimers of lower generations (<3) is physically more flexible than for those of higher generations. This feature provides Pb^{2+} with easier access into the interior binding sites in the dendrimer of lower generations. As generation number goes up (≥ 3), the exterior globular surface becomes more rigid, resulting in much reduced accessibility of the interior binding sites.

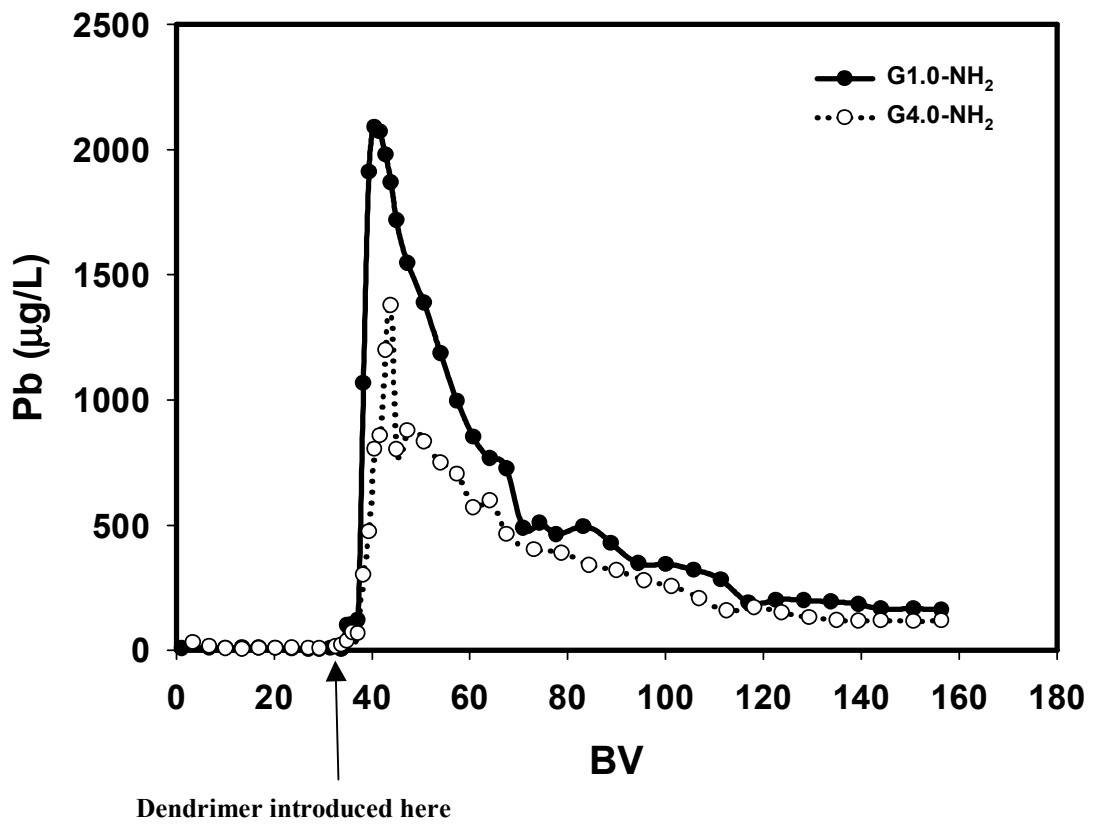


Figure 3-5. Elution histories of lead from a loamy sand soil using 0.1% G1.0-NH₂ and G4.0-NH₂ at pH 5.0.

3.3.5 Effect of pH

Results in **Table 3-4** indicate that the Pb^{2+} extraction effectiveness is strongly pH-dependent. For instance, at a dendrimer (G1.0-NH₂) concentration of 0.3%, a change in influent pH from 6.0 to 4.5 resulted in a 60% increase in Pb^{2+} removal from the sandy soil. When G1.5-COONa was used, a decrease in solution pH from 5.0 to 4.0 increased the Pb^{2+} removal from 43% to 92% (**Figure 3-6**). Apparently, lowering solution pH will increase the Pb^{2+} removal from the soils. **Table 3-4** also shows that pH in the effluent solution is either the same as or slightly (<0.3 pH unit) higher than in the influent.

The solution pH can affect both the availability of Pb^{2+} in a soil and the protonation characteristics of a dendrimer. **Figure 3-7** plots the uptake of Pb^{2+} by the two soils as a function of equilibrium solution pH. The sorption edge curves underwent a sharp change (from zero to maximum) within a narrow pH range of ~3 to ~5 for both soils. It is evident from **Figure 3-7** that when pH is lowered from 5.0 to 4.0, the Pb^{2+} sorption capacity would be reduced by nearly 50% for both soils, suggesting that Pb^{2+} removal is thermodynamically more favored at a lower pH. However, the fact that DI water alone at pH 4.0 could not desorb any appreciable Pb^{2+} (<0.08% in ~30 BVs) indicated that desorption is hindered by a greater activation energy barrier, which is also in accord with the observed sorption hysteresis effect (**Figure 3-1**).

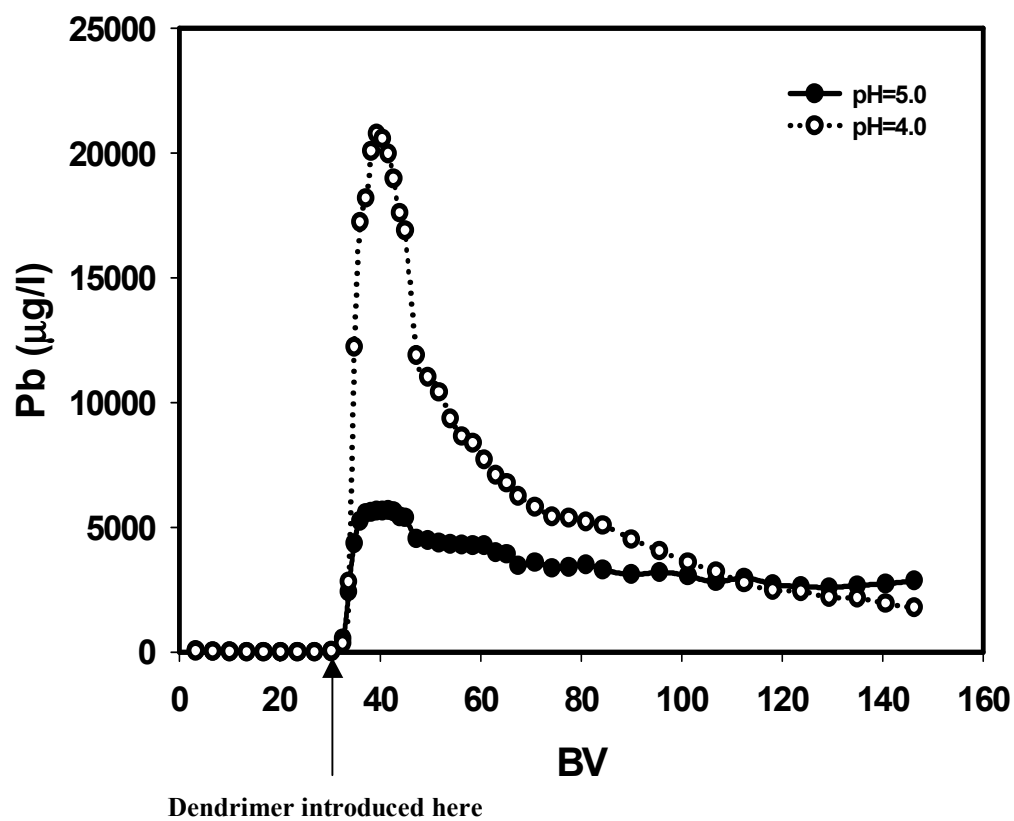


Figure 3-6. Elution histories of lead from a loamy sand soil with 0.3% of G1.5-COONa at pH 4.0 or 5.0.

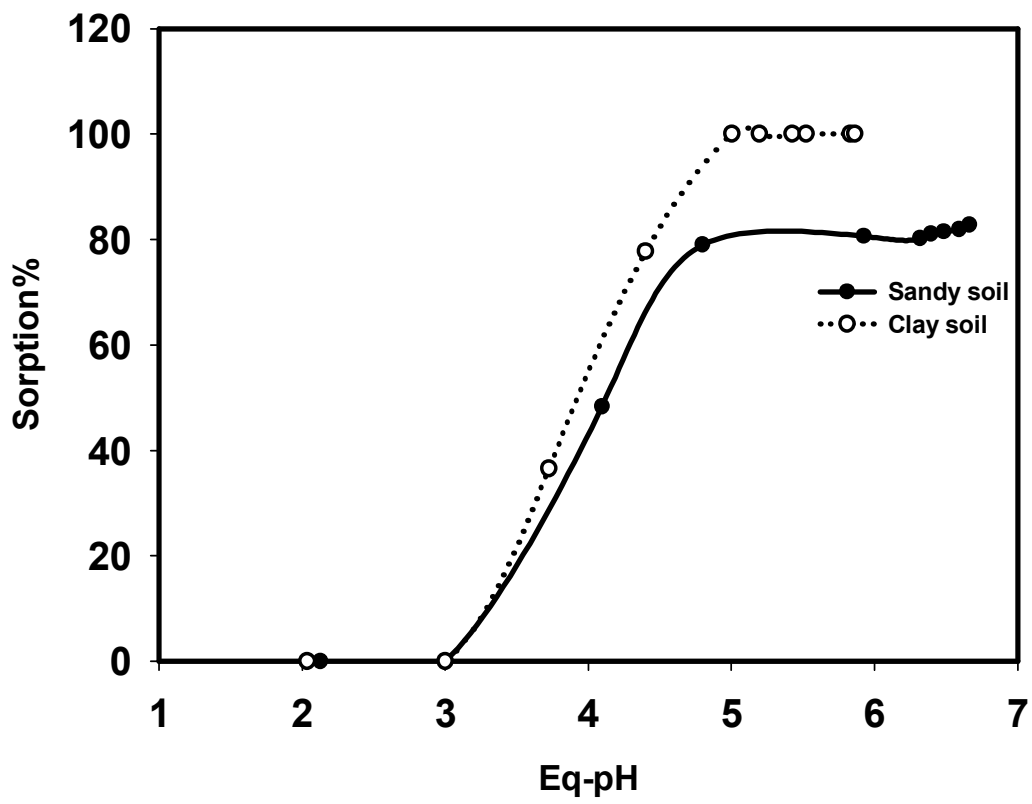


Figure 3-7. Lead sorption edges for the sandy and clay soils.

Protonation of dendrimers has attracted a great deal of research interest (Cakara et al. 2003; Diallo et al. 2004; Leinser and Imae 2003; Niu et al. 2003; Ottaviani et al. 1996; Tomalia et al. 1990). For G3.0 and G5.0 ethylenediamine core PAMAM dendrimers, pK_a values for the terminal primary amines have been reported to be in the range of 9.90-10.77 (Diallo et al. 2004). It is also believed that for ethylenediamine core PAMAM dendrimers, pK_a values for the terminal primary amines are much greater (~ 3 pH units) than those of interior amines, and the lowest pK_a value for a given dendrimer is found in the core or near-core micro-environment (Leinser and Imae 2003; Ottaviani et al. 1996). The reported pK_a values for interior tertiary amines are in the range of 3.4~7.6 for G3-NH₂ and G5-NH₂ dendrimers (Ottaviani et al. 1996). Cakara et al. (Cakara et al. 2003) observed through macroscopic titrations that at pH 3~5, all amine groups of G1.0-NH₂ were protonated except one of the central tertiary amine group. Based on EPR study of Cu(II) binding by G3.0-NH₂, G5.0-NH₂, and G7.0-NH₂, Ottaviani et al. (Ottaviani et al. 1997) reported that at pH = 4~5, the interior tertiary amine groups of these dendrimers were almost fully deprotonated and the exterior amine groups can interact with Cu(II) at pH>3.5. For G1.5-COO⁻, Ottaviani and co-workers (Ottaviani et al. 1994; Ottaviani et al. 1996; Ottaviani et al. 1997) reported that the surface carboxylate groups are available for the complexation with both Cu²⁺ and Mn²⁺ over a wide pH range (pH= 3~ 10). Evidently, at pH above 4.0, the functional groups in both G1.0-NH₂ and G1.5-COO⁻ remain largely dissociated and available for taking up Pb²⁺ ions from the soils. The increased thermodynamic driving force combined with the largely available binding capacity of the dendrimers resulted in the enhanced Pb²⁺ removal at pH 4.0.

3.3.6 Impact of dendrimer treatment on Pb²⁺ speciation and leachability

The toxicity and bioavailability of Pb²⁺ in soils is often governed by its solid-phase speciation and interactions with various soil components. **Figure 3-8** compares the operationally defined Pb²⁺ speciation profiles in the loamy sand soil before and after the treatment by ~120 BVs of 0.5% G1.0-NH₂ dendrimer at pH 5.0. The total lead in the original soil was 590 mg/kg, which was predominantly (98%) bound to carbonates (76%), SOM (12%), and ERO (9.7%). After the dendrimer treatment, ~60% (or 354 mg/kg) of lead was removed, i.e. the lead concentration was reduced to 236 mg/kg.

Individually, the dendrimer treatment reduced carbonate-bound Pb²⁺ from 448 to 156 mg/kg (a reduction of 65%), SOM-bound Pb²⁺ from 71 to 38 mg/kg (a reduction of 46%), and Pb²⁺ in ERO from 57 to 35 mg/kg (a reduction of 39%). Of all the forms of Pb²⁺ removed, the CARB fraction accounted for over 82%, the SOM form for 9%, and the ERO form for 6%. The most stable form of Pb²⁺ (i.e. the residual lead) was also reduced from 5.3 to 3.1 mg/kg, but accounted for only 0.62% of the total removal. According to the leaching procedure, the relative availability of the various forms of Pb²⁺ follows the sequence,

EXC > CARB > ERO > SOM > AmoFe > CryFe > RES.

The slightly higher removal of the SOM lead over ERO lead suggests that the former is likely kinetically more favored over the latter.

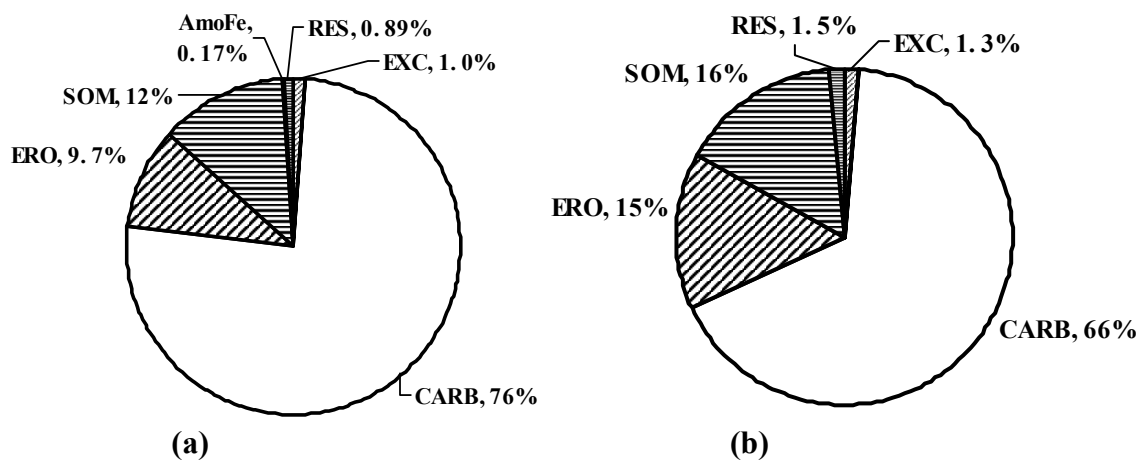


Figure 3-8. Operationally defined speciation of Pb^{2+} in: **(a)** untreated soil, and **(b)** dendrimer treated soil. All data are given as mean of duplicates. (Acronyms: EXC, Exchangeable lead; CARB, Carbonate-bound lead; ERO, Pb^{2+} to easily reducible oxides; SOM, Pb^{2+} to soil organic matter; AmoFe, Pb^{2+} to amorphous iron oxides; and RES, residual Pb^{2+}).

To further showcase the difference in physico-chemical availabilities of Pb^{2+} in soils before and after the dendrimer treatment, Pb^{2+} leachability tests were carried out following the standard Toxicity Characteristic Leaching Procedure (TCLP) (Cao et al. 2004; Lim et al. 2004a; Wu et al. 2004). The TCLP results indicated that the leachable lead was 12.5 mg/L for the untreated sandy soil and 13.2 mg/L for the untreated clay soil, which represented, respectively, 42.4% and 27.3% of the total Pb^{2+} pre-sorbed in the soils. Note that the Pb^{2+} concentration in both leachate exceeded the EPA limit concentration of 5.0 mg/L (<http://www.iwrc.org/summaries/TCLP.cfm>)(TCLP). After treated with ~120 BVs of 0.5% G1.0-NH₂ at pH 5.0, the leachable lead was reduced to 3.50 mg/L for the sandy soil and 4.80 mg/L for the clay soil, which corresponded to 28.4% and 18.8% of the initial mass, indicating that the residual lead in the treated soils is less leachable and safer.

3.3.7 Dendrimer retention by soil and recovery of spent dendrimers

Dendrimers are functionalized nanoscale molecules; therefore, they may interact with surface functional groups of various soil compositions, especially positively charged entities. Such interactions may result in retention of dendrimers in the soil bed and may undermine the viability of the metal extraction process. To examine the possible loss of the dendrimers during the course of extraction, dendrimer breakthrough curves were measured when 120 BVs of G1.0-NH₂ (0.1%) were passed through the loamy sand and sandy clay loam #1 bed, respectively. **Figure 3-9** shows that the dendrimer breakthrough for both soils took place almost immediately (after 1 BV) after the dendrimer solution was introduced into the soil bed. The full breakthrough was observed in ~3 BVs for the

loamy sand and in ~5 BVs for the sandy clay loam, i.e. the soil retention of dendrimers occurred in the few initial BVs. Considering a 120 BVs dendrimer dose and upon deduction of TOC from the methanol in the dendrimer stock solution, the dendrimer retention was determined to be less than 1% for the loamy sand and 1.8% for the sandy clay loam, indicating that the dendrimer is highly mobile in these soils. When the dendrimer-laden beds were subsequently rinsed *in-situ* with 5 BVs of DI water, ~96% of the dendrimer retained in the loamy sand and 84% in the sandy clay loam were rinsed off the soils, which suggest that the retention of dendrimers was highly reversible. The minimal soil retention of dendrimers offers the opportunity to recover the spent dendrimers and desorbed lead from the effluent.

Compared to other metal extracting agents such as EDTA or NTA, dendrimers offer some important advantages. First, spent dendrimers and dendrimer-associated metals can be recovered more easily owing to the much larger and well-defined molecular structure of dendrimers (Diallo et al. 2005); and second, the recovered dendrimers can be easily regenerated and reused. Recovery of G1.0-NH₂ and G4.0-NH₂ was tested in four consecutive nanofiltration runs. **Table 3-5** gives the recovery of the two dendrimers and Pb²⁺ in the spent dendrimer solution following each nano-filtration run. After the first nano-filtration run, ~94% of G1.0-NH₂ and ~95% of G4.0-NH₂ in the spent dendrimer solutions were retained. After four consecutive runs, the recovery was slightly increased to ~97 for both dendrimers (Note: because the MWCO of the membrane filter was less than the molecular weight for either of the dendrimers, the recovery for the two dendrimers was about the same despite the nearly one order of magnitude difference in their molecular weight). Upon acid regeneration, ~2% of the

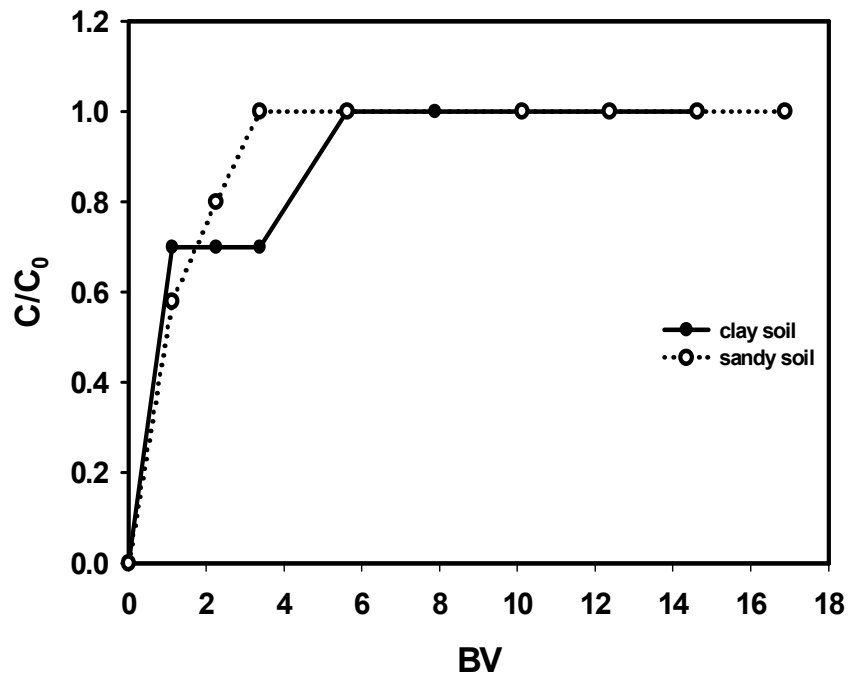


Figure 3-9. Dendrimer breakthrough curves in the loamy sand and sandy clay loam #1.

Table 3-5. Recovery of Spent Dendrimers and Pb²⁺ in the Spent Dendrimer Eluent.

Nanofiltration Run #	Dendrimer retained (%) (mean ± standard error)		Pb²⁺ retained (%) (mean ± standard error)	
	G1.0-NH ₂	G4.0-NH ₂	G1.0-NH ₂	G4.0-NH ₂
1	94.0±0.3	94.9±0.1	96.8± 0.6	95.8±0.8
2	95.6± 0.1	95.3±0.1	97.1±0.3	96.2±0.4
3	96.7± 0.5	95.9±0.4	97.5± 0.5	96.6±1.7
4	97.1± 0.5	97.4±0.6	97.5±0	97.0±0.4
After Acid Regeneration	95.1± 0.3	94.7±0.0	6.0±0.3	5.5±0.4

retained dendrimers leached through the filter, resulting in a net overall recovery of ~95% for both dendrimers. In addition, mass balances on Pb^{2+} in the spent dendrimer solution were measured. After the first run, ~96% of Pb^{2+} was retained for both cases; subsequent filtration runs added only 1% recovery. Upon the acid regeneration, ~94% of Pb^{2+} retained was leached through the filter for both dendrimers. The highly efficient regeneration copper-laden dendrimers with dilute acids was also reported by others (Rether and Schuster 2003). The regenerated dendrimers can then be reused for more metal extraction run.

3.4 Summary and Conclusions

Removal of lead from soils has been one of the most challenging environmental issues. This chapter aimed to test the technical feasibility of using selected dendrimers as a new class of recoverable and reusable extractants for removal and recovery of Pb^{2+} from various soils. The major findings from this chapter are summarized as follows:

1. Dendrimers with terminal groups of either primary amines or carboxylate can effectively remove Pb^{2+} from various soils, including a sandy soil, a clay soil, and an aged lead-contaminated field sandy clay loam. Up to 92% removal of lead was achieved using ~120 BVs of three dendrimers under various conditions (pH, dendrimer concentration).
2. Under the stated experimental conditions, dendrimers with different terminal groups offered comparable effectiveness for Pb^{2+} removal. This observation supports the notion that the interior tertiary amines of the dendrimers played an important role in

binding with Pb^{2+} , which is in accord with the reported assertion that the pK_a values for interior tertiary amines are much lower than for the terminal groups.

3. Dendrimers of lower generation removed more Pb^{2+} than those of higher generation on an equal weight basis.
4. In the tested pH range (4.0-6.0), lowering pH resulted in much greater Pb^{2+} removal in all cases.
5. Results from a sequential extraction procedure indicate that dendrimer treatment removed primarily (>82%) carbonate-bound Pb^{2+} ; and TCLP tests reveal that Pb^{2+} remaining in dendrimer-treated soils was much less leachable and the treated soils could pass the EPA's total extractable metal limit for Pb^{2+} .
6. Retention of dendrimers by either the sandy soil or the clay soil was minimal (<1.8% on a basis of 120 BVs of dendrimer solution applied). Over 96% (for the sandy soil) and 84% (for the clay soil) of the soil-retained dendrimers can be rinsed off the soil beds using less than 5 BVs of DI water.
7. More than 94% of the spent G1.0-NH₂ and G4.0-NH₂ dendrimers can be recovered in just one nanofiltration run, which also retained ~96% of Pb^{2+} in the spent dendrimer solution for both cases. The spent dendrimers can be regenerated efficiently using 2N HCl, and ~94% of the dendrimer bound Pb^{2+} was desorbed from the dendrimers upon the acid regeneration.

The results from this chapter revealed the promise of using some of the latest nanoscale reactive materials for environmental remediation. The dendrimers may serve as a recoverable extracting agent in lieu of currently used chelating agents for removal of Pb^{2+} from contaminated soils either *in-situ* or *ex-situ*.

CHAPTER 4. A REVISED ION EXCHANGE METHOD FOR ESTIMATION OF CONDITIONAL STABILITY CONSTANTS OF METAL-DENDRIMER COMPLEXES

In the previous two chapters, it has been demonstrated that PAMAM dendrimers were effective in removal of copper and lead from contaminated soils. To quantify metal binding affinity of various dendrimers, this study developed a simple and reproducible approach by modifying the classical Schubert ion exchange method for determination of the conditional stability constants (K_c) and the equilibrium metal-to-ligand molar ratio (n) for poly-nuclear complexes of metals (Cu^{2+} or Pb^{2+}) with various dendrimers.

4.1 Introduction

The metal-binding ability of poly(amidoamine) or PAMAM dendrimers has attracted growing research interest in recent years. Because of their well-controlled molecular architecture and functionalities, dendrimers can be used as a multifunctional ligands for binding various Lewis acids such as Cu^{2+} , Ag^+ , Mn^{2+} , and Fe^{3+} (Diallo et al. 1999; Diallo et al. 2004; Ottaviani et al. 1994; Ottaviani et al. 1996; Ottaviani et al. 1997; Zhou et al. 2001). Dendrimers have been found effective for removing Cu^{2+} from water (Diallo et al. 1999; Diallo et al. 2005). Our research has shown that selected low generations of PAMAM dendrimers were also found effective for extracting Cu(II) and

Pb(II) ions from contaminated soils. Dendrimers have also been used as stabilizers for preparing metal nanoparticles such as Pt and Cu (Zhao and Crooks 1999a; Zhao et al. 1998) .

However, there have been very few studies reported on the determination of the metal-dendrimer stability constants because, at least partially, of the size-dependent chemistry and rather different metal-chelating characteristics of dendrimers from classic ligands. To quantify the equilibrium distribution of Cu(II) between water and various PAMAM dendrimers, Diallo et al. (Diallo et al. 1999; Diallo et al. 2004) defined an equilibrium parameter known as “extent of binding” (EOB), which gives the number of moles of Cu(II) bound per mole of dendrimer, i.e. the equilibrium binding capacity of dendrimers. Later, Diallo et al. (Diallo et al. 2004; Diallo et al. 2005) postulated a two-site model, which claimed that the overall metal uptake by dendrimers was attributed to the binding to the amine groups and water molecules trapped in dendrimers. Based on the model, they defined a metal-dendrimer intrinsic association constant, which was further translated into the so-called binding constant to quantify the relative binding affinity. However, the model has not been validated through atomistic simulations (Diallo et al. 2004), and the different metal binding affinity between interior and outer shell sites was not considered (Sun and Crooks 2002).

In a recent theoretical study, Sun and Crooks (Sun and Crooks 2002) employed a statistical approach and a shell model to interpret the equilibrium binding of protons and metal ions to dendrimers. They concluded that metal binding to the inner shell of a dendrimer molecule was weaker than that to an outer shell. They also pointed out that the classical potentiometric pH titration method might not be proper for determining the

stability constant because of the large number of possible stability constants for metal-dendrimer complexes. However, Krot et al. (Krot et al. 2005) used the potentiometric pH titration method combined with a modeling package (HYPERQUAD 2000) to estimate the stability constant of copper and a generation zero PAMAM dendrimer with $-NH_2$ terminal functional groups. They identified five types of complexes with stability constants ranging from $10^{3.89}$ to $10^{42.30}$.

Although our knowledge on the local chemistry of dendrimers and its impact on the metal binding equilibrium is rather rudimentary, methods developed for estimating the stability constants of complexes between metal ions and other macromolecular ligands such as humic acids or fulvic acids may prove practical in facilitating a simple and sound estimation of the metal-dendrimer equilibrium constants. For instance, the equilibrium ion exchange (IX) method (also known as the Schubert method) (Lenhart et al. 2000; Martell and Calvin 1952; Pandey et al. 2000; Schnitzer and Skinner 1966; Schubert 1948; Schubert 1956; Schubert and Lindenbaum 1950; Schubert and Richter 1948; Schubert et al. 1950) has been used to estimate the conditional stability constants of mononuclear complexes (i.e. one metal ion complexes with one or more ligands) between a metal and fulvic acids, humic acids, citric, and tricarballic acid (Ochoa-Loza et al. 2001). More recently, it was also used to determine the stability constant of metal-biosurfactant complexes (Lenhart et al. 2000; Luster et al. 1994). In essence, this method employs a system consisting of a cation exchange resin and a solution containing the metal and the ligand of interest. Because the sorption equilibrium of a metal to an IX resin can be easily determined and interpreted using a common isotherm model (e.g. the linear sorption model), the presence of the resin in the metal-ligand solution can facilitate

the interpretation of the metal-ligand complexation, leading to a semi-empirical estimate of the metal-ligand stability constants. The IX method offers a rather straightforward and reproducible operational approach for estimating the “conditional stability constant” of complexes between metal and macromolecular ligands whose local chemistry and molecular structure are often poorly understood.

However, this approach bears with two limitations. First, it assumes that the sorption isotherm of the metal ions to the resin is linear or quasi-linear over a range of aqueous-phase concentration (Clark and Turner 1969; Schnitzer and Hansen 1970) which may not be the case for most ion exchange resins; Second, the method assumes that the metal-ligand complexes are mononuclear (Luster et al. 1994), which again may not hold for macromolecular, multi-dentate ligands such as dendrimers (Diallo et al. 2004; Diallo et al. 2005) (or even for humic or fulvic acids). To relax the first constraint, Luster *et al.* (Luster et al. 1994) introduced a revised procedure, which allowed the adsorption isotherms to be non-linear. However, the revised approach invoked a new restriction of a 1:1 metal-to-ligand complexation essentially confines the approach to only small ligands with a limited number of electron donors (Lewis base), i.e. the approach is not applicable to poly-dentate ligands with a large number of metal ion binding sites such as proteins and dendrimers (Diallo et al. 2005).

In addition, the selection of an appropriate resin has not been well addressed or even neglected. To ensure the proper use of the method, the ion exchange resin must satisfy some key criteria, including 1) the resin must not adsorb any significant amounts of the ligands, and 2) the resin-adsorbed metal ions should not take up any appreciable amounts of the ligands (i.e. no ternary complexes are formed at the resin surface). In the

past, strong-acid cation exchange resins with styrene-divinylbenzene (DVB) matrix and sulfonic functional groups such as Dowex 50WX8 have been typically employed (Kantar et al. 2005; Luster et al. 1994). However, the possible uptake of ligands involved and the impacts on the measurements were not adequately addressed despite the known strong interactions between the styrene-DVB matrix and various organic ligands.

The overall goal of this chapter is to revise the classic IX-based method for estimating the conditional stability constant of metal-dendrimer complexes that involve binding of multiple metal ions to one dendrimer molecule (i.e. multinuclear complexes). The specific objectives are to: 1) reformulate the equilibrium and mass balance equations for interpreting the ion exchange equilibrium and the metal-dendrimer complexation; 2) determine the most suitable IX resin for the desired uses; and 3) determine the metal-dendrimer conditional stability constant for Cu(II) and Pb(II) complexed with select dendrimers using the modified method. Compared to the classical IX method, the modified approach offers two distinguished features: first, it uses the Langmuir isotherm model to interpret the sorption isotherms of metal ions to the resin, thereby accommodating both linear and non-linear isotherms; and second, it is suitable for multinuclear complexes.

4.2 Materials and Methods

Dendrimers including G0.0-NH₂, G1.0-NH₂, G2.0-NH₂, G3.0-NH₂, G4.0-NH₂, and G1.5-COONa (*G_n* refers to the generation number and -NH₂ or -COONa indicate the type of terminal functional group) were purchased from Dendritech Inc. (Midland, MI, USA). The salient properties of these dendrimers are listed in **Table 4-1**.

Table 4-1. Salient Properties of Dendrimers Used in the Lead Removal Study.

Dendrimer	Core type	Molecular Weight	Measured Hydrodynamic Diameter	Number of interior tertiary amines	Number of Terminal Groups	pKa	
						Interior N	Terminal Groups
G0.0-NH ₂	ethylene diamine	517 ^a	15 ^a	2 ^a	4 ^a	(2.27-6.64) ^b	(8.35-9.78) ^b
G1.0-NH ₂	ethylene diamine	1430 ^a	22 ^a	6 ^a	8 ^a	(3.55~6.70) ^c 3.86 ^d	6.85 ^d , 9.00 ^c
G2.0-NH ₂	ethylene diamine	3256 ^a	29 ^a	14 ^a	16 ^a	Not available	Not Available
G3.0-NH ₂	ethylene diamine	6909 ^a	36 ^a	30 ^a	32 ^a	(5.3~7.6) ^e 6.52 ^f	(9.0~11.5) ^e 9.90 ^f
G4.0-NH ₂	ethylene diamine	14215 ^a	45 ^a	62 ^a	64 ^a	6.65 ^g , 6.85 ^f	9.2 ^g , 10.29 ^f
G1.5-COONa	ethylene diamine	2935 ^a	28 ^h	14 ^a	16 ^a	Not available	Not available

^aData supplied by Dendritech, Inc (Midland, MI).

^bData taken from ref. (Krot et al. 2005)

^cData taken from ref. (Cakara et al. 2003)

^dData taken from ref. (Tomalia et al. 1990)

^eData taken from ref. (Ottaviani et al. 1996)

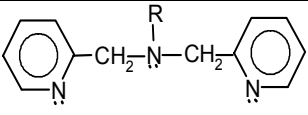
^fData taken from ref. (Diallo et al. 2004)

^gData taken from ref. (Leinser and Imae 2003)

^hData taken from ref. (Li et al. 2005)

To identify a suitable IX resin, four different classes IX resins (IRC-50, IRC-748, IR-120, and DOW-3N) were tested for their equilibrium uptake of dendrimers in the presence of Cu^{2+} or Pb^{2+} ions. The resins were purchased from Sigma-Aldrich (Milwaukee, WI, USA). **Table 4-2** gives important properties of these resins. Before uses, the resins were rinsed with DI water, and then prepared in the sodium form by conditioning with NaCl solution. Regent grade PbNO_3 and CuCl_2 were also purchased from Sigma-Aldrich.

Table 4-2. Important Properties of the Ion Exchange Resins.

Resin	IRC-50	IRC-748	IR-120	DOW-3N
Manufacturer	Rohm and Haas	Rohm and Haas	Rohm and Haas	DOW Chemical
Functional group (R: repeating polymer unit)	$\text{R}-\overset{\text{O}}{\parallel}{\text{C}}-\text{O}^{-}-\text{H}^{+}$ <p>Carboxylic acid</p>	$\begin{array}{c} \text{O} \\ \parallel \\ \text{CH}_2-\text{C}-\text{O}^{-}-\text{H}^{+} \\ \\ \text{CH}_2-\text{N} \\ \\ \text{CH}_2-\text{C}-\text{O}^{-}-\text{H}^{+} \\ \parallel \\ \text{O} \end{array}$ <p>Iminodiacetic acid</p>	$\text{R}-\overset{\text{O}}{\parallel}{\text{S}}(\text{O})-\text{O}^{-}-\text{H}^{+}$ <p>Sulfonic acid</p>	 <p>Di-picolyamine</p>
Matrix	Methacrylic, Macro-reticular	Polystyrene-DVB, Macro-reticular	Polystyrene-DVB, Gel	Polystyrene-DVB, Macro-reticular
Capacity (meq/g-dry)	3.5 ^a	4.4 ^a	5.35 ^b	3.0 ^c
BET surface area (m ² /g)	NA	NA	NA	139 ^c

^aData taken from Aldrich Catalog 2005-2006

^bData taken from ref. (Nabi et al. 2005)

^cData taken from ref. (Zhao and SenGupta 2000)

To facilitate the selection of a suitable IX resin, the extent of dendrimer uptake by the IX resins was quantified through duplicated batch sorption isotherm experiments in 40 mL glass vials with Teflon-lined caps. Two types of dendrimers with different terminal groups, G1.0-NH₂ and G1.5-COONa, were tested in the experiments. In each vial, 0.0040 g of a resin and 0.025 g or 0.050 g of a dendrimer were added to 20 mL of a solution containing 11.6 mg/L of Cu²⁺ or 15.2 mg/L of Pb²⁺. In addition, parallel experiments were also conducted in the absence of Cu²⁺ or Pb²⁺. In all tests, the solution pH was maintained at 5.0 through intermittent adjusting. The vials were shaken for 4 days to reach equilibrium. The dendrimer concentration in the solution was measured as total organic carbon (TOC), which was determined using a UV-persulfate TOC analyzer (Phoenix 8000, Teledyne Tekmar, Mason, OH, USA). Control tests were also carried out for each resin with a solution containing no dendrimer but with the same background compositions (pH and methanol) to correct the effect of methanol or any organic leachate from the resin on the TOC measurements.

For its minimal dendrimer uptake, IRC-50 was chosen as the most suitable resin for this study. Sorption isotherms of Cu²⁺ or Pb²⁺ to IRC-50 were constructed through duplicated batch sorption tests in 40 mL glass vials with Teflon-lined screw caps and in the absence of dendrimers. In each vial, ~0.0040 g of the resin was added to 20 mL solution containing an initial Cu²⁺ or Pb²⁺ concentration spanning from 1.5 mg/L to 20 mg/L. The mixture was shaken for 4 days at ~21 °C to reach equilibrium, and pH was maintained at a desired final pH (5.0 or 7.0 for Cu²⁺, and 5.0 for Pb²⁺) by intermittent pH adjusting. At equilibrium, the metal concentration in the solution phase was analyzed, and the metal uptake by the resin was determined through mass balance calculations.

Metal-dendrimer complexation equilibrium tests in the presence of the IX resin were also carried out in batch reactors to facilitate the determination of the conditional stability constants. First, glass vials with Teflon-lined caps were each filled with 20 mL of a solution containing 11.6 mg/L Cu²⁺ or 15.2 mg/L Pb²⁺. Then, each vial received 0.0040 g of the resin and, respectively, 0.025, 0.050, 0.10, 0.15, and 0.20 g of a dendrimer. The mixtures were then allowed to equilibrate under mechanical shaking for 4 days, with pH being kept at 5.0 or 7.0 for Cu²⁺ solution and 5.0 for Pb²⁺ solution through intermittent adjusting. At equilibrium, metal ions remaining in the solution, which included both free metal ions and dendrimer-complexed metal ions, were analyzed using flame atomic-absorption spectrophotometer (AAS) (Varian 220FS). Then, the metal uptake by the resin was determined by mass balance calculations.

4.3 Model Formulation

Consider that each mole of a dendrimer (D) complexes with n (≥ 1) moles of a metal (M) (Cu²⁺ or Pb²⁺). Eqn (4-1) gives the overall metal-dendrimer complexation reaction:



where n is the stoichiometric coefficient. The equilibrium conditional stability constant for the resultant complex M_nD is thus defined as

$$K_c = \frac{\{M_nD\}}{\{M\}^n \{D\}} \quad (4-2)$$

where the curve brackets indicate the activities of the metal-dendrimer complex, free metal ions, and the dendrimer (mol/L), which are approximated using the corresponding

concentrations in this study. Note that the K_c defined in eqn (4-2) does not distinguish among the different metal affinity of various binding sites in a dendrimer molecule (An et al. 2005; Groves and White 1984; Zhao and SenGupta 2000) rather, it represents an overall equilibrium binding constant.

Consider a resin-ligand-solution system consisting of a resin, a dendrimer, and metal ions, the equilibrium metal uptake (q_R , mol/g) by the resin can be determined through the mass balance equation:

$$q_R = \frac{V(C_0 - C_e)}{M} \quad (4-3)$$

where V is the solution volume (L), C_0 the initial concentration of the metal ions in the solution (mol/L), C_e the equilibrium concentration of metal ions in the solution (mol/L), and M the mass of the resin in the system (g). Since a cation exchange resin sorbs only free metal ions, q_R represents the free metal ions in the resin phase, whereas C_0 and C_e include both free and complexed metal ions in the solution phase.

On the other hand, the equilibrium distribution of the free metal ions can be described by the Langmuir isotherm model,

$$q_R = \frac{bQC_f}{1 + bC_f} \quad (4-4)$$

where Q is the Langmuir capacity of resin (mol/g); b is the Langmuir affinity coefficient (L/mol), and C_f is the equilibrium free metal concentration in the aqueous phase (mol/L). In the classical Schubert method, the equilibrium metal distribution was interpreted with a constant distribution coefficient (i.e. a linear isotherm model). In this study, Cu^{2+} and Pb^{2+} sorption isotherms for IRC-50 were constructed in the absence of dendrimers, and Q

and b were then obtained by fitting eqn (4-4) to the respective experimental isotherm data. Eqn (4-4) was then used to calculate the corresponding concentration of free metal ions (C_f) in the presence of a dendrimer. Consequently, the concentration of complexed metal ions was calculated by the difference of total metal and free metal in the solution, i.e. ($C_e - C_f$).

The conditional stability constant described by eqn (4-2) can then be rewritten as

$$K_c = \frac{\frac{1}{n}(C_e - C_f)}{(C_f)^n [D_t - \frac{1}{n}(C_e - C_f)]} \quad (4-5)$$

where D_t is the total dendrimer concentration (mol/L) in the resin-dendrimer-solution system. When the total dendrimer (D_t) added is much greater than the fraction of dendrimer that is complexed with the metal ions ($C_e - C_f$), as is the case for this study, eqn (4-5) is further reduced to

$$K_c = \frac{\frac{1}{n}(C_e - C_f)}{(C_f)^n D_t} \quad (4-6)$$

Eqn (4-6) can be conveniently linearized to yield

$$\log\left(\frac{C_e - C_f}{D_t}\right) = n \log C_f + \log(nK_c) \quad (4-7)$$

A linear regression of eqn (4-7) to the experimental data plotted as $\log\left(\frac{C_e - C_f}{D_t}\right)$ vs $\log C_f$ yields the conditional stability constant K_c and the metal-to-dendrimer molar ratio of n .

4.3 Results and Discussion

4.3.1 Resin selection

In the ion exchange method, the IX resin must not take up any significant amounts of dendrimers when the resin is mixed with a solution containing the metal ions and dendrimers. Unfortunately, this important point was not adequately addressed in the literature, and the choice of a suitable resin has not yet been systematically examined. In search for a suitable IX resin, the uptake of two dendrimers (G1.0-NH₂ and G1.5-COONa) by four representative IX resins (IRC-50, IRC-748, IR-120, and DOW-3N), respectively, was quantified in the presence or absence of Cu²⁺ or Pb²⁺. **Table 4-3** provides the percentage mass reduction of a dendrimer by each of the resins.

In all cases, the resin sorbed more dendrimers when Cu²⁺ was present in the system, which was especially true for the two chelating resins (IRC-748 and DOW 3N). When Cu²⁺ is absent in the solution, the dendrimers can only be taken up through physisorption (e.g. hole-filling and/or hydrophobic interactions) to the resin's matrix. As a result, the dendrimer uptake was low (<2.53%) in all cases. However, when Cu²⁺ is present, a fraction of Cu²⁺ ions will be sorbed to the resin's surface, and the sorbed Cu²⁺ ions then act as ligand exchange sites that further bind with ligands (dendrimers) from the solution phase (An et al. 2005; Groves and White 1984; Zhao and SenGupta 2000). Consequently, the presence of Cu²⁺ greatly enhanced the dendrimer uptake to the resin, which can potentially lead to failure of the ion exchange method. Because of the considerable dendrimer-resin interactions, chelating resins were not suitable for the purpose of interest. Of the two standard cation exchangers, IRC-50 is based on a

Table 4-3. Percentage of Dendrimer Loss from the Aqueous Phase under Various Conditions (data given as mean of duplicates \pm standard deviation).

Dendrimer	G1.0-NH ₂				G1.5-COONa	
	without Cu ²⁺	with Cu ²⁺	with Cu ²⁺	with Pb ²⁺	with Cu ²⁺	With Pb ²⁺
Initial dendrimer concentration (mg/L)	2.5	2.5	1.25	1.25	1.25	1.25
Dendrimer uptake by IRC-50 (%)	0.46 \pm 0.02	0.95 \pm 0.06	4.27 \pm 0.73	4.03 \pm 0.36	6.31 \pm 0.57	4.52 \pm 1.74
Dendrimer uptake by IR-120 (%)	2.53 \pm 0.18	3.37 \pm 1.02	12.38 \pm 1.42	NA	20.99 \pm 2.10	NA
Dendrimer uptake by IRC-748 (%)	1.98 \pm 0.12	6.06 \pm 1.56	7.18 \pm 1.50	NA	22.12 \pm 1.34	NA
Dendrimer uptake by DOW-3N (%)	0.91 \pm 0.05	6.60 \pm 0.95	10.97 \pm 1.04	NA	15.49 \pm 1.23	NA

NA: Not analyzed.

macroporous, methacrylic matrix, whereas IR-120 is on a gel-type, polystyrene polymer. As a result, IR-120 is more vulnerable to organic fouling (i.e. irreversible uptake of organics) because of its more hydrophobic and gel-type (non-porous) matrix, while IRC-50 displayed a much lower uptake of either dendrimers compared to all other resins. The dendrimer loss onto IRC-50 was also investigated in the presence of Pb^{2+} ions at an initial dendrimer concentration of 1.25 mg/L. For both dendrimers, the IRC-50 resin sorbed less amounts of dendrimers in the Pb^{2+} system than in the Cu^{2+} system. However, the percentage dendrimer uptake was dependent on the initial concentration of dendrimers, and thus, may become significant when the total dendrimer mass in the system is below 0.025 g. Therefore, it is necessary to control the resin-to-dendrimer mass ratio for a given system to ensure that the resin's dendrimer uptake is minimal. Based on **Table 4-3**, IRC-50 was chosen as the IX resin used for measuring the conditional stability constants of various metal-dendrimer complexes. In all cases, the maximum dendrimer uptake was less than 5%.

4.3.2 Metal sorption isotherms

To facilitate the measurements, sorption isotherms of Cu^{2+} and Pb^{2+} to IRC-50 were constructed. IRC-50 is a weak acid cation exchange resin, and its sorption capacity is likely pH dependent. Therefore, the Cu^{2+} or Pb^{2+} sorption isotherms should be constructed at equilibrium pH values consistent with the subsequent experiments for the stability constant measurements, i.e. pH 5.0 and 7.0, respectively, for Cu^{2+} and pH 5.0 for Pb^{2+} . **Figure 4-1** shows the experimental isotherm data (symbols) and the Langmuir model fit (lines) for (a) Cu^{2+} and (b) Pb^{2+} . Note the markedly different copper sorption

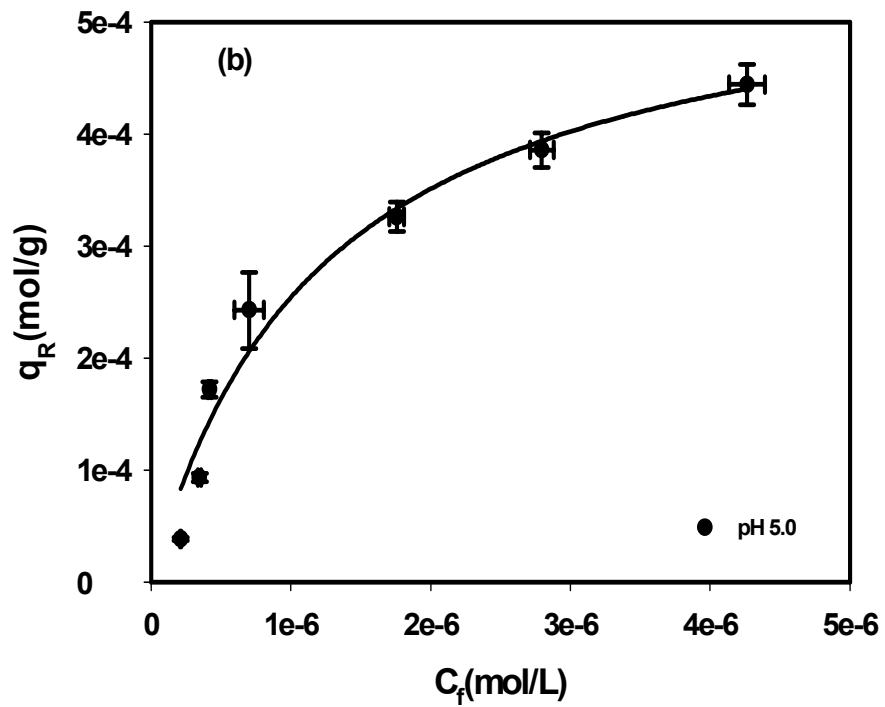
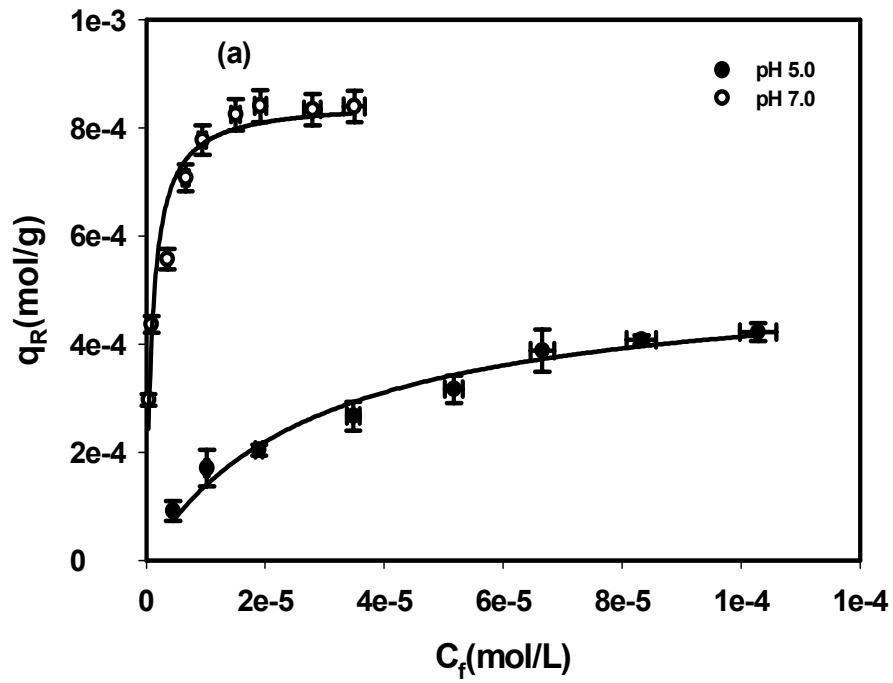


Figure 4-1. Sorption isotherms IRC-50 in the absence of dendrimer: (a) Cu^{2+} and (b) Pb^{2+} (data plotted as mean of duplicates, errors refer to standard deviations).

Table 4-4. Best-fitted Langmuir Model Parameters and R^2 values for Cu^{2+} and Pb^{2+} .

	Q_{\max} (mol/g)	b (L/mol)	R^2
Cu^{2+}, pH 5.0	5.13×10^{-4}	3.53×10^4	0.97
Cu^{2+}, pH 7.0	8.50×10^{-4}	1.02×10^6	0.94
Pb^{2+}, pH 5.0	5.68×10^{-4}	8.10×10^5	0.96

capacity of IRC-50 at pH 5.0 and pH 7.0. Table 4-4 gives the best-fitted model parameters and values of the coefficient of determination (R^2). The isotherm equations were then applied to the resin-dendrimer-solution system to calculate the free metal concentrations.

4.3.3 Complexation of Cu^{2+} with G1.0-NH₂ at pH 5.0 and 7.0

The conditional stability constant K_c and the Cu^{2+} -to-dendrimer molar ratio were determined for G1.0-NH₂ at pH 5.0 and 7.0 by fitting eqn (4-7) to the experimental equilibrium data plotted as $\log\left(\frac{C_e - C_f}{D_t}\right)$ vs $\log C_f$ (**Figure 4-2**). The linear regression gives both K_c and the copper-to-dendrimer ratio (n) of the Cu-G1.0-NH₂ complexes.

At pH 5.0, the method resulted in a K_c value of $10^{20.0}$ and an n value of 3, which suggests that each G1.0-NH₂ molecule in complexed with 3 Cu^{2+} ions. The K_c value is comparable to the reported stability constant of $10^{18.7}$ for the Cu-EDTA complexes (Martell and Smith 1974). The protonation and metal binding properties of dendrimers have been investigated extensively (Diallo et al. 2004; Ottaviani et al. 1997; Tarazona-Vasquez and Balbuena 2004; Tran et al. 2004; Zhou et al. 2001). Tomalia et al. (Tomalia et al. 1990) studied the protonation behavior of G1.0-NH₂ through acid titration and found that there existed two distinctive ionization constants, i.e. $\text{p}K_{a1} \approx 3.86$ for the interior amines and $\text{p}K_{a2} \approx 6.85$ for the terminal primary amines of G1.0-NH₂. Therefore, the terminal amine groups are not available for binding with Cu^{2+} at the experimental pH 5.0. In other words, the three copper ions are likely bound with the interior nitrogen donors and H₂O molecules trapped in the dendrimer (Diallo et al. 2004; Ottaviani et al. 1997).

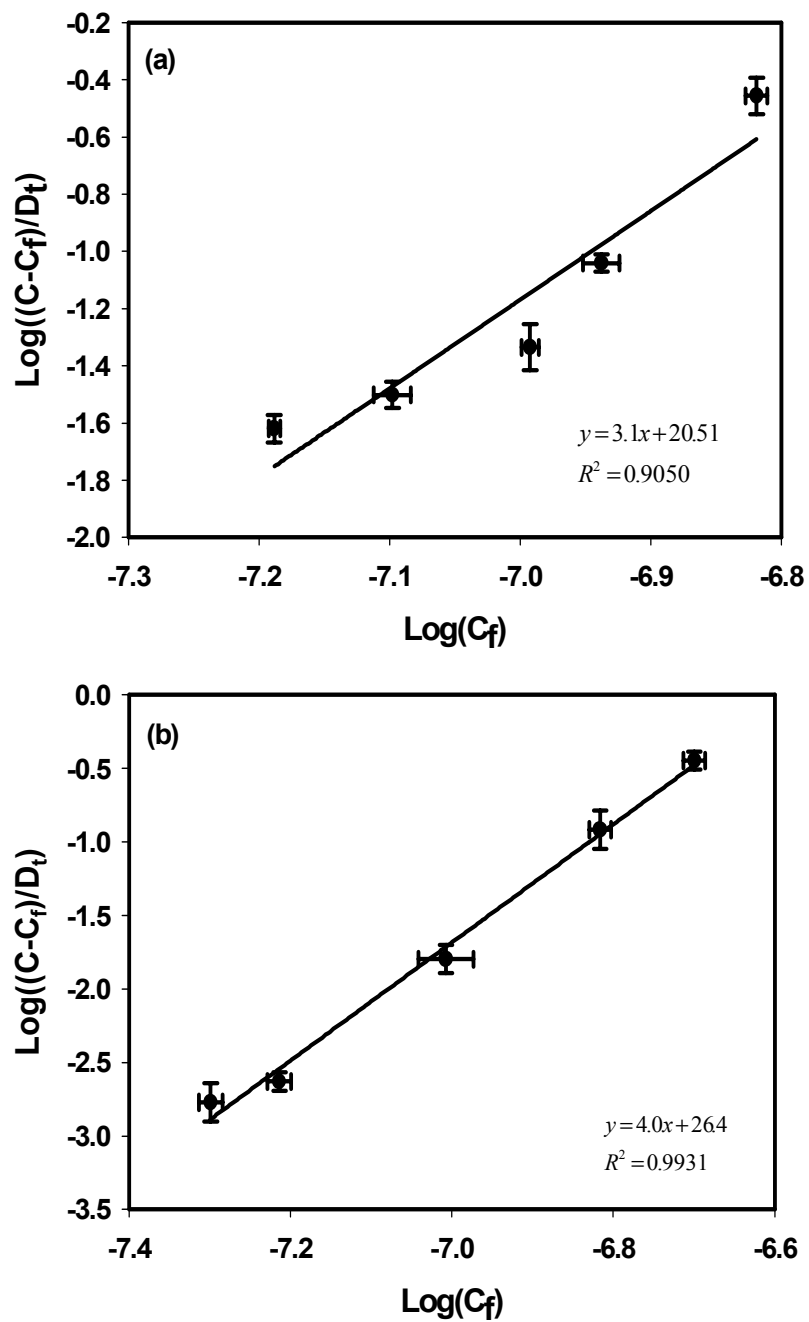


Figure 4-2. Determination of the conditional stability constant and the molar ratio of Cu^{2+} -to-dendrimer of Cu^{2+} -G1.0- NH_2 complexes: (a) pH 5.0; (b) pH 7.0.

At pH 7.0, the terminal -NH_2 groups in G1.0- NH_2 are deprotonated and become available to bind with Cu^{2+} . As a result, the Cu^{2+} -to-dendrimer ratio is increased to 4 and the conditional stability constant is raised to $10^{25.8}$. It was reported that at pH above 6.0, Cu^{2+} can bind with two terminal -NH_2 groups and two internal tertiary nitrogen donor atoms, based on a study of G3.0-, G5.0-, and G7.0- NH_2 dendrimers by EPR technique (Ottaviani et al. 1997). The fact that the conditional stability constant at pH 7.0 is 5.8 orders of magnitude greater than at pH 5.0 appears consistent with the reported assertion that the metal binding ability of the nitrogen donors follows the sequence: primary amines > tertiary amines > secondary amine (Ottaviani et al. 1997). In addition, Niu et al. (Niu et al. 2003) reported that the star-burst structure of a PAMAM dendrimer molecule tends to shrink as pH increases, which also favors a stronger binding with Cu^{2+} at an elevated pH.

4.3.4 Complexation of Cu^{2+} with dendrimers of various generations

Ottaviani et al. (Ottaviani et al. 1997) found that the nature and mode of Cu^{2+} -dendrimer complexation can differ widely as the dendrimer generation goes up. To quantify the effects of the dendrimer generation on Cu^{2+} binding, the K_c values for Cu^{2+} in complexation with five generations of a dendrimer homolog from G0.0- NH_2 to G4.0- NH_2 were determined following the modified IX-based method. **Table 4-5** lists the resultant Cu^{2+} -to-dendrimer molar ratio (n) and logarithm of the conditional stability constant, $\text{Log}(K_c)$. As the dendrimer grows from generation zero to generation four, the number of tertiary amines in one dendrimer molecule increases from 2 to 62, and the number of primary amines increases from 4 to 64 (**Table 4-1**). Accordingly, the number of Cu^{2+} ions

bound with each dendrimer molecule goes up from 1 to 12, and the K_c value rises by nearly 18 orders of magnitude.

For G0.0-NH₂, [Cu(dendrimer)H₄]⁶⁺ has been reported to be the predominant species at pH 5.0 and two tertiary nitrogen atoms are involved in binding with Cu²⁺ (Krot et al. 2005). As the generation goes up, the number of nitrogen donor atoms more than doubles per generation increment, and more importantly, the p*K_a* value of the interior tertiary amines decreases. As a result, the higher the generation number, the more tertiary amines are available for binding with Cu²⁺ at pH 5.0. For example, one G1.0-NH₂ (p*K_a* ≈ 3.86 (Tomalia et al. 1990)) is able to bind with two more Cu²⁺ ions than G0.0-NH₂ (p*K_a*= 2.77 ~ 6.64 (Krot et al. 2005)).

Ottaviani et al. (Ottaviani et al. 1997) investigated the Cu²⁺ binding properties of G3.0-NH₂ to G7.0-NH₂ at pH 4.2 to 5.3. They found that binding was predominantly facilitated in the form of Cu-N₄ (a complex with two surface NH₂ groups and two tertiary NR₃ groups). In another study, Ottaviani et al. (Ottaviani et al. 1994) reported that the mobility of the Cu²⁺ ions in the higher generation dendrimers decreased due to the more compact structure and the increase in molecular weight. These findings appear to agree with the observed increase in the conditional stability constant for higher generations of dendrimers.

Table 4-5. Conditional Stability Constant K_c and Cu^{2+} -to-Dendrimer Molar Ratio n for Complexes Cu^{2+} Bound with Various Generations of Dendrimers.

Dendrimer	n	Log(K)	R^2
G0-NH₂	1	16.2	0.9775
G1.0-NH₂	3	20.0	0.9050
G2.0-NH₂	5	25.6	0.9836
G3.0-NH₂	8	30.2	0.9797
G4.0-NH₂	11	34.1	0.8216

4.3.5 Complexation of Pb²⁺ with G1.0-NH₂ and G1.5-COONa

The Pb-dendrimer complexation is interpreted by fitting eqn (4-7) to the experimental equilibrium data in the Pb²⁺-resin-dendrimer systems plotted as

$\log\left(\frac{C_e - C_f}{D_t}\right)$ vs $\log C_f$ (**Figure 4-3**). The linear regression yields a K_c value of $10^{17.2}$

for the Pb-G1.0-NH₂ complex and $10^{21.9}$ for the Pb-G1.5-COONa complex, and a Pb-to-dendrimer ratio (n) of 3.0 for G1.0-NH₂ dendrimer and 4.0 for G1.5-COONa dendrimer.

The conditional stability constants for the Pb-dendrimer complexes appear comparable to the reported stability constant of $10^{17.88}$ for Pb-EDTA complexes (Martell and Smith 1974).

A G1.0-NH₂ dendrimer molecule has 8 terminal primary amine groups and 6 interior tertiary amines (**Table 4-1**). Both the primary and tertiary amines have been reported to be able to bind with metals such as Cu²⁺ (Ottaviani et al. 1994; Ottaviani et al. 1996; Ottaviani et al. 1997; Tran et al. 2004). However, the degree of metal binding is strongly pH-dependent because of the weakly-basic nature of the amine groups (Ottaviani et al. 1997). At the experimental pH of 5.0 in our study, the terminal primary amines would be fully protonated and are not available for binding Pb²⁺. Therefore, the above conditional stability constant reflects the binding of Pb²⁺ with the interior nitrogen donor atoms.

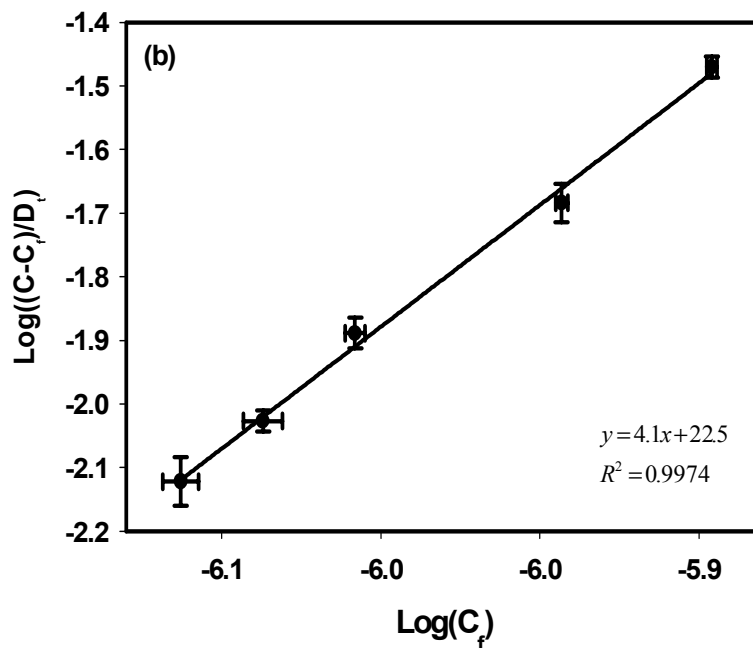
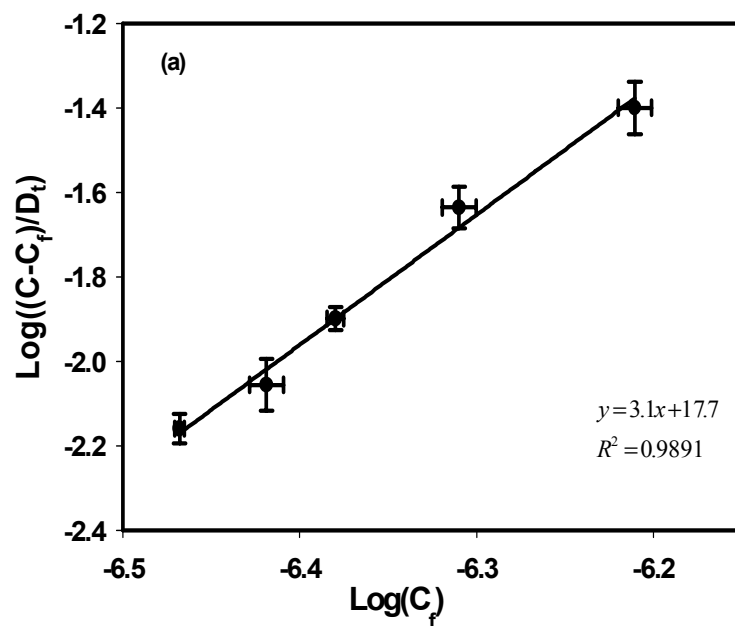


Figure 4-3. Determination of the conditional stability constant and the Pb^{2+} -to-dendrimer molar ratio of Pb^{2+} -dendrimer complexes: (a). Pb-G1.0-NH_2 , and (b). Pb-G1.5-COONa (data plotted as mean of duplicates, errors indicate standard deviation).

A G1.5-COO⁻ molecule shares a similar interior structure with G1.0-NH₂. However, G1.5-COO⁻ possesses 16 terminal COO⁻ groups and 14 interior tertiary amines. Although no pK_a values for G1.5-COO⁻ have been reported, metal binding with G3.5-COO⁻, G5.5-COO⁻, and G7.5-COO⁻ has been studied by Ottaviani et al. (Ottaviani et al. 1994; Ottaviani et al. 1996; Ottaviani et al. 1997) , who reported that both the interior amines and surface carboxylate groups in these half-generation dendrimers are likely to complex with Cu²⁺ over a wide pH range (pH= 3~10). The pK_a value for the terminal groups of an analogue dendrimer, G3.5-COO⁻, was reported to be 3.79 (Manriquez et al. 2003); and that for G5.5-COO⁻ was reported in the range of 1.5~3.9 (Ottaviani et al. 1996). It is also known that for homologous dendrimers the pK_a values decrease with increasing generation number; and for a given dendrimer the pK_a values of the inner-shell amines are lower than those of outer-shell amines (Ottaviani et al. 1996). Ottaviani et al. (Ottaviani et al. 1997) has also pointed out that at pH 5.0, copper ions can form stable complexes with the terminal carboxylate groups. Based on these observations, it is plausible that both the terminal carboxylate groups and the interior N donor atoms of G1.5-COO⁻ may have been involved in binding with Pb²⁺. Because of the synergistic interactions, G1.5-COO⁻ was able to bind with one more Pb²⁺ per molecule and offered a stability constant three orders of magnitude greater compared to G1.0-NH₂.

The above results show that the binding capacity of G1.0-NH₂ for Cu²⁺ and Pb²⁺ are the same at pH 5.0. However, the conditional stability constant of the Cu²⁺ complex with G1.0-NH₂ is nearly three orders of magnitude greater than that for Pb²⁺, indicating that copper forms much stronger complexes with the dendrimer than lead. At pH 5.0, Lewis acid-base interaction between Cu²⁺/Pb²⁺ and the interior nitrogen is the primary

mechanism. Our observation appears consistent with the notion that Cu^{2+} is a stronger Lewis acid than Pb^{2+} .

4.4 Summary and Conclusions

An ion exchange procedure was developed by modifying the classical IX-based approach for measuring the conditional stability constant of metal-dendrimer complexes and the metal binding capacity of various PAMAM dendrimers. The method provides a simple and reproducible approach to quantify the metal-binding affinity and capacity of poly-dentate ligands such as dendrimers. The revised method extends the traditional Shubert method for mononuclear metal-ligand complexes to polynuclear complexes. In addition, the revised method employs the Langmuir isotherm model, rather than the linear partitioning model, to interpret the metal's distribution between the IX resin and solution, thereby allowing for more versatile and more accurate estimate of the stability constants over a wide range of metal concentration. To ensure proper uses of the method, the IX resin used must not adsorb any significant amounts of ligands in the presence of the metal ions. To this end, non-chelating cation exchange resins with macroporous, acrylic matrix are preferred. Chelating resins or resins with polystyrene or gel-type matrices should be avoided for their much greater dendrimer retention.

This study revealed that the conditional stability constant for Cu^{2+} -G1.0-NH₂ complexes increased from $10^{20.0}$ at pH 5.0 to $10^{25.8}$ at pH 7.0, and a dendrimer can bind more Cu^{2+} ions at a higher pH. The conditional stability constant was $10^{17.2}$ for Pb-G1.0-NH₂ and $10^{21.9}$ for Pb-G1.5-COO⁻ complexes at pH 5.0. When the dendrimer generation increased from zero to four, the conditional stability constant was increased from $10^{16.2}$ to

$10^{34.1}$ and the number of Cu^{2+} ions in the metal-dendrimer complexes was increased from 1 to 12 at pH 5.0.

CHAPTER 5. MODELING THE ELUTION HISTORIES OF COPPER AND LEAD FROM A CONTAMINATED SOIL TREATED BY POLY(AMIDOAMINE) (PAMAM) DENDRIMERS

In this chapter, a dynamic “two-site” model was formulated and tested for simulating the elution histories of copper (II) and lead (II) from a contaminated soil by various dendrimers and under various experimental conditions. The soil sorption site was kinetically divided into two compartments: a site with a fast desorption rate and a site with a slow desorption rate. The model was also used to simulate the copper (II) and lead (II) elution histories by dendrimers from a sandy loam soil. The predicting power of the model was investigated for varying dendrimer doses, solution pH, and initial metal concentration in soil.

5.1 Introduction

In recent years, extraction of heavy metals from contaminated soils by various chelating agents has been widely studied (Allen and Chen 1993; Di Palma and Ferrantelli 2005; Furukawa and Tokunnaga 2004; Hong et al. 1999; Lim et al. 2004b; Lo and Yang 1999; Mulligan et al. 2001; Neilson et al. 2003; Rampley and Ogden 1998a; Samani et al. 1998). Results from chapters 2 and 3 indicate that poly(amidoamine) PAMAM dendrimers can effectively remove Cu^{2+} and Pb^{2+} from contaminated soils. To facilitate

further process design and cost-benefit analysis, it is necessary to develop a mechanistically sound model that can predict the performance and efficiency of the remediation process. Furthermore, model simulation of the metal extraction process may also aid in process optimization and assessing the fate and transport of metal ions in the soil-groundwater systems.

Various mathematical models have been reported for describing the desorption and transport of metals in porous media. The conventional approach to describe the reactive transport includes the processes of convection, dispersion, and adsorption (Clement et al. 2000; Clement et al. 1998; Tran et al. 2002), where equilibrium conditions are often invoked to describe the local sorption/desorption isotherms such as the classic Langmuir, Freundlich, or the linear isotherm models (Fetter 2001; Peters and Shem 1992). However, the classical models can not simulate the dynamic leaching process of heavy metals desorbed by the water soluble chelators such as dendrimers since the models do not account for the metal-chelator interactions.

Column studies have shown that the leaching of metals from soils by chelating agents is mostly controlled by the slow solubilization kinetics rather than diffusion-limited mass transport (Kedziorek et al. 1998b). Shi et al. (Shi et al. 2005) used a two-site model to simulate the kinetics of Cu and Zn release from soils with a stirred-flow method. Qafoku et al. (Qafoku et al. 2005) investigated the desorption and sorption of U(VI) during reactive transport in a sediment by column experiments with a one-dimension distributed rate coefficient model. Kedziorek et al. (Kedziorek et al. 1998b) developed a model with a second-order kinetic metal solubilization reaction to simulate the leaching of Cd and Pb from soil during the percolation of ethylenediamine tetraacetic acid

(EDTA). This model accounted for both the uncomplexed EDTA and the fraction of extractable metal in the soil. Samani et al. (Samani et al. 1998) simulated lead removal process based on equilibrium and kinetic dissolution in a contaminated soil column using EDTA and showed that the model could adequately predict the observed removal process. Thayalakumaran et al. (Thayalakumaran et al. 2003) developed a more sophisticated model to simulate Cu leaching following the application of EDTA while considering the competition between copper and iron for EDTA. Bryan et al. (Bryan et al. 2005) applied a mixed equilibrium-kinetic model to simulate the column experimental data involving transport of metal ions and humic substances.

We constructed a “two-site” model using the classical convection-dispersion equation coupled with a kinetic source/sink term to predict the desorption kinetics and dynamics of metal ions from a contaminated soil in the presence of a dendrimer. The overall goal of this work is to develop a numerical modeling framework to simulate the elution histories of Cu^{2+} and Pb^{2+} in soils following application of various dendrimers and under various operating conditions such as dendrimer concentration, solution pH, and metal concentration in soils. The specific objectives are to: (1) formulate a modified two-site model for simulating/predicting the dendrimer-facilitated transport of metal ions in the metal-dendrimer-soil-groundwater system; and (2) test the model by applying the model for interpreting observed Cu^{2+} and Pb^{2+} elution histories from bench-scale column experiments.

5.2 Experiment

5.2.1 Materials

The star-burst PAMAM dendrimers used in this study included a generation 4.5 dendrimer terminated with carboxylic groups (G4.5-COOH), a generation 1.0 dendrimer with primary amine groups (G1.0-NH₂), and a generation 4.0 dendrimer with primary amine groups (G4.0-NH₂). G4.5-COOH was purchased from Aldrich Chemical CO., Milwaukee, WI, and G1.0-NH₂ and G4.0-NH₂ were purchased from Dendritech Inc., Midland, MI, USA. They were all obtained as stock solutions (5% for G4.5-COOH, 39.49% for G1.0-NH₂, and 26.00% for G4.0-NH₂) in methyl alcohol solution (the dendrimer concentration is expressed in percent by weight throughout this paper).

A surface sandy loam soil sample from top 0-12 cm was collected from a local farm in Auburn, AL, USA. Before use, the soil was sieved through a 2 mm screen. For subsequent batch and column elution tests, Cu²⁺ and Pb²⁺ were pre-loaded to the soil to yield an initial concentration of 590 mg/kg for Cu and 965mg/kg for Pb. The detailed soil compositions, mineral analysis, and the loading method were reported in Chapter 2 and Chapter 3.

5.2.2 Experiment setup

The Cu²⁺ and Pb²⁺ elution using dendrimers was investigated through column experiments. A series of column runs were conducted to test the effects of dendrimer concentration, pH, and terminal functional groups on the elution profiles of copper and lead. The column setup included a HPLC pump (Series II), a glass column (inner

diameter of 1.0 cm and length of 10 cm, Omnifit, Cambridge, UK), and a fraction collector (Eldex Laboratories, Napa, CA).

Two sets of tracer tests were performed with potassium bromide (KBr) to determine the dispersion coefficient of the soil bed. For the Cu-loaded soil, the tracer test was carried out with a soil bed of 3.14 mL and at an empty bed contact time (EBCT) of 17 min. For the Pb-loaded soil, a smaller soil bed volume (1.60 mL) was used and the EBCT was 27 min. For Cu-loaded soil, the influent tracer solution contained 100 mg/L Br⁻ and 0.1% of G4.5-COOH, and the solution pH was adjusted to 6.0. Before introducing the KBr solution, ~14 bed volumes (BVs) of DI water at pH 6.0 were passed through the soil. The bromide concentration in the effluent was analyzed using a DIONEX ion chromatograph (IC, DX-120) until full breakthrough. The tracer test for the Pb-loaded soil was similar to the Cu-soil column, except that 0.1% G1.0-NH₂ was used in the influent solution and the influent pH was adjusted to 5.0. **Table 5-1** summarizes the experimental conditions and hydro-dynamic parameters for the column runs. These parameters were also used in the subsequent model simulations.

To facilitate model simulation, batch desorption experiments were carried out to obtain the relationship of Cu²⁺ desorption coefficient at a solution pH of 5.0, 6.0 and 7.0, respectively, and in the presence of 0.04% G4.5-COOH. In each test, five grams of a Cu-loaded soil sample were added to a flask containing 200 mL of a dendrimer solution. The mixtures were then continuously shaken for 2 hours, during which 1-mL solution samples were taken every 3 minutes. The solution pH was intermittently adjusted with dilute

Table 5-1. General Experimental Conditions Used in Cu²⁺ and Pb²⁺ Column Experiments.

	Bed volume (mL)	Bed length (cm)	Flow rate (mL/s)	True velocity (cm/s)	Dispersion coefficient D (cm²/s)
Cu²⁺ Elution	3.14	4.0	3.0×10^{-3}	1.13×10^{-2}	1.15×10^{-3}
Pb²⁺ Elution	1.60	2.0	1.0×10^{-3}	3.4×10^{-3}	8.80×10^{-4}

NaOH or HCl to maintain the desired pH of 5.0, 6.0 or 7.0. An Orion pH meter (Model 520A) with an Orion electrode (model 8102BN) was used to measure the pH.

5.3 Model

5.3.1 Model formulation

When applied to a metal contaminated soil, a fraction of dendrimer molecules will complex with the metal ions, while the rest will remain in their free form. The transport of the free dendrimer molecules and the dendrimer-metal complexes through a one dimensional (x) column is described by following set of advection-dispersion equations which are coupled with a kinetic sink or source term:

$$\frac{\partial C_d}{\partial t} = D \frac{\partial^2 C_d}{\partial x^2} - v \frac{\partial C_d}{\partial x} + \frac{\rho}{\varepsilon} \frac{\partial C_{ms}}{\partial t} \quad (5-1)$$

$$\frac{\partial C_{dm}}{\partial t} = D \frac{\partial^2 C_{dm}}{\partial x^2} - v \frac{\partial C_{dm}}{\partial x} - \frac{\rho}{\varepsilon} \frac{\partial C_{ms}}{\partial t} \quad (5-2)$$

Eqn (5-1) describes the transport of free dendrimers along the column, where C_d is the concentration of free dendrimer molecules, mmol/L; D is the dispersion coefficient, cm^2/s ; v is the pore velocity, cm/s ; ρ is the dry bulk soil density, g/L ; ε is the porosity, dimensionless; C_{ms} is the metal concentration in soil, mmol/g ; and $\rho \partial C_{ms} / \varepsilon \partial t$ is the sink term for the dendrimer. Eqn (5-2) describes the transport of dendrimer-metal complexes, where C_{dm} is the concentration of the metal-dendrimer complexes in mmol/L and $(-\rho \partial C_{ms} / \varepsilon \partial t)$ is the source term. Since ρ and ε are constants they can be combined with C_{ms} (mmol/g) to express the copper concentration in soil C_m ,

mmol/L. In the previous work, indicated that the retention of the dendrimers by the soil was negligible.

Under the same governing equations, this work formulated and tested three types of kinetic equations to describe the desorption of metal ions from the soil by complexation with dendrimers. The first kinetic model is referred to as “one-site and constant-desorption-rate” model where all sorption sites are considered as equal and the metal desorption kinetics is described by a second-order rate equation with respect to the free dendrimer concentration and to the fraction of available metal in the soil as shown by eqn (5-3):

$$\frac{\partial C_m}{\partial t} = -KnC_d \frac{C_m}{C_{mi}} \quad (5-3)$$

Where K is the kinetic desorption rate constant, s^{-1} ; n is the equilibrium metal/dendrimer ratio in the metal-dendrimer complexes; C_{mi} is the initial metal concentration in soil expressed as mmol/L, which is calculated using eqn (5-4):

$$C_{mi} = \frac{\rho C_{msi}}{\varepsilon} \quad (5-4)$$

where C_{msi} is the initial metal concentration in soil expressed as mmol/g. For homogeneous (i.e. pure solution) systems, the values of n have been reported (Diallo et al. 1999; Zhao et al. 1998). However, for the heterogeneous soil-solution systems, the metal binding may not be at equilibrium. Consequently, the n value may not be determined through separate equilibrium tests. In this work, the parameter n is lumped with the desorption rate constant K to yield an observed desorption coefficient K_d (s^{-1}), i.e.

$$K_d = Kn \quad (5-5)$$

The parameter K_d value is affected by temperature, pH, metal-dendrimer complexing stoichiometry, and particle shape (Montero et al. 1994). Combining eqns (5-1), (5-2), (5-3), and (5-5), the “one-site” model for describing the desorption and transport of free dendrimer and dendrimer-metal complexes can be written as:

$$\frac{\partial C_d}{\partial t} = D \frac{\partial^2 C_d}{\partial x^2} - v \frac{\partial C_d}{\partial x} + \frac{\partial C_m}{\partial t} \quad (5-6)$$

$$\frac{\partial C_{dm}}{\partial t} = D \frac{\partial^2 C_{dm}}{\partial x^2} - v \frac{\partial C_{dm}}{\partial x} - \frac{\partial C_m}{\partial t} \quad (5-7)$$

$$\frac{\partial C_m}{\partial t} = -K_d C_d \frac{C_m}{C_{mi}} \quad (5-8)$$

The second kinetic model is a “gamma distribution” model, in which K_d is assumed to follow a gamma distribution. Gamma distribution has been used in the modeling of sorption/desorption of organic and inorganic compounds in soils and sediments (Ahn et al. 1999; Chen and Wagenet 1995; Connaughton et al. 1993; Culver et al. 1997; Qafoku et al. 2005). The advantage of gamma distribution is its flexibility (Dovore 1995). The expression for K_d is given by (Ahn et al. 1999; Chen and Wagenet 1995; Connaughton et al. 1993):

$$f(K_d) = \frac{\beta^\eta (K_d)^{\eta-1}}{\Gamma(\eta)} \exp(-\beta K_d) \quad (5-9)$$

where β is the scale parameter and η is the shape parameter; they are both positive parameters. $\Gamma(\eta)$ is the gamma function described by the integral:

$$\Gamma(\eta) = \int_0^\infty x^{\eta-1} \exp(-x) dx \quad (5-10)$$

where x is a dummy variable for integration. Eqns. (5-6), (5-7), (5-8), (5-9), and (5-10) must be solved simultaneously to simulate the desorption and transport of heavy metals

from soil in the presence of a dendrimer. The parameters β and η can be determined by fitting the model to a set of experimental metal elution data.

However, due to the heterogeneity and complexity of soils, the models based on one uniform site often fail to simulate the actual contaminant transport process (Dang et al. 1994; Fanguero et al. 2005; Kuo and Mikkelsen 1980). To overcome the limitations, researchers have modified the one-site models by considering two or more kinetic compartments, each with a different kinetic constant (Lenhart and Saiers 2003; Pang et al. 2005; Shi et al. 2005; Van Noort et al. 2003). In this work, a “two-site” model is developed by dividing the soil’s metal desorption sites into two compartments: a fast desorption site and a slow desorption site. Accordingly, Eqn (5-8) can be applied to describing the desorption kinetics for each class of the sites:

$$\frac{\partial C_{m1}}{\partial t} = -K_{d1} C_d \frac{C_{m1}}{f C_{mi}} \quad (5-11)$$

$$\frac{\partial C_{m2}}{\partial t} = -K_{d2} C_d \frac{C_{m2}}{(1-f) C_{mi}} \quad (5-12)$$

$$\frac{\partial C_m}{\partial t} = \frac{\partial C_{m1}}{\partial t} + \frac{\partial C_{m2}}{\partial t} \quad (5-13)$$

where C_{m1} is the metal concentration in the fast desorption site, mmol/L; f is the fraction of fast desorption site; C_{m2} is the metal concentration in the slow desorption site, mmol/L; K_{d1} and K_{d2} are the desorption coefficient for the fast and slow site, respectively, s^{-1} .

To solve the transport eqns (5-6) and (5-7), the following boundary condition(BC) and initial conditions(IC) are specified:

$$C_d = 0 \quad x \geq 0, t = 0 \quad (5-14)$$

$$C_{dm} = 0 \quad x \geq 0, t = 0 \quad (5-15)$$

$$C_d = C_{d, \text{influent dendrimer concentration}} \quad x = 0, t \geq 0 \quad (5-16)$$

$$C_{dm} = 0 \quad x = 0, t \geq 0 \quad (5-17)$$

$$\frac{\partial^2 C_d}{\partial x^2} = 0 \quad (\text{Widdowson et al. 1988}) \quad x = L, t \geq 0 \quad (5-18)$$

$$\frac{\partial^2 C_{dm}}{\partial x^2} = 0 \quad x = L, t \geq 0 \quad (5-19)$$

Eqn (5-6) and (5-7) were solved using a fully implicit finite difference scheme along with a characteristics advection tracking scheme (Clement et al. 1996). Spatial and temporal grids were adjusted to set Courant number one to fully eliminate numerical dispersion. Reaction equations (5-8), (5-11), and (5-12) were solved using the 4th order Runge-Kutta method. Model fittings were completed by minimizing the squares of the differences between the experimental data and the model predictions (SDBEM).

5.3.2 Parameter estimation

The soil particle density was determined using pycnometer method, and the soil porosity was calculated using particle density and bulk density. The dispersion coefficient D and true velocity V were obtained by fitting the advection-dispersion model to the tracer breakthrough curves (BTC). Other model parameters including K_d , β , η , f , K_{d1} , and K_{d2} were obtained by fitting the calculated dendrimer-metal elution histories to the corresponding experimental data.

5.4 Results and Discussion

5.4.1 Simulating Cu²⁺/Pb²⁺ transport

Figure 5-1 shows the experimentally observed Cu²⁺ elution profiles (symbols) and the best fitted elution curves using: the “one-site” model, the “gamma distribution” model, and the “two-site” model for the release of Cu²⁺ with G4.5-COOH dendrimer at a concentration of 0.1% and at pH 6.0.

All three models were able to correctly simulate the incipient peaking time as well as the peak height of the copper elution curve. However, the simulation quality differed markedly in the tailing stage, with the two-site model being the best and the one-site model the worst. At a constant desorption coefficient (K_d) of $2.1 \times 10^{-5} \text{ s}^{-1}$, the “one-site” model failed to interpret the observed tailing profile, displaying a broader peak but a shorter duration of tailing. The “gamma distribution” model also fitted the observed curve adequately although the deviation was increasing as the tailing went on. In contrast, the “two-site” model ($f = 0.35$, $K_{d1} = 8.3 \times 10^{-3}$, and $K_{d2} = 8.1 \times 10^{-4}$) was able to adequately simulate the experimental elution curve throughout the experimental period. **Table 5-2** lists the best-fitted parameters of the “two-site” model. The desorption coefficient of the slow desorption site is one magnitude smaller than that for the fast desorption site. While the slow site accounted for ~65% of the total site, our simulation sensitivity analyses indicated that the fast desorption site controls the height and width of the peak whereas the slow desorption site controls the tailing profile.

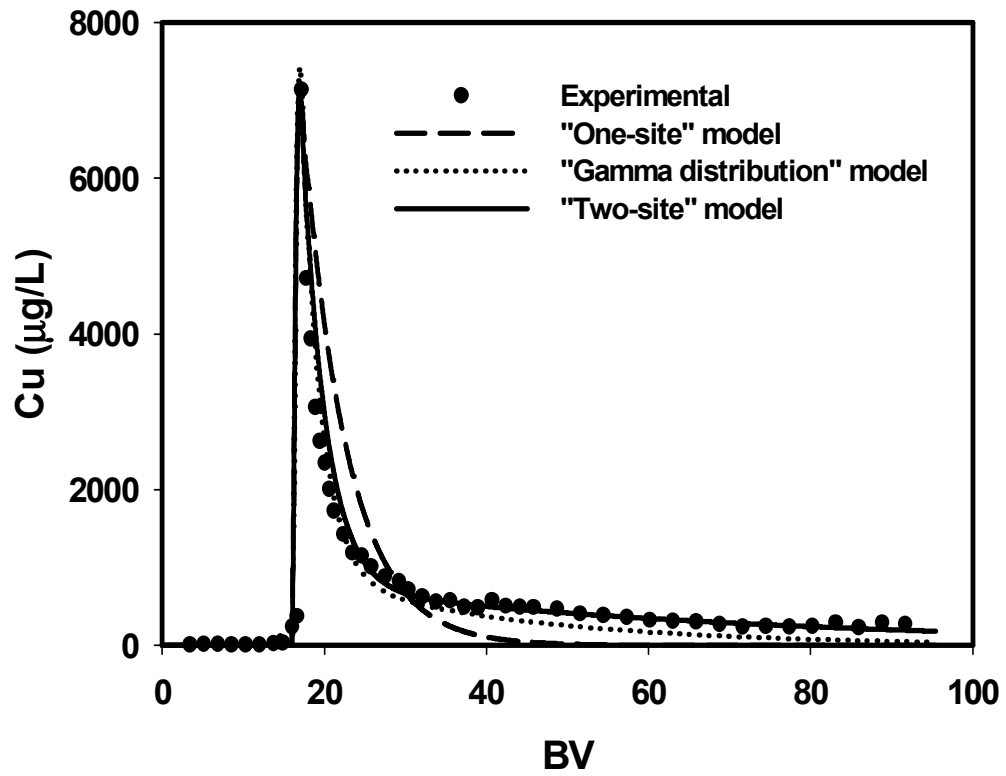


Figure 5-1. Experimentally observed and model-simulated elution histories of Cu^{2+} from a soil treated with 0.1% of G4.5-COOH. (Influent pH = 6.0; Initial Cu in soil = 30mg/kg).

Table 5-2. Best Fitted Parameters of the Two Sites Model under Various Experimental Conditions.

	Experimental Conditions	<i>f</i>	<i>K_{d1}</i> (s ⁻¹)	<i>K_{d2}</i> (s ⁻¹)
Cu	G4.5-COOH = 0.1%, pH = 6.0, initial Cu in soil = 30 mg/kg (Figure 5-1)	0.35	8.3×10 ⁻³	8.1×10 ⁻⁴
	G4.0-NH ₂ = 0.04%, pH = 6.0, initial Cu in soil = 30 mg/kg (Figure 5-3)	0.33	3.9×10 ⁻³	2.2×10 ⁻⁴
Pb	G1.0-NH ₂ =0.1%, pH = 5.0, initial Pb in soil = 590 mg/kg (Figure 5-2)	0.02	1.3×10 ⁻⁵	8.2×10 ⁻⁶

The “two-site” model has been typically used to describe the biphasic desorption pattern where a sorbate is desorbed through a rapid initial release followed by a much slower release (Ahn et al. 1999; Pignatello et al. 1993; Van Noort et al. 2003). Separate kinetic experiments indicate that the release of Cu^{2+} conforms to this type of desorption pattern (data not shown). Consequently, the “two-site” model simulated the experimental data much better than the one-site model.

The advantage of the two-site model became more remarkable when the models were applied to simulating Pb^{2+} elution histories. **Figure 5-2** compares the model simulations of the Pb^{2+} elution history with 0.1% G1.0-NH₂ and at pH 5.0. Like the case of Cu^{2+} elution, the Pb^{2+} peaking also occurred with a sharp rise followed by a long tailing. Three models were applied to fit the experimental data. As shown in **Figure 5-2**, the best fit of the “one-site” model with $K_d = 5.5 \times 10^{-4}$ almost got a flat line after 40 BVs. It could neither get the peak nor the tailing. The “gamma distribution” model failed to describe the experimental data too. As indicated in **Figure 5-2**, the “two-site” model ($f = 0.02$, $K_{d1} = 1.3 \times 10^{-5}$, and $K_{d2} = 8.2 \times 10^{-6}$) provided the best description to the observed data. Compared to the copper release as shown in **Figure 5-1**, the “one-site” model and the “gamma distribution” model are more way off from the experimental data for the Pb^{2+} case. As shown in **Table 5-2**, lead has a much smaller fraction of fast release site and a bigger fraction of the slow release site than copper does. This makes it harder for the other two models to catch the peak and tailing because the small fraction of the fast desorption site controls the height and width of the peak while the slow desorption site controls the tailing profile.

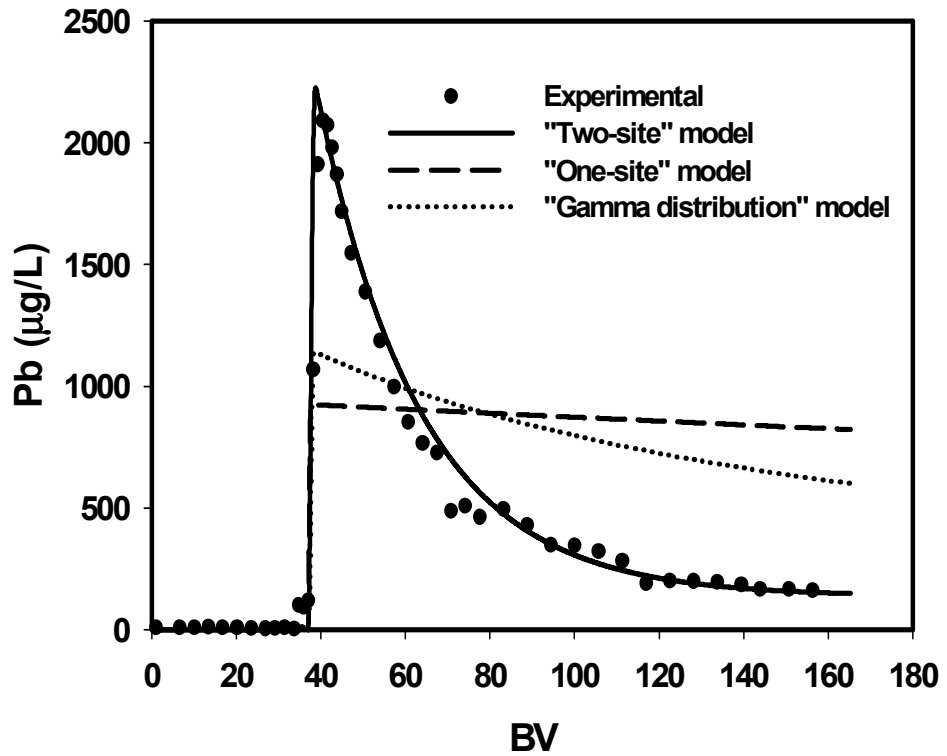


Figure 5-2. Experimentally observed and model-simulated elution histories of Pb^{2+} from a soil treated with 0.1% of G1.0-NH₂. (Influent pH = 5.0; Initial Pb in soil = 590 mg/kg).

The Cu^{2+} or Pb^{2+} bound to the fast releasing sites was relatively more available. Cu^{2+} has a greater fraction (31% ~ 35%) of the fast releasing sites than Pb^{2+} (2%) (**Table 5-2**). This is in accord with the sequential extraction results: 38% of the total Cu^{2+} and 1.0% of Pb^{2+} is in the easily available exchangeable form (EXE) in the untreated soil. Parameters in **Table 5-2** also show that the desorption rate of the two sites for Cu^{2+} is two magnitude faster than Pb^{2+} . The elution of heavy metals is affected by the lability of heavy metals in soil. Cu is usually the most labile and Pb is the least labile compared to Zn and Cd (Sun et al. 2001). This implies that the removal of Pb^{2+} from contaminated soil is more time-dependent than Cu^{2+} .

Figure 5-3 shows that the two-site model also adequately simulated the Cu^{2+} elution history when a different dendrimer, 0.04% of G4.0-NH₂, was applied at pH 6.0. The model parameters (f , K_{d1} , and K_{d2}) in **Table 5-2** indicate that the f value for Cu^{2+} with the two dendrimers was quite comparable (0.33 and 0.35).

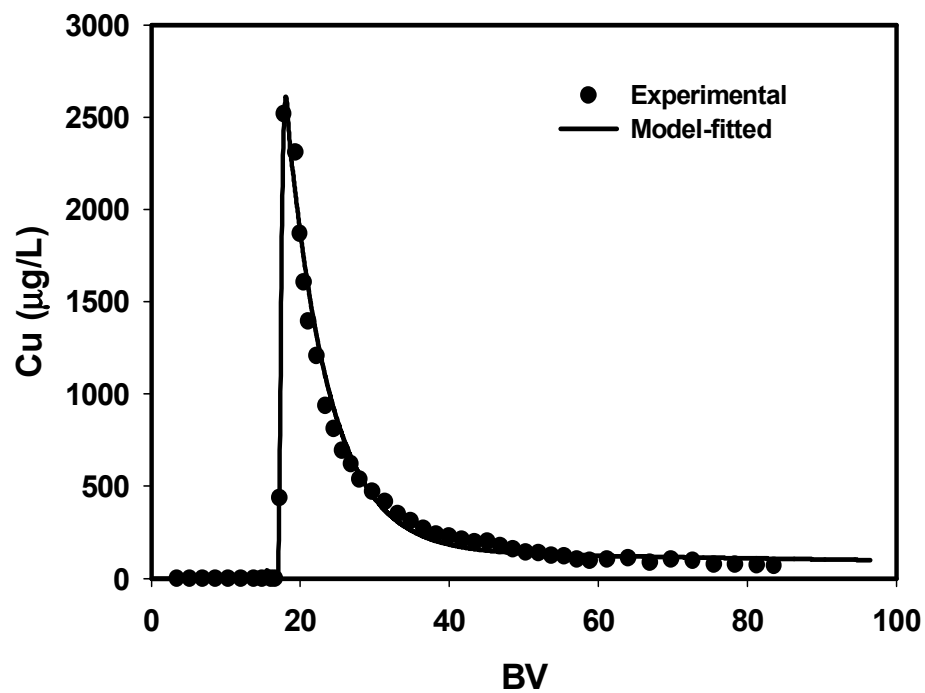


Figure 5-3. Experimentally observed and model-simulated elution histories of Cu^{2+} from a soil treated with 0.04% of G4.0-NH₂. (Influent pH = 6.0; Initial Cu in soil = 30 mg/kg).

5.4.2 Predicting the Cu²⁺/Pb²⁺ elution histories

The predictive power of the “two-site” model was tested with Cu²⁺ as the model metal. The prediction was carried out at varied initial Cu²⁺ concentration in soil, dendrimer concentration, or pH of the dendrimer solution.

5.4.2.1 Prediction at different initial Cu²⁺ concentrations in soil

Figure 5-4 shows the observed and model-predicted elution history of copper from the soil with an initial Cu concentration of 12 mg/kg based on the model parameters (**Table 5-2**) obtained by fitting the two-site model to the experimental elution curve where the initial copper concentration was 30 mg/kg while the other conditions were the same (**Figure 5-3**). As shown in **Figure 5-4**, the two-site model was able to adequately predict the Cu elution curves at the two initial concentrations of Cu in the soil. Despite the 2.5 times difference in the initial Cu concentration, the elution peaking profiles (peak height and of width) of **Figures 5-3** and **5-4** differ only slightly. This observation suggests that the elution dynamics of Cu²⁺ is controlled by the dendrimer concentration and rather than the initial Cu²⁺ concentration in the soil.

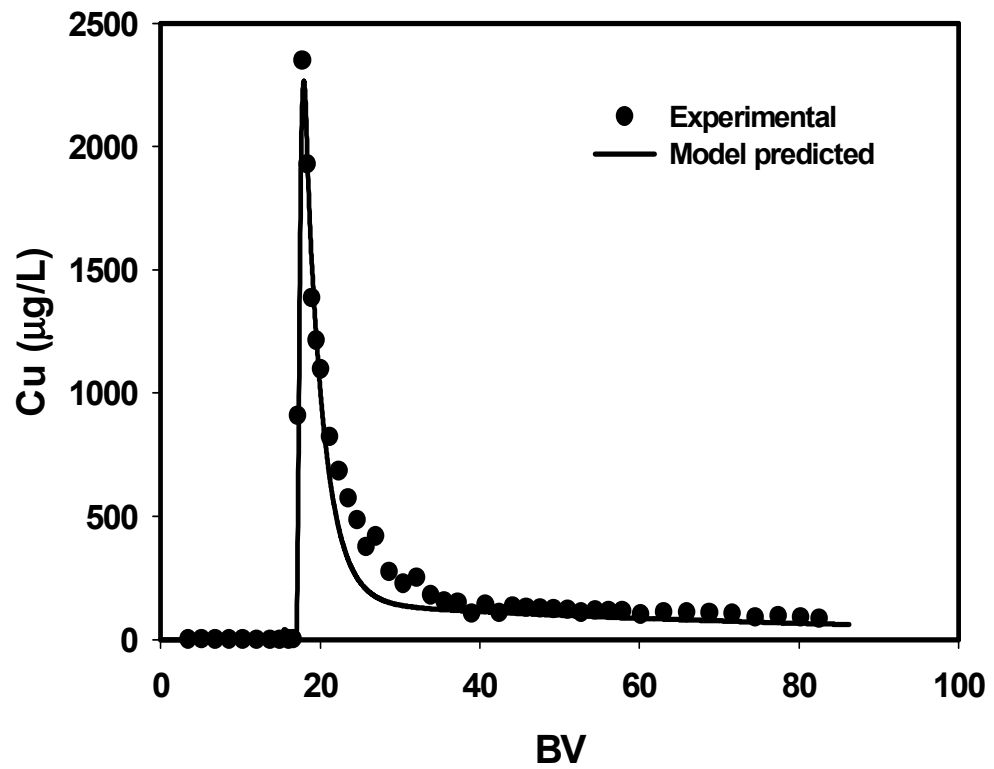


Figure 5-4. Observed and model-predicted Cu²⁺ elution histories from a soil treated with 0.04% of G4.0-NH₂. (Influent pH = 6.0; Initial Cu in soil = 12 mg/k).

5.4.2.2 Prediction at various dendrimer concentrations

The “two-site” model was further tested to predict Cu^{2+} elution curves at various dendrimer concentrations and for two different dendrimers, G4.5-COOH and G4.0-NH₂. First, the two-site model parameters were determined from **Figure 5-1**, where the concentration of G4.5-COOH was 0.1%, and from **Figure 5-3**, where the concentration of G4.0-NH₂ was 0.04%. Then, the model was applied to predicting the Cu^{2+} elution histories obtained at different dendrimer concentrations. **Figures 5-5** and **5-6** show the predicted Cu^{2+} elution histories when the soil was treated with 0.04% of G4.5-COOH and 0.1% G4.0-NH₂, respectively. Evidently, the predictions in both cases were quite successful.

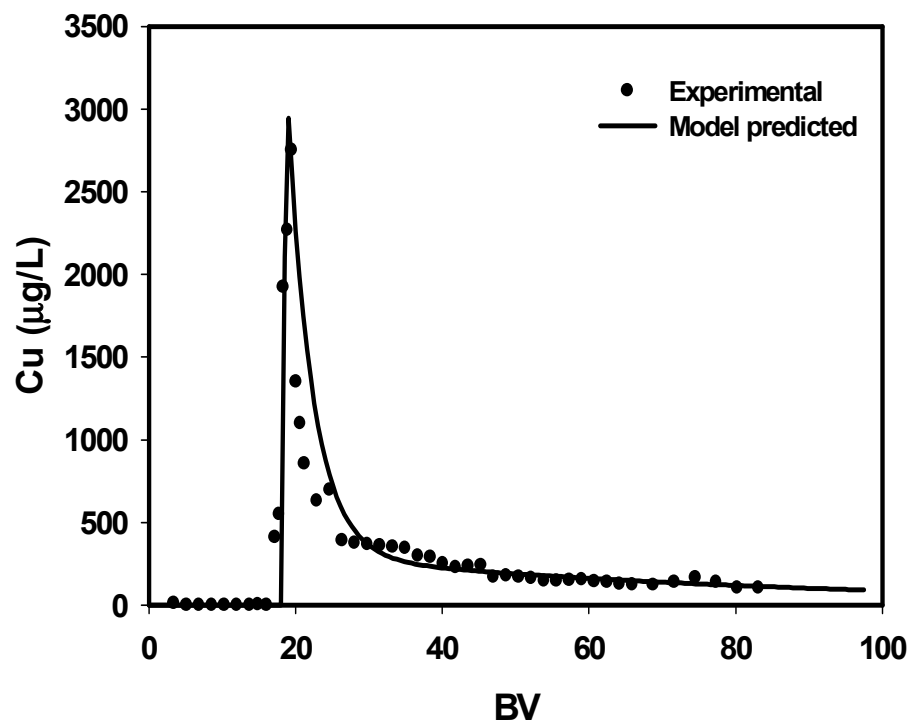


Figure 5-5. Observed and model-predicted Cu²⁺ elution histories from a soil treated by 0.04% of G4.5-COOH and under otherwise identical conditions as in **Figure 5-1**. (Model parameters were derived from **Figure 5-1**).

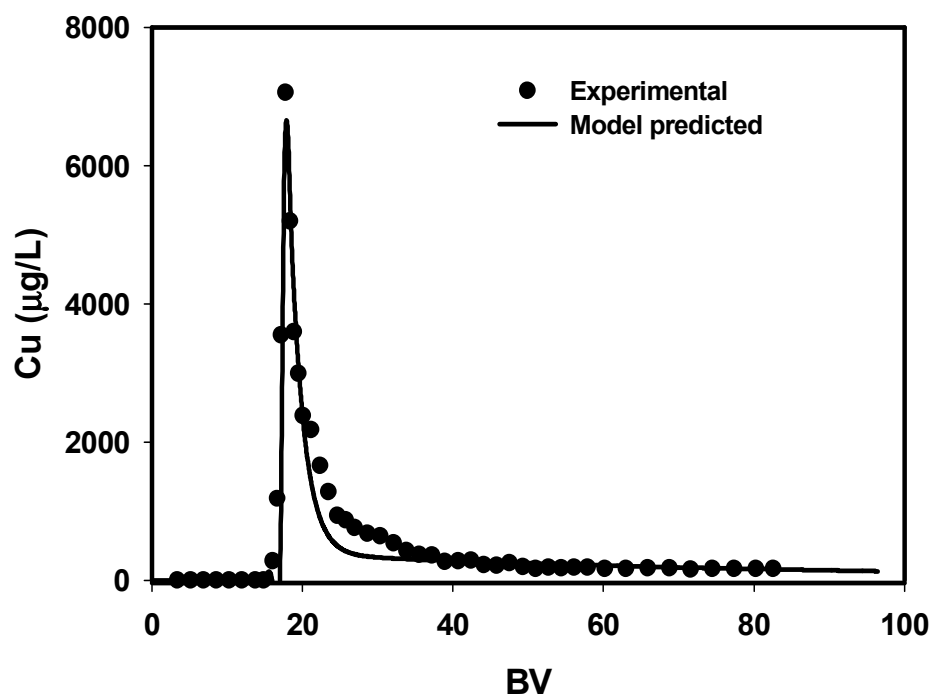


Figure 5-6. Observed and model-predicted Cu^{2+} elution histories from a soil treated by 0.1% of G4.0-NH₂ and under otherwise identical conditions as in Figure 3. (Model parameters were derived from **Figure 5-3**).

5.4.2.3 Prediction at various pH levels

Because of the competition of protons with the metal ions for the binding sites of soils and dendrimers, the metal desorption rate by a dendrimer is expected to be pH-dependent. The pH effect on the dissolution rate can be described by (Drever 1994; Lasaga et al. 1994; Sukreeyapongse et al. 2002; Wieland et al. 1988):

$$\text{Release rate} = a[\text{H}^+]^b \quad (5-20)$$

where a is a constant independent of pH and b is an empirical constant related to molar proton/metal exchange ratio. The relationship of K_d at different pH values is expressed by:

$$\frac{K_{d_i, pH2}}{K_{d_i, pH1}} = 10^{b(pH1 - pH2)} \quad (j=1, 2) \quad (5-21)$$

In a batch reactor, the dendrimer-facilitated desorption kinetics can also be described by the two-site model via:

$$\frac{M}{V} \frac{dC_{ms1}}{dt} = -K_{d1, batch} Cd \frac{C_{ms1}}{fC_{ms}} \quad (5-22)$$

$$\frac{M}{V} \frac{dC_{ms2}}{dt} = -K_{d2, batch} Cd \frac{C_{ms2}}{(1-f)C_{ms}} \quad (5-23)$$

$$\frac{dC_{ms}}{dt} = \frac{dC_{ms1}}{dt} + \frac{dC_{ms2}}{dt} \quad (5-24)$$

where M is the amount of the soil added into the batch reactor (5 g); V is the solution volume (0.2 L); C_{ms} is metal concentration in soil, mmol/g; C_{ms1} and C_{ms2} are metal concentration at the fast and slow desorption sites, respectively, mmol/g; $K_{d1, batch}$ and

$K_{d2, batch}$ refer to the desorption coefficient for the fast and slow sites in the batch reactor, respectively, s^{-1} . Note that K_d in the batch is likely to be different from in the column due to the different operating conditions. The change in solution volume during the batch test was 5.5%, thus, the associated effect on desorption kinetics was negligible.

The batch kinetic equations were solved numerically with appropriate boundary and initial conditions, and then the solutions were fitted to the batch kinetic data (**Figure 5-7**) at a fixed solution pH 5.0, 6.0 and 7.0, respectively. The best-fitted $K_{d1, batch}$ and $K_{d2, batch}$ are, respectively, $1.5 \times 10^{-3} s^{-1}$ and $5.8 \times 10^{-5} s^{-1}$ for pH 5.0; $9.5 \times 10^{-4} s^{-1}$ and $3.4 \times 10^{-5} s^{-1}$ for pH 6.0; and 6.3×10^{-4} and 2.1×10^{-5} for pH 7.0. Based on these K_d values and using Eq. (21), a mean value of b is determined to be 0.21 (**Table 5-3**). This value is smaller than the reported b in the literature: 1.3 (Shi et al. 2005) and 1.2-1.7 (Kinniburgh et al. 1999). The discrepancy is due to the fact that the solution pH affects the binding sites on both the soil and the dendrimer. Lowering pH increases the availability of copper ions in the soil, but also reduces the sorption capacities of the dendrimers. The two opposing effects result in the lower proton/metal exchange ratio than that in the literature where pH was considered only to affect the soil binding sites (Kinniburgh et al. 1999; Shi et al. 2005).

The batch-determined b value was then used to calculate the desorption coefficient for the column experiments from pH 6.0 to pH 5.0 and 7.0, respectively. Again, Eq. (21) was used, and the K_{d1} and K_{d2} values at pH 6.0 (**Figure 5-1**) served as the starting model parameters. **Table 5-3** gives the calculated K_{d1} and K_{d2} values. Based on these values and the model-fitted f value from **Figure 5-1**, the two-site model was able to

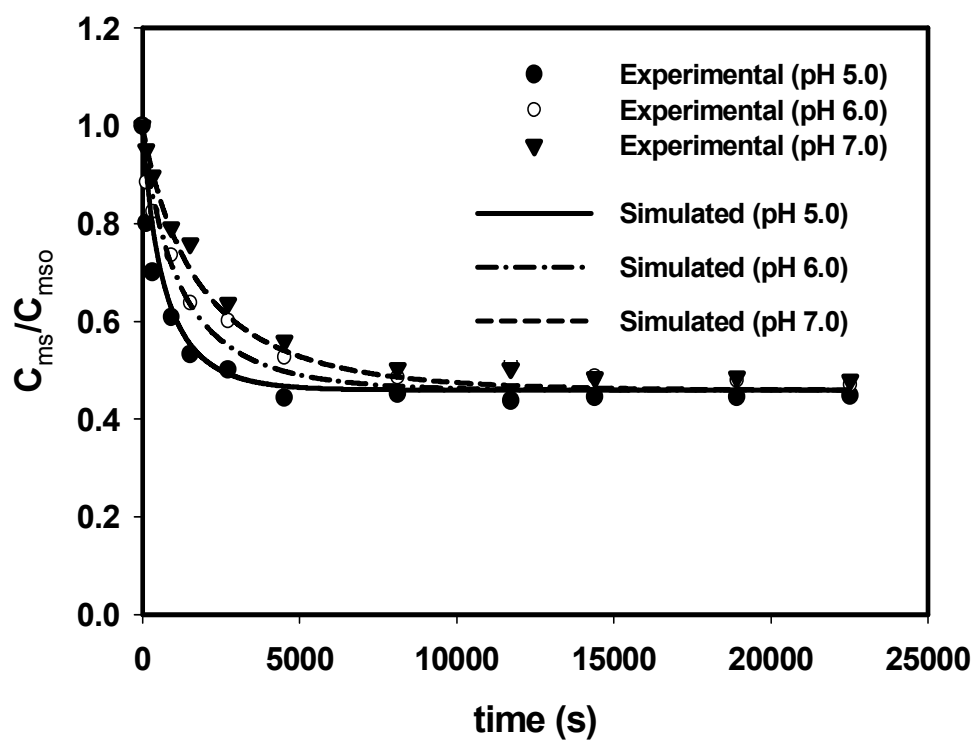
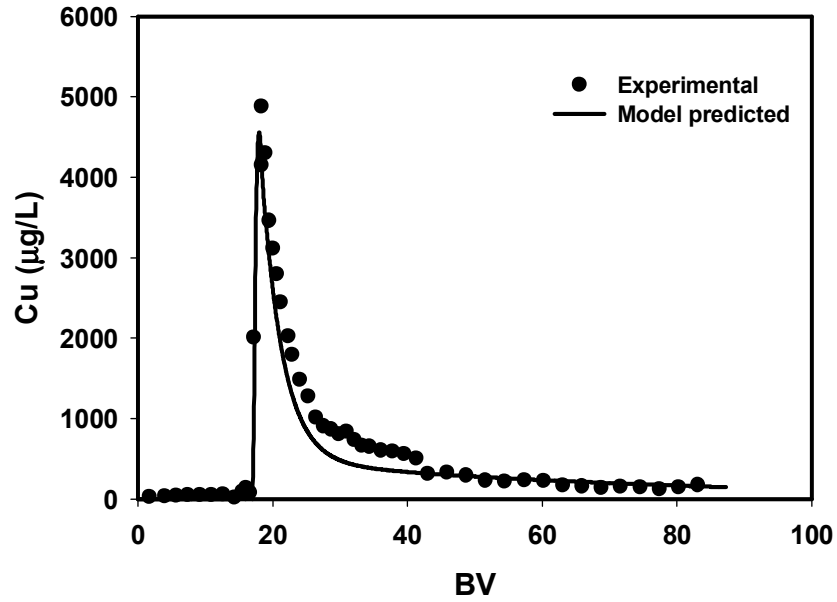


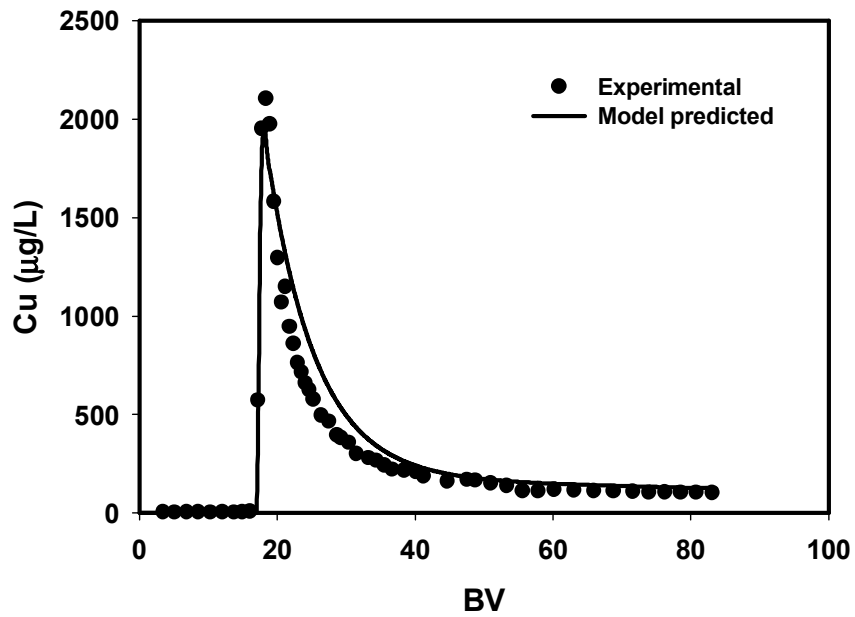
Figure 5-7. Observed and model-simulated Cu^{2+} desorption kinetics in a batch reactor and in the presence of 0.04% of G4.5-COOH at pH 5.0, 6.0, and 7.0, respectively.

Table 5-3. Values of Molar Proton/Metal Exchange Ratio (*b*) Determined from Batch Experiments and by Eq. (5-21) and the Resultant Desorption Coefficient (*K_d*).

pH	<i>b</i> based on <i>K_{d1, batch}</i> from Figure 5-7 (s ⁻¹)	<i>K_{d1}</i> for the two-site column model (s ⁻¹)	<i>b</i> based on <i>K_{d2, batch}</i> from Figure 5-7 (s ⁻¹)	<i>K_{d2}</i> for the two-site column model (s ⁻¹)
5.0	0.20	1.3×10 ⁻² (calculated)	0.23	1.3×10 ⁻³ (calculated)
6.0		8.3×10 ⁻³ (from Figure 1)		8.1×10 ⁻⁴ (from Figure 1)
7.0	0.19	5.1×10 ⁻³ (calculated)	0.20	5.0×10 ⁻⁴ (calculated)
Mean <i>b</i>	0.21 ± 0.02 (mean ± standard deviation)			



(a)



(b)

Figure 5-8. Observed and model-predicted Cu^{2+} elution histories from a soil treated by 0.04% of G4.5-COOH and at pH 5.0 (a) and 7.0 (b). Model parameters are listed in

Table 5-3.

adequately predict the column elution histories of Cu^{2+} at pH 5.0 and pH 7.0, respectively (Figure 5-8).

5.5 Summary and Conclusions

This study formulated a modified “two-site” model, and is the first to simulate dendrimer-facilitated desorption kinetics and transport dynamics of metal ions from contaminated soils. Evidently, the one-dimension advection-dispersion equation coupled with a two-site kinetic sink or source term is capable of simulating the dynamic metal elution processes of Cu^{2+} and Pb^{2+} in a soil column.

Among the three tested models, the two-site model clearly over-performs the one-site model and the gamma-distribution for simulating/predicting the dendrimer-facilitated dynamic elution histories of Cu^{2+} and Pb^{2+} . Modeling results show that the desorption rate of Cu^{2+} is ~two-orders of magnitude faster than Pb^{2+} at both classes of the sites, and also Pb^{2+} has a 15 times smaller fraction of fast release site than Cu^{2+} .

The “two-site” model was able to predict Cu^{2+} removal from the soil with different initial copper concentrations but under otherwise identical conditions. It also successfully predicted the Cu^{2+} elution histories as dendrimer concentration was varied from 0.04% to 0.1%. The effect of pH was incorporated in the model by considering the proton competition with metal ions for the binding sites. A molar proton/metal exchange ratio of 0.21 was determined through batch desorption experiments, the b value was then used to facilitate the prediction of Cu^{2+} elution histories for various pH values (6.0 to 5.0 and to 7.0). The two-site model provides a convenient means for facilitating process design and analyses of the dendrimer-based metal removal technology. The successful model

prediction along with our column experimental results also supports the previously hypothesized mechanisms (chapters 2 and 3) for desorption of copper and lead by dendrimers.

CHAPTER 6. REDUCTIVE IMMOBILIZATION OF CHROMATE IN WATER AND SOIL BY STABILIZED IRON NANOPARTICLES

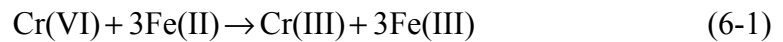
This chapter studies the feasibility of using a new class of stabilized zero-valent iron (ZVI) nanoparticles, which were developed by He and Zhao (2006) to reduce and immobilize Cr(VI) in soils through a series of batch and column experiments.

6.1. Introduction

Chromium has been widely detected in groundwater and soils, particularly in the industrial sites associated with metal plating, leather tanning, metal corrosion inhibition, and pigment production (Kavanaugh 1994a). From 1987 to 1993, chromium compound releases to land and water totaled nearly 200 million pounds (EPA web page: http://www.epa.gov/safewater/contaminants/dw_contamfs/chromium.html). Compared to the less soluble Cr(III) species, the more soluble Cr(VI) species is much more mobile, toxic and carcinogenic (Legrand et al. 2004). To address this concern, the U.S. Environmental Protection Agency (EPA) has set a maximum contaminant level (MCL) of 0.1 mg/L for total chromium in drinking water.

Traditionally, Cr(VI) is removed from water and soil through reduction of Cr(VI) to Cr(III) using a reducing agent such as ferrous sulfate, sulfur dioxide, or sodium bisulfite, followed by precipitation of Cr(III) (Guha and Bhargava 2005). In recent years,

researchers also demonstrated that Cr(VI) can be effectively reduced by Fe(II) according to the following reaction (Buerge and Hug 1999; Legrand et al. 2004; Pettine et al. 1998; Pratt et al. 1997; Schlautman and Han 2001; Seaman et al. 1999) (Legrand et al. 2004; Singh and Singh 2003):



More recently, reduction of Cr(VI) to Cr(III) by zero-valent iron particles has been investigated in a number of laboratory and field studies (Alowitz and Scherer 2002; Blowes et al. 1997; Cantrell et al. 1995; Gandhi et al. 2002; Gould 1982; Melitas et al. 2001; Powell et al. 1995; Pratt et al. 1997; Puls et al. 1999; Singh and Singh 2003; Wilkin et al. 2005). For example, permeable reactive barriers (PRBs) with commercially available Fe(0) powder have attracted great interest for *in situ* treatment of groundwater contaminated with various redox active compounds including Cr(VI) (Astrup et al. 2000; Melitas et al. 2001). A field-scale PRB using Fe(0) to remove Cr(VI) from groundwater was installed at the U.S. Coast Guard Support Center in North Carolina in June of 1996 (Furukawa et al. 2002; Mayer et al. 2001; Puls et al. 1999; Wilkin et al. 2003; Wilkin et al. 2005). After eight years of operation, the PRB still remains effective for reducing the concentration of Cr(VI) from higher than 1500 µg/L to less than 1 µg/L (Wilkin et al. 2005).

It is suggested that the metal reduction rate by zero-valent iron particles follows the general equation (Ponder et al. 2000):

$$v = kA_s [Me] \quad (6-2)$$

where v is the reaction rate, k is the rate constant ($M^{-1}m^2s^{-1}$), Me is the metal ion concentration (M), and A_s is the specific surface area of the iron particles (m^2/g). Eqn (6-2) indicates that the reaction rate is directly proportional to the specific surface area. Consequently, reducing particle size is expected to enhance the reduction reaction rate substantially. For example, according to Eqn (6-2), reducing the particle size from 10 μm to 10 nm would result in a surge in specific surface area, or the reaction rate, by six orders of magnitude. Ponder et al. (Ponder et al. 2000) reported a resin-supported nanoscale Fe(0) particles (Ferragels, 10-30 nm in diameter) to reduce Cr(VI) and Pb(II) in the aqueous solutions. They found that the reduction of Cr(VI) is 20-30 times greater than the commercial iron filings or iron powder on a Fe molar basis (Ponder et al. 2000).

However, Fe nanoparticles prepared using current methods tend to either agglomerate rapidly or react quickly with the surrounding media (i.e. dissolved oxygen or water), resulting in rapid loss in reactivity and mobility in soils (He and Zhao 2005a).

To prevent particles from agglomeration, researchers have been trying to prepare more stable and chemically more reactive Fe(0) nanoparticles using a dispersion agent as stabilizer. Chen et al. (Chen et al. 2004) reported a class of nanoscale iron particles cetylpyridinium chloride (CPC) as stabilizer, for nitrate removal from water. The nanoparticles offered a specific surface area of 25.4 m^2/g . He and Zhao (He and Zhao 2005b) reported a new class of starch-stabilized bimetallic nanoparticles to degrade TCE and PCBs. The surface area of the stabilized Fe nanoparticles was estimated to be $\sim 55m^2/g$ (He and Zhao 2005b). The permeability of the stabilized nano-particles was significantly enhanced in both sand and soils (Schrack et al. 2004). Other stabilizing agents were also reported to disperse nanoparticles, including macroporous polymeric

cation exchanger (Cumbal and Sengupta 2005), polyamidoamine (PAMAM) dendrimers (Zhao and Crooks 1999b; Zhao et al. 1998), Poly (acrylic acid) (PAA) (Schrick et al. 2002; Si et al. 2004), and carboxymethyl cellulose (CMC) (Magdassi et al. 2003; Si et al. 2004).

Recently, He and Zhao (He and Zhao 2005a; He and Zhao 2005b; He et al. 2006) developed a technique to prepare palladized iron (Fe-Pd) nanoparticles by applying low concentrations of a starch and cellulose (CMC) as stabilizers. TEM analyses indicated that the stabilized nanoparticles were present as discrete particles as opposed to dendritic flocs for non-stabilized particles. The stabilized nanoparticles exhibited markedly greater and sustained reactivity when used for dechlorination of TCE or PCBs in water.

The overall goal of this research was to test the feasibility of using the CMC-stabilized Fe nanoparticles for the reductive immobilization of Cr(VI) from Cr(VI) contaminated soil. The specific objectives of this work were to: (1) test the effectiveness of the CMC-stabilized nanoparticles for reducing Cr(VI) in water and a sandy-loam soil slurry under various experimental conditions, and (2) test the particles for reductive immobilization of Cr(VI) in a contaminated sandy-loam through batch and fixed-bed column experiments.

6.2 Materials and Methods

Chemicals used in this research include iron (II) sulfate heptahydrate ($\text{FeSO}_4 \cdot 7\text{H}_2\text{O}$, Acros Organics, Morris Plains, NJ, USA), sodium borohydride (NaBH_4 , ICN Biomedicals, Aurora, OH, USA), carboxymethyl cellulose (CMC, Acros Organics, Morris Plains, NJ, USA) in sodium form, sodium chromate tetrahydrate ($\text{Na}_2\text{CrO}_4 \cdot 4\text{H}_2\text{O}$,

Aldrich, Milwaukee, WI, USA), 1, 5-diphenylcarbohydrazide and acetone (Aldrich, Milwaukee, WI, USA).

A loamy sand soil, obtained from a local farm in Auburn, AL, USA was used in this study. The composition of the soil is listed in **Table 2-2**. Before use, the raw soil was sieved with a 2 mm standard sieve. The soil contains only 0.43% of organic matter and it was not contaminated with Cr(VI) initially. Cr(VI) was loaded to the soil by equilibrating 1 L of solution containing 315 mg/L Cr(VI) with 180 g of an air-dried soil sample in a batch reactor at pH 6.5, which resulted in a 83 mg/kg Cr(VI) concentration in the air-dried soil.

The stabilized zero-valent iron (Fe) nanoparticles were prepared in water by reducing Fe^{2+} to Fe^0 using BH_4^- in the presence of CMC as a stabilizer. Detailed preparation procedures are reported elsewhere (He and Zhao 2005b). In brief, stock FeSO_4 solution was added to a CMC solution to yield a solution with a desired concentration of Fe (0.04~0.12 g/L) and CMC (0.2%, w/w). Then, NaBH_4 stock solution was added to the flask dropwise through a burette and at 1.4 times of the stoichiometric amount. The stabilized Fe suspension was sealed and stored for 20 minutes before every use.

The stabilized Fe nanoparticles were then tested in batch experiments for reducing Cr(VI) in water. The batch kinetic tests were carried out in twenty of 15 mL glass vials. The reduction was initiated by injecting a Cr(VI) stock solution (Cr = 440 mg/L) into 15 mL of the Fe nanoparticle suspension, which resulted in an Fe concentration ranging from 0.04 to 0.12 g/L and an initial Cr(VI) concentration of 33.6 mg/L. Zero headspace was maintained in all vials. The mixtures were then shaken on a rotator and two vials

were sacrificed for analysis at pre-determined time intervals. The samples were transferred to centrifuge tubes and centrifuged at 5000 g-force with a high-speed centrifuge (AcuuSpin™ 400, Fisher Scientific, Pittsburgh, PA, USA). The total Cr as well as Cr(VI) concentration in the supernatant after centrifuging was analyzed, and the Cr(VI) reduction rate was calculated based on mass balance calculations. The initial and final pH was measured. A control test was conducted in parallel at an Fe concentration of 0.08 g/L and under otherwise identical conditions. All the experimental points were duplicated to assure data quality.

The reduction kinetics of Cr(VI) preloaded in the soil by Fe-nanoparticles was tested in both batch and column experiments. A total of three sets of batch kinetic tests were carried out, with an initial pH 9.0, 7.0 and 5.0, respectively. Each experimental set consisted of 20 15-mL testing vials, each of which received 1.5 g of the Cr(VI)-loaded soil and 15 mL of a nanoparticle suspension (Fe = 0.08 g/L) (soil : solution = 1 : 10). At predetermined times, the vials in duplicates were centrifuged at 5000 g-force, and the concentration of total Cr and Cr(VI) in the supernatant was measured. The final pH was also adjusted to the desired pH as 5.0, 7.0, and 9.0. For comparison, control tests were also carried out in parallel.

To test the effectiveness of the CMC-stabilized Fe nanoparticles for *in situ* reductive immobilization of Cr(VI), fixed-bed column experiments were conducted. The column setup consisted of an HPLC pump (Series II), a glass column (inner diameter of 1.0 cm and length of 10 cm; Omnifit, Cambridge, England) with adjustable ends (Omnifit, Cambridge, England), and a fraction collector (Eldex Laboratories, Napa, CA, USA). Five grams of the Cr(VI)-loaded soil were packed in the column, which resulted in a soil bed

volume (BV) of 3.14 mL. The hydraulic conductivity of the column was 0.25 cm/min. The Cr(VI)-laden soil bed was then treated by passing ~6 BVs of the Fe nanoparticle suspension (Fe = 0.08 g/L and pH = 5.6) through the soil bed in the up-flow mode. The flow rate was kept constant at 0.15 mL/min, which translates to an empty contact time (EBCT) of 21 min and a superficial velocity (SLV) of 4.24×10^{-5} m/s. A control column test was also performed in parallel but using deionized water at pH 5.6 as the influent. The concentration of total Cr and Cr(VI) in the column effluent was then followed. To quantify the soil transportability of the Fe nanoparticles, the concentration of total Fe in the influent and effluent was also analyzed and compared.

To investigate transportability of reduced Cr in the presence of the CMC stabilizer, an additional ‘two-bed’ column run was carried out, where another 5.0 g of the clean soil was packed on top of the original 5.0 g of the Cr-loaded soil bed. The experiment was conducted under otherwise the same conditions as in the one-bed column experiment. The Cr elution history at the exit of the two-bed column was analyzed and then compared with that of the one-bed column.

The effectiveness of Cr-immobilization by Fe nanoparticles was measured by comparing the leachability of Cr in the soil before and after the nanoparticle treatment. The leachability was quantified following the Toxicity Characteristic Leaching Procedure (TCLP, EPA method 1311) and Waste Extraction Test (WET, California HML Method 910). In TCLP tests, the prescribed Fluid #1 was used as the extractant. Soil samples were mixed with the TCLP fluid at a solid : solution ratio of 1 : 20. The mixtures were then rotated at 30 rpm at room temperature (21 °C) for 19 hours and then centrifuged at 500 g-force for 20 min. The supernatant was acidified to pH <2.0 with 1 N HNO₃ and

analyzed for Cr concentration. In the WET tests, soil samples were extracted with a citrate buffer solution for 48 hours at a solid : solution ratio of 1 : 10 on a rotating shaker. The mixtures were then centrifuged at 500 g-force, and the supernatants filtered with 0.45 micro membrane filters. The filtrate was then acidified to 5% by volume acid content with nitrate acid, and analyzed for Cr.

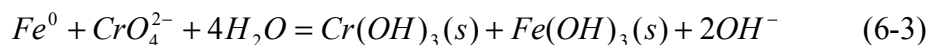
Total Cr was analyzed using a graphite atom absorption spectrophotometer (GF-AA, Perkin Elmer 3110). Cr(VI) was analyzed following the diphenylcarbohydrazide method (Standard Method 3500B), which employed a UV-Visible spectrophotometer (HP 8453) operated at 540 nm wavelength . Total Fe was analyzed using a flame atomic-absorption spectrophotometer (FLAA, Varian model 220FS).

6.3 Results and Discussion

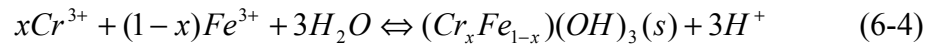
6.3.1 Reduction of Cr(VI) in water by Fe nanoparticles

Figure 6-1 shows the batch kinetic data during the reduction of Cr(VI) by CMC-stabilized Fe nanoparticles at an initial pH of ~9.0. For comparison, results from the control tests (without Fe but with the same concentrations of NaCMC and NaBH₄) were also plotted in **Figure 6-1**. It is evident that after reacting for 48 hours, the 0.08 g/L CMC-stabilized Fe nanoparticles reduced 53% of Cr(VI), while the control tests did not show any significant reduction.

It has been proposed that elemental Fe reduces Cr(VI) to Cr(III) according to Eqn (6-3) (Astrup et al. 2000; Buerge and Hug 1998; Melitas et al. 2001; Powell et al. 1995):



In the absence of a stabilizer, the resultant $\text{Cr}(\text{OH})_3$ is a sparingly soluble compound ($K_{sp} = 6.3 \times 10^{-31}$), and thus, can be easily separated from water. In addition, Cr(III) can also be removed by a surface precipitation process by forming the Fe(III)-Cr(III) hydroxide according to Eqn (6-4) (Astrup et al. 2000; Blowes et al. 1997; Patterson et al. 1997; Powell et al. 1995; Wilkin et al. 2005):



where, x is equal to 0.75. The solubility of $\text{Cr}_x\text{Fe}_{1-x}(\text{OH})_3$ is less than that of pure $\text{Cr}(\text{OH})_3$. Another form of the Cr precipitation $\text{Cr}_x\text{Fe}_{1-x}\text{OOH}$ has also been reported (Cao and Zhang 2006).

The initial (<4 hours) reduction rate of Cr(VI) can be described by a pseudo-first-order kinetic model (Alowitz and Scherer 2002; Ponder et al. 2000):

$$\frac{d[C]}{dt} = -k_{obs}[C] \quad (6-5)$$

where C is the concentration of Cr(VI) in water (mg/L), t the time (h), and k_{obs} the observed first-order rate constant (h^{-1}). The value of k_{obs} was determined to be 0.08 h^{-1} by fitting the solution of Eqn (6-5) to the initial reduction rate data of Cr(VI) in **Figure 6-1**. A similar approach was also used by (Alowitz and Scherer 2002) and Ponder et al. (2000) for determining the initial rate constant. The observed value of k_{obs} in this study is lower than the reported 1.18 h^{-1} where a resin supported Fe was employed at an Fe(0) concentration of 0.226 g/L and with an initial Cr(VI) concentration of 26 mg/L (Ponder et al. 2000). It has been reported that the rate constant increases linearly with the increasing

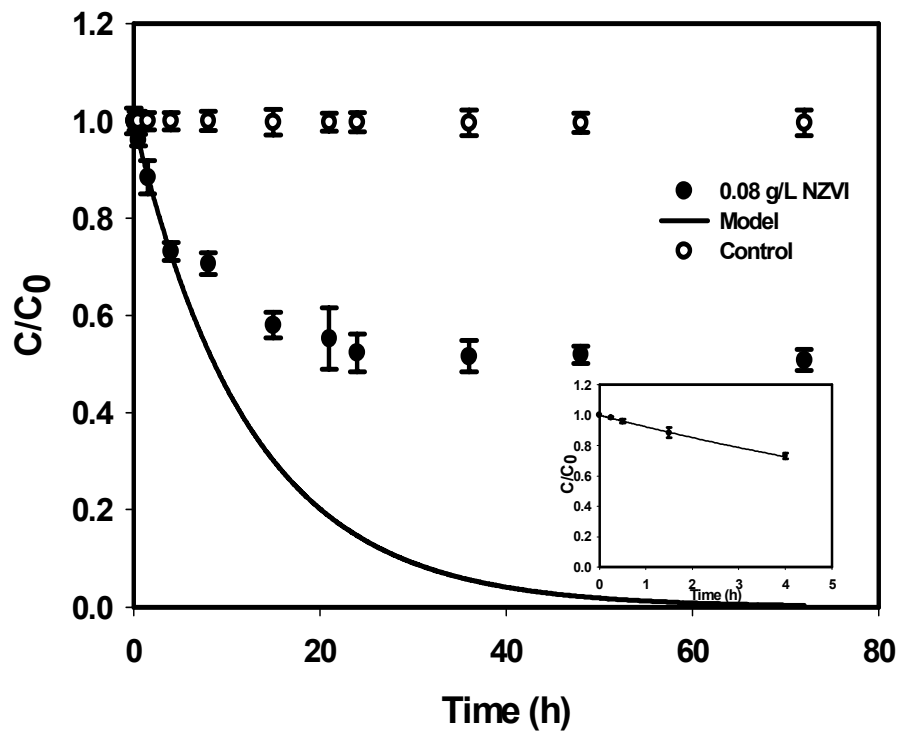


Figure 6-1. Reduction of Cr(VI) in water by CMC-stabilized Fe nanoparticles. NaCMC = 0.2% (w/w); Fe = 0.08 g/L; initial Cr = 33.6 mg/L (inset: Cr(VI) removal within the first 4 hours fitted with the first-order reaction model; Symbols: experimental data, Lines: model fitting. Data given as means of duplicates and errors refer to standard deviation).

Fe concentration (Alowitz and Scherer 2002; Ponder et al. 2000) but decreases with increasing initial Cr(VI) concentration. The Fe concentration in this study was 2.8 times lower than that used by Ponder et al. (2000) and the initial Cr(VI) concentration of 34 mg/L in this study was ~31% greater than that (26 mg/L) by Ponder et al. (Ponder et al. 2000).

Ponder et al. (Ponder et al. 2000) also reported that 90% of the Cr(VI) reduction occurred within the first 48 for both resin-supported or unsupported Fe nanoparticles based on batch tests running for 60 days. **Figure 6-1** indicates that equilibrium was reached after 40 hours in this study, which is slightly faster than that observed by Ponder et al. (2000).

According to Eqn (6-3), the stoichiometric amount of Fe required to completely reduce the initial 34 mg/L Cr(VI) is 0.035 g/L. The Fe dosage (0.08 g/L) in **Figure 6-1** is ~2.3 times greater than the stoichiometric quantity. However, only 53% of Cr(VI) was reduced at equilibrium, which was reached after ~40 hours. **Figure 6-1** also indicates that Cr(VI) removal after 4 hours remarkably deviates from the first-order rate model, i.e. the reaction rate becomes much slower than the model-predicted rate. The decrease of the reaction rate is attributed to two factors. First, the Fe nanoparticles are extremely reactive when they are fresh. In addition to the reaction with the targeted Cr(VI), the Fe nanoparticles can also undergo reaction with water via (Ponder et al. 2001):



This side reaction can diminish both the reaction rate and extent of Cr(VI) reduction. Second, the CMC molecules in the system not only stabilize the Fe nanoparticles, they

can also complex with Cr^{3+} and Fe^{3+} ions and their hydroxides. In other words, CMC also stabilizes the metal hydroxide precipitates. The initial pH of the solution in the batch tests was ~ 9.0 , and the final pH was increased to $9.2\sim 9.4$, which was high enough for $\text{Cr}(\text{OH})_3$ to precipitate based on the K_{sp} of 6.3×10^{-31} . However, no visible precipitation of $\text{Cr}(\text{OH})_3$ was observed during the reaction. The accumulation of Cr^{3+} in the system may also slow down the reaction according to Eqn (6-3).

To further test the effect of the competitive side reaction on the extent of Cr(VI) reduction, parallel batch experiments were carried out with an Fe concentration of 0.04 g/L, 0.08 g/L, and 0.12 g/L, respectively, and under otherwise identical conditions. As shown in **Figure 6-2**, after 48 hours reaction, the percentage removal of Cr(VI) increased from 24% to 90% as the Fe dosage was increased from 0.04 g/L to 0.12 g/L. Evidently, at an Fe dosage of ~ 3.4 times the stoichiometric amount, the stabilized nanoparticles can reduce over 90% Cr(VI) under ambient conditions. Compared to the results obtained by Ponder et al. (Ponder et al. 2000), who reported a 24% Cr(VI) reduction at an Fe(0) dosage of >8.7 times the stoichiometric amount for 8 days, the CMC stabilized ZVI nanoparticles was more effective.

6.3.2 Reduction of Cr(VI) sorbed in soil

After having investigated the effectiveness of NZVI to reduce Cr(VI) in aqueous phase, we then applied NZVI to reduce and immobilize Cr(VI) in the contaminated soil. **Figure 6-3** shows the kinetic results of Cr(VI) reduction from soil at pH 9.0. Both total Cr and Cr(VI) were analyzed for each point. Equilibrium was reached after 21 hours. In the presence of NZVI, 18% of the initially loaded Cr was released at equilibrium. There

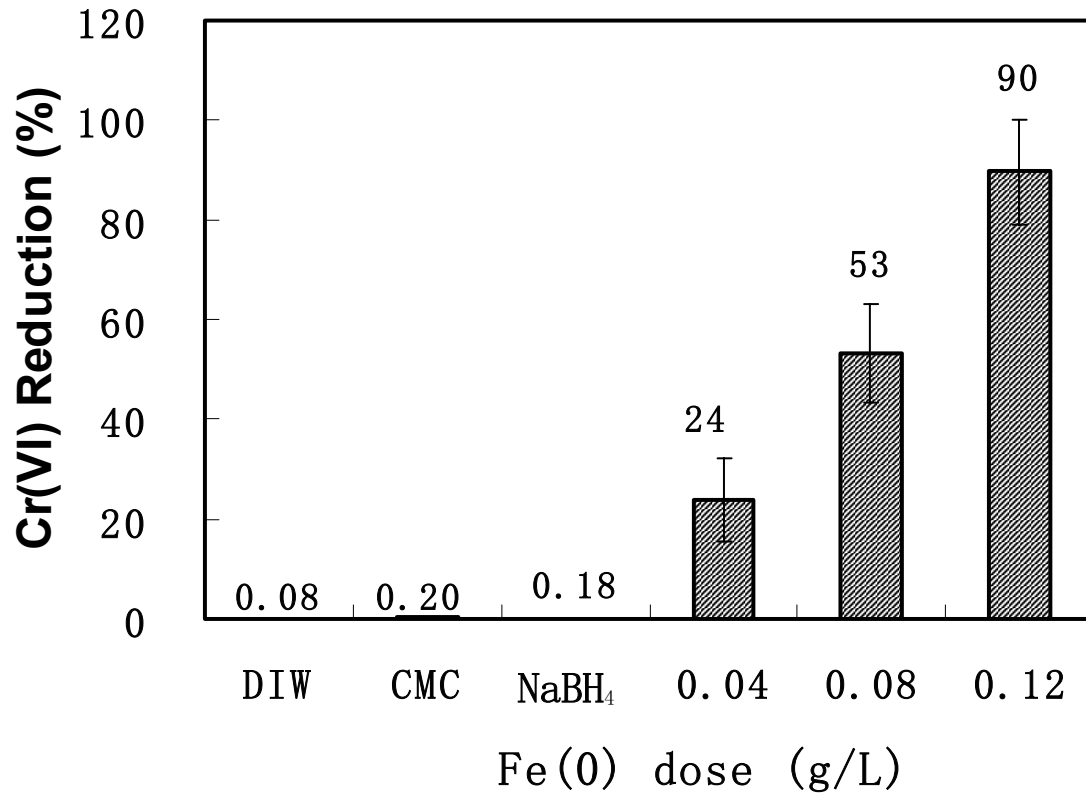


Figure 6-2. Cr(VI) reduction by NZVI with different Fe(0) dose and with DIW, CMC, or NaBH₄.

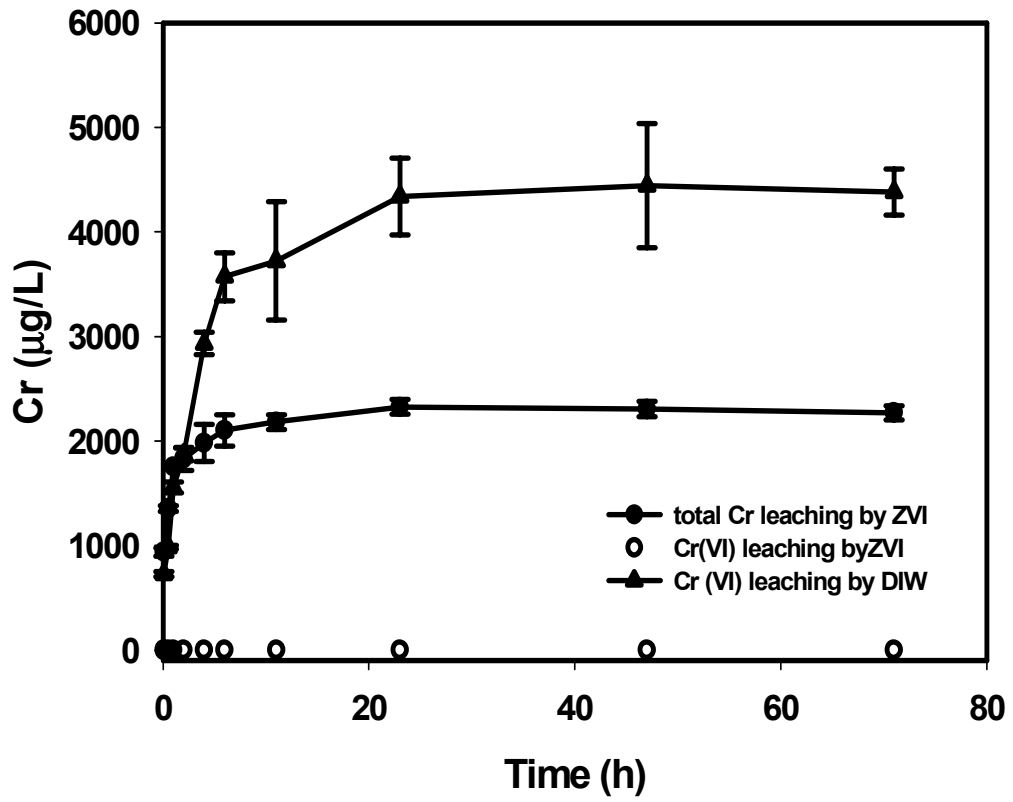


Figure 6-3. Leaching of Cr from contaminated soil using 0.08 g/L ZVI nanoparticles or DI water in batch test.

was no Cr(VI) detected in the solution, which means all the desorbed Cr(VI) was reduced to Cr³⁺ by Fe(0).

To assess the effect of solution pH on Cr(VI) reduction and immobilization in contaminated soil, batch tests were conducted at three pH values: 9.0, 7.0, and 5.0.

Figure 6-4 shows that total amount of Cr released from the soil at equilibrium for the same soil either untreated (with DI water only) or treated with 0.08 g/L Fe suspension and at the three pH levels. As the solution pH was increased from 9.0 to 5.0, the DI-water desorbed Cr(VI) was reduced from 30% to 20%. This observation is no surprising given that at higher pH the soil sorption sites become more negative and OH⁻ ions compete more fiercely with CrO₄²⁻ for the binding sites. However, for the Fe-treated soil, only 11% ~ 12% of the pre-sorbed Cr(VI) was released in the pH range of 5.0~9.0, and all desorbed Cr was detected as Cr(III). In addition, desorption of Cr from the treated soil was less pH dependent, and the total Cr release was only increased by less than 2% when pH was changed from 9.0 to 5.0. The less pH dependence of Cr release is attributed to the stabilizer CMC, which stabilized the Cr³⁺ and Fe³⁺ cations in the solution.

These results indicate that NZVI is a good candidate for removal of Cr(VI) from soil by two means: 1) it reduced Cr(VI) to Cr(III) by the mechanism described by eqn (6-3); and 2) it inhibits the release of Cr from soil to aqueous phase. The precipitated Cr(OH)₃, Cr_xFe_{1-x}OOH, Cr_xFe_{1-x}(OH)₃, and the adsorbed NZVI on the soil surface provides long term protection of Cr leaching to aqueous (Cao and Zhang 2006).

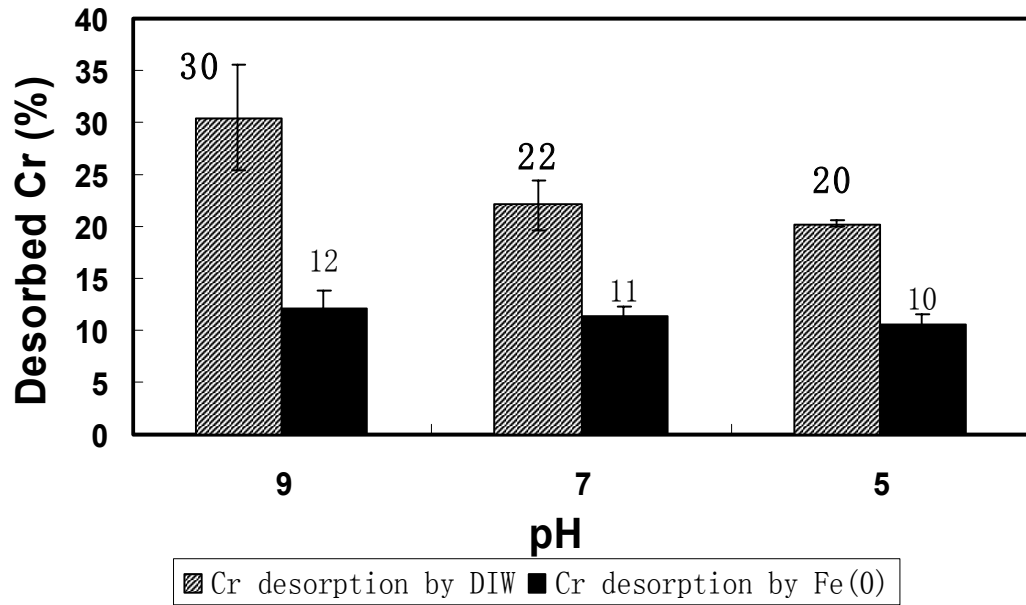
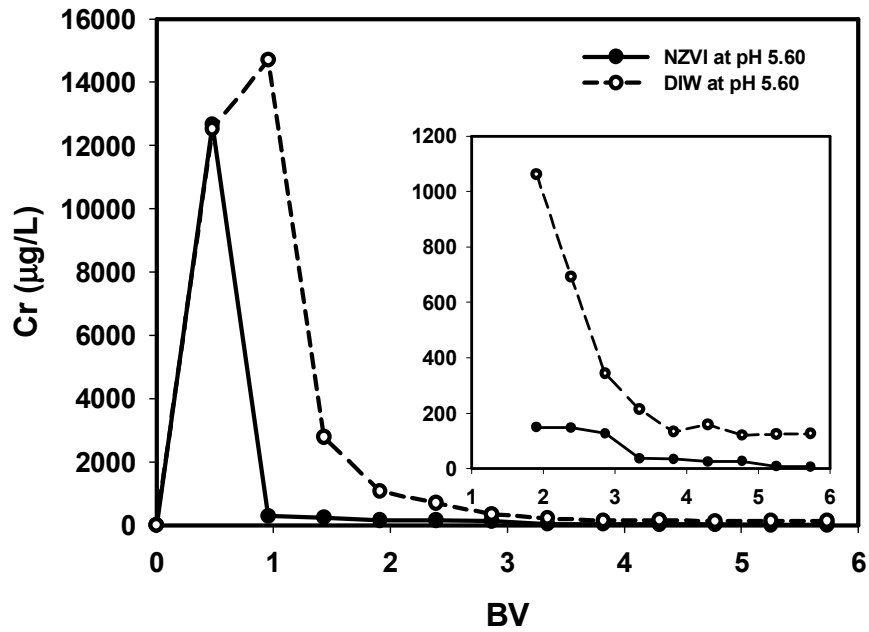


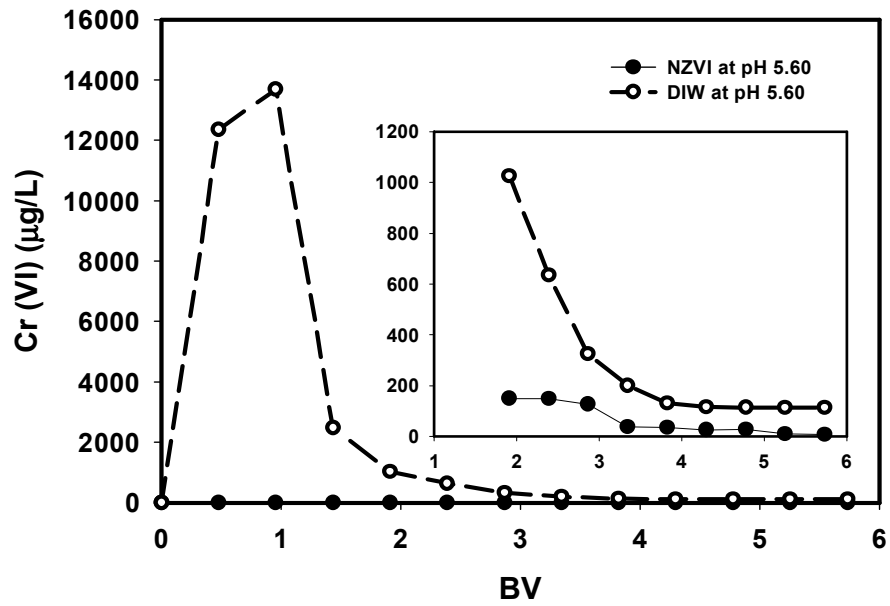
Figure 6-4. Cr(VI) desorption from contaminated soil by nanoscale Fe(0) or DI water at pH 9.0, 7.0, and 5.0.

6.3.3 Reductive immobilization of Cr(VI) in soil: column tests

The foregoing batch test results reveal the great promise of the CMC-stabilized Fe nanoparticles for reductive immobilization of Cr(VI) in soils and water. However, to facilitate the *in situ* application of the Fe nanoparticles, some key technical criteria must be satisfied, including 1) the Fe nanoparticles must be transportable or injectable in soils, and 2) the application of the CMC-stabilized Fe nanoparticles must not cause any more mobilization/dissolution of Cr than groundwater as in the natural subsurface environment. To address these issues, the Fe nanoparticles are also tested in a set of fixed-bed column experiments. **Figure 6-5** shows the chromium elution histories during two separate column runs when 0.08 g/L Fe nanoparticle suspension at pH 5.60 or DI-water was pumped through the Cr-loaded soil bed under otherwise identical conditions. As shown in **Figure 6-5 (a)**, the elution of total Cr with DIW displayed a much higher and broader peak as well as and a longer tailing than with the Fe nanoparticle suspension. Mass balance calculation reveals that DI-water eluted a total of ~12% of the pre-sorbed Cr(VI), while the Fe suspension leached only ~4.9%.. When plotted as Cr(VI), **Figure 6-5 (b)** shows that the Fe nanoparticle suspension essentially eluted no chromate, i.e. the Fe nanoparticles converted all of the 4.9% Cr(VI) eluted from the soil bed to Cr(III) during the treatment.



(a)



(b)

Figure 6-5. Cr elution histories during two separate column runs using NZVI or DIW at pH 5.60 ((a) total Cr; (b) Cr(VI); insets: Cr elution histories after 1.9 BVs).

To compare the physico-chemical availability of Cr in the soil before and after the treatment with ~5.7 BVs of the Fe nanoparticle suspension (**Figure 6-5**), Cr leachability tests were performed following the standard TCLP approach (EPA method 1311) and WET (California HML Method 910). The TCLP results indicated that the equilibrium Cr concentration in the TCLP extractant was 0.4 mg/L for the untreated soil. In contrast, when the same soil was treated with ~5.7 BVs of the Fe nanoparticles at pH 5.60, the TCLP-leached Cr concentration was reduced to 0.04 mg/L, i.e. the brief treatment can reduce the soil's TCLP leachability by one order of magnitude or 90%. In addition, all TCLP-leached Cr for the treated soil was found in the less toxic form of Cr(III). Compared to the TCLP fluid, the WET employs a much more aggressive extracting agent (citric acid for WET vs. acetic acid for TCLP). As a result, the leached Cr in the WET extractant was 1.2 mg/L for the same untreated soil (3 times greater than in the TCLP fluid). Upon the treatment by Fe nanoparticles treatment, the WET-leached Cr concentration was reduced to 0.28 mg/L, a reduction of ~76%.

The extracted Cr in both TCLP and WET tests was far below the regulated TCLP or WET limit (5 mg/L for TCLP and WET), which is commonly applied to classifying hazardous wastes in the U.S. The above results suggest that the Fe-nanoparticles may also be applied to treat Cr(VI)-laden solid wastes, which may greatly minimize Cr(VI) leachability and cut down the handling and disposal cost of hazardous materials.

The influent pH of 5.6 was chosen to mimic the groundwater pH. In both cases, the effluent pH was at around 5.2 ~ 5.7. Rai and Zachara (Rai and Zachara 1986) have reported that, in the pH range of 4.0 to 6.5, CrOH^{2+} ions are the dominant species of Cr^{3+} . They are either adsorbed on the iron surface or precipitate as chromium-iron hydroxide

solid. Compared to the column results by DIW, the mobility of Cr was reduced by more than 58%. The fact that ZVI still eluted some Cr indicates that the Cr^{3+} ions were still stabilized by CMC. This form of Cr is non-toxic and after a long time run when CMC is degraded, it will precipitate.

The column results indicate that the stabilized NZVI was able to go through the soil bed and react with Cr(VI) sorbed on soil. During the column run of ~6BVs' NZVI, the flow rate remained constant, which tells that the NZVI did not agglomerate on the soil surface. Although the less eluted Cr indicates that Cr was immobilized by reactions (3) and (4), the precipitation had no effect on the flow rate. The iron concentration in the effluent was also analyzed and over 80% of the initial Fe passed through the pump.

In the two-bed column runs, a clean soil bed with the same volume was packed on the contaminated soil bed. The unit bed volume of one bed was used for the calculation of BVs of the effluent in all cases. When the two beds column was run with NZVI, one unit bed volume was still used for the calculation of solution BVs for the x-axis in **Figure 6-6** for the purpose of comparison. **Figure 6-6** shows that the elution of total Cr had a lower peak than that of the one bed column. About 4.3% of the total sorbed Cr was eluted and no Cr(VI) was detected. The difference tells that the clean soil bed took up some of the eluted Cr. In the field, if the reduced Cr^{3+} goes through a long distance, less Cr will be leached out.

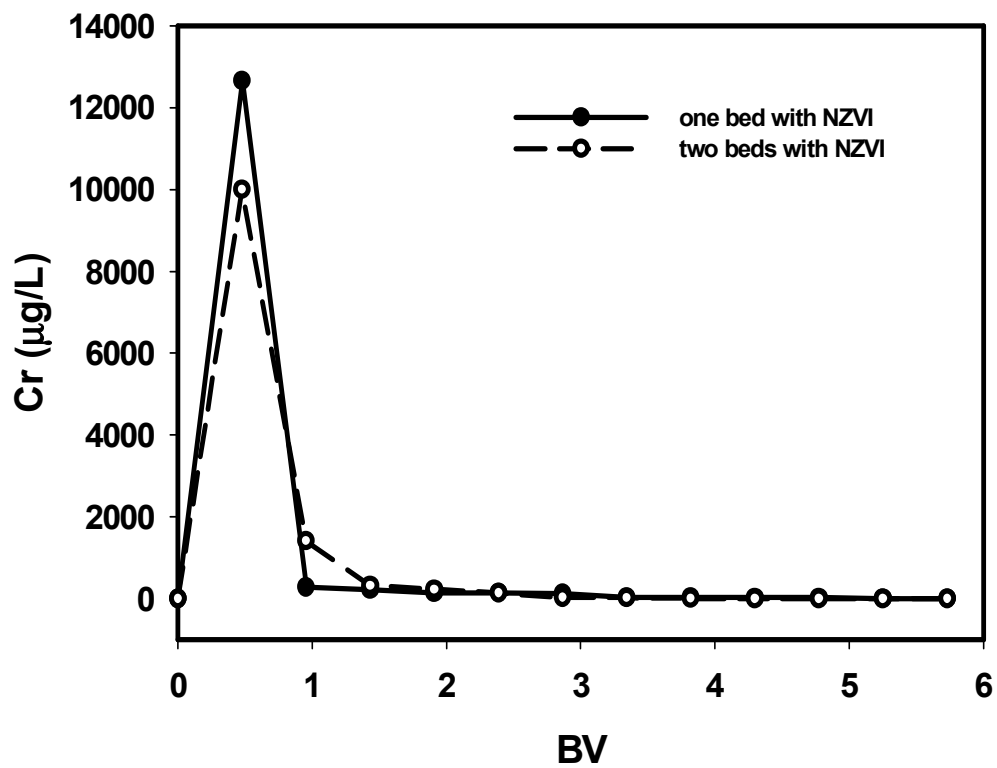


Figure 6-6. Cr elution histories during two separate column runs with one or two beds using NZVI at pH 5.60.

6.4 Summary and Conclusions

Hexavalent chromium reduction from soil has been one of the most challenging environmental issues. This study investigated the feasibility of using CMC stabilized nanoscale zero-valent iron to reduce Cr(VI) in aqueous phase and soil phase by batch and column experiments. The major results are summarized as follows:

- (1) NZVI is able to reduce Cr(VI) in both aqueous phase and soil phase.
- (2) The Cr(VI) reduction rate was 0.08 h^{-1} at an initial Cr(VI) concentration of 34 mg/L with 0.08 g/L NZVI, which was relatively high at this low initial Fe(0)/Cr(VI) ratio.
- (3) When the NZVI dose was increased from 0.04 g/L to 0.12 g/L, the Cr(VI) reduction rate in aqueous phase was increased from 24% to 90%.
- (4) Compared to Cr leach from soil by DIW, NZVI not only reduced the leachability, but also reduced all the Cr(VI) form to Cr(III) in the leached Cr. Batch experiments for Cr(VI) reduction in soil showed that pH had insignificant effect on Cr release because CMC stabilized Cr(III) and Fe(III).
- (5) CMC stabilized NZVI showed great transportability through soil bed in the column tests. The leachability of Cr was reduced by 59% with NZVI. All the leached Cr was in the less toxic form of Cr(III).
- (6) The availability of Cr in the soil was greatly reduced after NZVI treatment. Compared to the untreated soil, WET results indicated a availability reduction of 76% while TCLP had a reduction of 90%.

Results obtained from this study suggest that stabilized nanoscale zero-valent iron is able to reduce and immobilized Cr(VI) in soil. This research provides promising evidence for the *in situ* remediation of Cr(VI) contaminated soil using stabilized NZVI. Meanwhile,

additional work is needed to better understand the reaction mechanism and speciation of the reaction products between Cr(VI) and ZVI nanoparticles.

CHAPTER 7. CONCLUSIONS AND SUGGESTIONS FOR FUTURE RESEARCH

7.1 Summary and Conclusions

Application of various synthetic nanoparticles for environmental remediation has attracted great interests in recent years. For the first time, this research investigated the feasibility of using poly(amidoamine) (PAMAM) dendrimers, a class of nanoscale macromolecules, for extraction of heavy metals (Cu^{2+} and Pb^{2+}) from various contaminated soils. Detailed experimental investigations were also carried out to determine the effects of various operating parameters such as dendrimer dosage, generation number, pH, terminal groups, ionic strength, and soil type on the metal extraction efficiency.

Over 90% of copper initially sorbed in a sandy soil was removed using ~66 bed volumes of 0.10% (w/w) of a generation 4.5 dendrimer with carboxylate terminal groups at pH 6.0. A lead removal of 92% from the sandy soil was achieved using ~120 BVs of 0.3% (w/w) of a generation 1.5 dendrimer with carboxylate terminal groups at pH 4.0. Based on equal equivalent dose, dendrimers of lower generation removed more copper or lead, and lowering pH enhanced copper or lead removal for all dendrimers tested. The lead removal was more effective for a sandy soil than for a clay soil. In contrast, types of terminal groups (carboxylate, amine, or hydroxyl) showed modest effect on the removal efficiency. Results from a sequential extraction procedure suggested that the dendrimer

treatment of a soil removed primarily exchangeable and carbonate-bound copper, which corresponds to the most easily available fraction of Cu sorbed in the soil. The residual copper in dendrimer-treated soil was predominantly bound with soil organic matter (SOM), which is much less available physical-chemically or biologically. The sequential extraction also indicated that dendrimer treatment removed primarily (>82%) carbonate-bound Pb^{2+} , and TCLP test revealed that the residual lead in the dendrimer-treated soil was much less leachable. About 95% of the spent dendrimers was recovered by a commercially available nanofiltration device. The metal sorption capacity was then fully recovered upon regeneration of recovered dendrimers with dilute 2N hydrochloric acid. About 96% of Pb^{2+} in the solution can be retained by the nano-filter, and ~94% of the retained Pb^{2+} can be desorbed upon acid regeneration. After acid regeneration, recovered dendrimers were reused for extracting pre-sorbed Cu^{2+} in soils, and they performed equally well as the virgin dendrimers. The dendrimers may be used as reusable, high-capacity extracting agents for in-situ removal of heavy metals from contaminated soils.

A modified ion exchange method was developed to determine the conditional stability constant (K_c) and the metal-to-dendrimer molar ratio (n) of the metal-dendrimer complexes. This method employs a system containing an ion exchange resin, a dendrimer, and a metal solution. It considers the multi-dentate nature of dendrimer molecules, and employs a non-linear (Langmuir) isotherm model to interpret the ion exchange isotherm. For its minimal interaction with dendrimers, a weak acid cation exchange resin, IRC-50, was chosen for the study. For a generation 1.0 dendrimer with primary amine terminal groups (G1.0-NH₂), the K_c value for Cu^{2+} -dendrimer complexes was determined to be $10^{20.0}$ at pH 5.0 and $10^{25.8}$ at pH 7.0. For the same family of dendrimers, the K_c value

increased from $10^{16.2}$ to $10^{34.1}$ and the n value increased from 1 to 12 as the generation number rose from 0 to 4. The conditional stability constant for Pb^{2+} -(G1.0-NH₂) complexes was determined to be $10^{17.2}$ at pH 5, compared to $10^{20.9}$ for complexes of Pb^{2+} with a generation 1.5 dendrimer with carboxylate terminal groups. The revised method may provide a simple and useful means for quantifying poly-nuclear binding of metals with poly-dentate ligands such as dendrimers.

A two-site model was developed to simulate the copper (II) and lead (II) elution histories from a sandy soil using various dendrimers. Tell how the model was developed? Modeling results indicate that Cu^{2+} bound to soil had a greater (33% for Copper and 2% for lead) fraction of fast desorption site than Pb^{2+} , and the desorption rate of Cu^{2+} was faster than Pb^{2+} for both fractions. Compared to the classical “one-site” model and the modified “gamma distribution” model, the “two-site” model not only provided much improved power for simulating the observed metal elution data from the column experiments, but it also served as a powerful tool for predicting the metal elution histories under various experimental conditions including initial metal concentration in soil, dendrimer dosage, and treatment pH.

Laboratory batch and column experiments were conducted to investigate the feasibility of using stabilized zero-valent iron nanoparticles to reduce and immobilize Cr(VI) in soil. In the batch tests for aqueous Cr(VI) reduction, the presence of 0.08 g/L Fe nanoparticles was able to reduce 53% of the initial 34 mg/L Cr(VI) at pH 9.0 with an initial observed first-order rate constant of 0.08 h^{-1} . The extent of Cr(VI) reduction was increased from 24% to 90% when the Fe concentration was increased from 0.04 g/L to 0.12 g/L. When tested in a column filled with a sandy-loam, the stabilized Fe

nanoparticles were highly transportable in the soil bed. When the Cr-laden soil bed was treated with 5.7 BVs of 0.08 g/L Fe nanoparticles at pH , the TCLP-based leachability of Cr from the soil was reduced by 90%, and WET-based leachability by 76%. Only 4.9% of the total Cr was eluted during the treatment compared to 12% when deionized water was passed through the soil bed under otherwise the same conditions.

Results obtained from this research show that it is very promising to apply the CMC-stabilized Fe nanoparticles for the *in situ* reductive immobilization of chromate in various contaminated soils.

7.2 Suggestions for Future Work

Dendrimers have been widely investigated for drug delivery systems, but only limited studies have been reported on the toxicity and biodistribution of dendrimers as DNA transfection reagents by means of *in vitro* and *in vivo* have been published. Malik et al. (Malik et al. 2000) and Jevprasephant et al. (Jevprasesphant et al. 2003) found that the whole generation PAMAM dendrimers with $-NH_2$ terminal groups displayed concentration and generation dependent cytotoxicity and changes in red cell morphology. They suggested that the dendrimer structure must be carefully tailored to avoid rapid hepatic uptake. Jevprasephant et al. (Jevprasesphant et al. 2003) also found that the cytotoxicity of the whole generations of dendrimer was greater than that of the half generations. Hong et al. (Hong et al. 2004) investigated the mechanism of how PAMAM dendrimers altered cells using fluorescence microscopy, lactate dehydrogenase (LDH), luciferase (Luc) assays, and flow cytometry. They revealed that a G7.0- NH_2 dendrimer could form holes of 15-40 nm in diameter in aqueous, supported bilayers, while a G5.0-

NH₂ dendrimer did not initiate the formation of holes but expanded holes at existing defects. These studies suggest that it is possible to synthesize non-toxic and biodegradable dendrimers through a judicious selection of the dendrimer building blocks such as core and terminal group.

However, to the best of our knowledge, no investigations on the hydrolytic, oxidative, photochemical, and biological stability of nanomaterials including dendrimers and Fe(0) nanoparticles in natural and engineered environmental systems have been published. Although this research showed attractive results for the remediation of heavy metal contaminated soils using the nanoparticles, two questions remain unanswered. One is the fate and transport of the nanoparticles in environment, and the other is the environmental impacts of nanoparticles. The environmental fate and toxicity of a material are of critical importance in selection and design of environmental remediation techniques.

Research on nanoparticle toxicology and research on their fate and transport have been two of the common research priorities for nanotechnology environment and safety research (Dunphy Guzman et al. 2006). Research related to this area has established its foundations even before the establishment of National Nanotechnology Initiative (NNI). However, researchers have focused mainly on the nanoparticulate aerosols by the atmospheric toxicologists and ultrafine particles (UFP) by toxicologists (Biswas and Wu 2005). It has been reported that concentrations of incidental nanoparticle aerosols would decay with distance from the source (Smith and Harrison 1996). In a review of toxicology of nanoparticles based on the observations of UFP toxicology (Oberdorster et al. 2005), it was pointed out that some smaller nanoparticles showed increased toxicity

due to the increased surface area. However, particle structure and composition may also play a role in toxicity other than particle size (Dunphy Guzman et al. 2006).

The overall understanding of the environmental impact of nanoparticles is dependent on the investigation of how environmental conditions such as pressure, biochemical reactions over time, solution chemistry, and presence or absence of coatings. More information is needed in order to gain regulatory and public acceptance for using nanomaterials in environmental remediation because of their unknown toxicity and environmental impact. Therefore, future work should consider the transport and fate of nanoparticles in environment.

Modeling the reductive immobilization of Cr(VI) by ZVI nanoparticles is also an interesting area. In addition, this research focused on the lab experiments for remediation of heavy metal contaminated soils using nanoparticles. Pilot/field tests and cost analysis are necessary for the development of a new technology.

REFERENCES

- Adesina, A. A. (2004). "Industrial Exploitation of Photocatalysis: Progress, Perspectives and Prospects." *Catalysis Surveys from Asia*, 8(4), 265-273.
- Ahn, I.-S., Lion, L. W., and Shuler, M. L. (1999). "Validation of a Hybrid "Two-Site Gamma" Model for Naphthalene Desorption Kinetics." *Environmental Science and Technology*, 33(18), 3241-3248.
- Al-Hamdan, A., and Reddy, K. (2006). "Geochemical Reconnaissance of Heavy Metals in Kaolin after Electrokinetic Remediation." *Journal of Environmental Science and Health, Part A: Toxic/Hazardous Substances & Environmental Engineering*, 41(1), 17-33.
- Alkorta, I., Hernandez-Allica, J., Becerril, J. M., Amezaga, I., Albizu, I., and Garbisu, C. (2004). "Recent Findings on the Phytoremediation of Soils Contaminated with Environmentally Toxic Heavy Metals and Metalloids Such as Zinc, Cadmium, Lead, and Arsenic." *Reviews in Environmental Science and Bio/Technology*, 3(1), 71-90.
- Allen, H. E., and Chen, P.-H. (1993). "Remediation of Metal Contaminated Soil by EDTA Incorporating Electrochemical Recovery of Metal and EDTA." *Environmental Progress*, 12(4), 284-293.

- Alowitz, M. J., and Scherer, M. M. (2002). "Kinetics of Nitrate, Nitrite, and Cr(VI) Reduction by Iron Metal." *Environmental Science and Technology*, 36(3), 299-306.
- Alvarez-Ayuso, E., Garcia-Sanchez, A., and Querol, X. (2003). "Purification of metal electroplating wastewaters using zeolites." *Water Research*, 37(20), 4855-4862.
- An, B., Steinwinder, T. R., and Zhao, D. (2005). "Selective removal of arsenate from drinking water using a polymeric ligand exchanger." *Water Research*, 39(20), 4993-5004.
- Asahi, R., Morikawa, T., Ohwaki, T., Aoki, K., and Taga, Y. (2001). "Visible-light photocatalysis in nitrogen-doped titanium oxides." *Science (Washington, DC, United States)*, 293(5528), 269-271.
- Astrup, T., Stipp, S. L. S., and Christensen, T. H. (2000). "Immobilization of Chromate from Coal Fly Ash Leachate Using an Attenuating Barrier Containing Zero-valent Iron." *Environmental Science and Technology*, 34(19), 4163-4168.
- Bae, E., and Choi, W. (2003). "Highly Enhanced Photoreductive Degradation of Perchlorinated Compounds on Dye-Sensitized Metal/TiO₂ under Visible Light." *Environmental Science and Technology*, 37(1), 147-152.
- Balogh, L., Swanson, D. R., Tomalia, D. A., Hagnauer, G. L., and McManus, A. T. (2001). "Dendrimer-Silver Complexes and Nanocomposites as Antimicrobial Agents." *Nano Letters*, 1(1), 18-21.
- Bartlett, R. R., and James, B. R. (1998). *Chromium in the natural and human environments*, Wiley & Sons, New York, USA.

- Berti, W. R., and Cunningham, S. D. (1997). "In-Place Inactivation of Pb in Pb-Contaminated Soils." *Environmental Science and Technology*, 31, 1359-1364.
- Biswas, P., and Wu, C.-Y. (2005). "Nanoparticles and the environment." *Journal of the Air & Waste Management Association*, 55(6), 708-746.
- Blowes, D. W., Ptacek, C. J., and Jambor, J. L. (1997). "In-Situ Remediation of Cr(VI)-Contaminated Groundwater Using Permeable Reactive Walls: Laboratory Studies." *Environmental Science and Technology*, 31(12), 3348-3357.
- Brewster, M. D., Peters, R. W., Miller, G. A., Li, W., Patton, T. L., and Martino, L. E. (1995). "Physical/Chemical Treatment of Metals-Contaminated Soils." *Waste Processing and Recycling in Mineral and Metallurgical Industries II, Proceedings of the International Symposium on Waste Processing and Recycling in Mineral and Metallurgical Industries, 2nd, Vancouver, B. C., Aug. 20-24, 1995*, 539-65.
- Bryan, N. D., Barlow, J., Warwick, P., Stephens, S., Higgs, J. J. W., and Griffin, D. (2005). "The Simultaneous Modeling of Metal Ion and Humic Substance Transport in Column Experiments." *Journal of Environmental Monitoring*, 7(3), 196-202.
- Buerge, I. J., and Hug, S. J. (1998). "Influence of Organic Ligands on Chromium(VI) Reduction by Iron(II)." *Environmental Science and Technology*, 32(14), 2092-2099.
- Buerge, I. J., and Hug, S. J. (1999). "Influence of Mineral Surfaces on Chromium(VI) Reduction by Iron(II)." *Environmental Science and Technology*, 33(23), 4285-4291.

- Cakara, D., Kleimann, J., and Borkovec, M. (2003). "Microscopic Protonation Equilibria of Poly(amidoamine) Dendrimers from Macroscopic Titrations." *Macromolecules*, 36(11), 4201-4207.
- Cameron, R. E. (1992). "Guide to Site and soil description for hazardous waste site characterization. Volume 1: Metals. Environmental Protection Agency EPA/600/4-91/029."
- Cantrell, K. J., Kaplan, D. I., and Wietsma, T. W. (1995). "Zero-Valent Iron for the *In Situ* Remediation of Selected Metals in Groundwater." *J. Hazard. Mater.*, 42(2), 201-12.
- Cao, J., and Zhang, W.-X. (2006). "Stabilization of chromium ore processing residue (COPR) with nanoscale iron particles." *J. Hazard. Mater.*, 132(2-3), 213-219.
- Cao, X., Ma, L. Q., Rhue, D. R., and Appel, C. S. (2004). "Mechanisms of Lead, Copper, and Zinc Retention by Phosphate Rock." *Environmental Pollution (Amsterdam, Netherlands)*, 131(3), 435-444.
- Chechik, V., and Crooks, R. M. (2000). "Dendrimer-Encapsulated Pd Nanoparticles as Fluorous Phase-Soluble Catalysts." *Journal of the American Chemical Society*, 122(6), 1243-1244.
- Chen, S.-S., Hsu, H.-D., and Li, C.-W. (2004). "A New Method to Produce Nanoscale Iron for Nitrate Removal." *Journal of Nanoparticle Research*, 6(6), 639-647.
- Chen, W., Tomalia, D. A., and Thomas, J. L. (2000). "Unusual pH-Dependent Polarity Changes in PAMAM Dendrimers: Evidence for pH-Responsive Conformational Changes." *Macromolecules*, 33(25), 9169-9172.

- Chen, W., and Wagenet, R. J. (1995). "Solute Transport in Porous Media with Sorption-Site Heterogeneity." *Environmental Science and Technology*, 29(11), 2725-34.
- Chitose, N., Ueta, S., Seino, S., and Yamamoto, T. A. (2003). "Radiolysis of Aqueous Phenol Solutions with Nanoparticles. 1. Phenol Degradation and TOC Removal in Solutions Containing TiO₂ induced by UV, g-ray and Electron Beams." *Chemosphere*, 50(8), 1007-1013.
- Clark, J. S., and Turner, R. C. (1969). "An Examination of the Resin Exchange Method for the Determination of Stability Constant of Metal-soil Organic Matter Complexes." *Soil Sci.*, 107, 8-11.
- Clement, T. P., Hooker, B. S., and Skeen, R. S. (1996). "Numerical Modeling of Biologically Reactive Transport from a Nutrient Injection Well." *ASCE Journal of Environmental Engineering*, 122(9), 833-839.
- Clement, T. P., Johnson, C. D., Sun, Y., Klecka, G. M., and Bartlett, C. (2000). "Natural Attenuation of Chlorinated Solvent Compounds: Model Development and Field-Scale Application." *Journal of Contaminant Hydrology*, 42, 113-140.
- Clement, T. P., Sun, Y., Hooker, B. S., and Petersen, J. N. (1998). "Modeling Multi-species Reactive Transport in Groundwater Aquifers." *Groundwater Monitoring & Remediation Journal*, 18(2), 79-92.
- Cline, S. R., and Reed, B. E. (1995). "Lead Removal from Soils via Bench-Scale Soil Washing Techniques." *Journal of Environmental Engineering*, 10, 700-705.
- Connaughton, D. F., Stedinger, J. R., Lion, L. W., and Shuler, M. L. (1993). "Description of Time-Varying Desorption Kinetics: Release of Naphthalene from Contaminated Soils." *Environmental Science and Technology*, 27(12), 2397-2403.

- Crooks, R. M., Zhao, M., Sun, L., Chechik, V., and Yeung, L. K. (2001). "Dendrimer-Encapsulated Metal Nanoparticles: Synthesis, Characterization, and Applications to Catalysis." *Accounts of Chemical Research*, 34(3), 181-190.
- Culver, T. B., Hallisey, S. P., Sahoo, D., Deitsch, J. J., and Smith, J. A. (1997). "Modeling the Desorption of Organic Contaminants from Long-Term Contaminated Soil Using Distributed Mass Transfer Rates." *Environmental Science and Technology*, 31(6), 1581-1588.
- Cumbal, L., and Sengupta, A. K. (2005). "Arsenic Removal Using Polymer-Supported Hydrated Iron(III) Oxide Nanoparticles: Role of Donnan Membrane Effect." *Environmental Science and Technology*, 39, 6508-6515.
- Dang, Y. P., Dalal, R. C., Edwards, D. G., and Tiller, K. G. (1994). "Kinetics of zinc desorption from Vertisols." *Soil Science Society of America Journal*, 58(5), 1392-1399.
- Dendritech. "Technical data supplied by Dendritech, Inc. (Midland, MI)."
- Dendritech, W. o. "<http://www.dendritech.com/pricing.html>." accessed August 2005.
- Di Palma, L., and Ferrantelli, P. (2005). "Copper Leaching from a Sandy Soil: Mechanism and Parameters Affecting EDTA Extraction." *Journal of Hazardous Materials*, 122(1-2), 85-90.
- Di Palma, L., Ferrantelli, P., and Medici, F. (2005). "Heavy Metals Extraction from Contaminated Soil: Recovery of the Flushing Solution." *Journal of Environmental Management*, 77(3), 205-211.
- Diallo, M. S., Balogh, L., Shafagati, A., Johnson, J. H., Jr., Goddard, W. A., III, and Tomalia, D. A. (1999). "Poly(amidoamine) Dendrimers: A New Class of High

- Capacity Chelating Agents for Cu(II) Ions." *Environmental Science and Technology*, 33(5), 820-824.
- Diallo, M. S., Christie, S., Swaminathan, P., Balogh, L., Shi, X. Y., Um, W. Y., Papelis, C., Goddard, W. A., III, and Johnson, J. H., Jr. (2004). "Dendritic Chelating Agents. 1. Cu(II) Binding to Ethylene Diamine Core Poly(amidoamine) Dendrimers in Aqueous Solutions." *Langmuir*, 20, 2640-2651.
- Diallo, M. S., Christie, S., Swaminathan, P., Johnson, J. H., Jr., and Goddard, W. A., III. (2005). "Dendrimer Enhanced Ultrafiltration. 1. Recovery of Cu(II) from Aqueous Solutions Using PAMAM Dendrimers with Ethylene Diamine Core and Terminal NH₂ Groups." *Environmental Science and Technology*, 39(5), 1366-1377.
- Dienemann, E., Goldfard, W., and Ahlert, R. C. (1992). "Evolution of the Superfund Remedy Selection Process, Including an Assessment of Implementation of Permanent and Alternative Remedial Technologies." *Environmental Progress*, 11, 165-172.
- Dovore, J. L. (1995). "Probability and Statistics for Engineering and the Science." 4th Edition, Duxbury Press, P167-170.
- Drever, J. I. (1994). "The Effect of Land Plants on Weathering Rates of Silicate Minerals." *Geochimica et Cosmochimica Acta*, 58(10), 2325-32.
- Dunphy Guzman, K. A., Taylor, M. R., and Banfield, J. F. (2006). "Environmental Risks of Nanotechnology: National Nanotechnology Initiative Funding, 2000-2004." *Environmental Science and Technology*, 40(5), 1401-1407.

- Dzombak, D. A., and Morel, F. M. M. (1990). *Surface Complexation Modeling: Hydrous Ferric Oxide*, John Wiley & Sons, New York, NY.
- Eary, L. E., and Rai, D. (1988). "Chromate Removal from Aqueous Wastes by Reduction with Ferrous Ion." *Environmental Science and Technology*, 22(8), 972-7.
- Eary, L. E., and Rai, D. (1991). "Chromate Reduction by Subsurface Soils under Acidic Conditions." *Soil Science Society of America Journal*, 55(3), 676-83.
- Elliott, D. W., and Zhang, W. X. (2001). "Field Assessment of Nanoscale Bimetallic Particles for Groundwater Treatment." *Environmental science and technology*, 35(24), 4922-6.
- Elliott, H. A., and Brown, G. A. (1989). "Comparative Evaluation of NTA and EDTA for Extractive Decontamination of Pb-Polluted Soils." *Water Air and Soil Pollution*, 45, 361-369.
- Fangueiro, D., Bermond, A., Santos, E., Carapuca, H., and Duarte, A. (2005). "Kinetic Approach to Heavy Metal Mobilization Assessment in Sediments: Choose of Kinetic Equations and Models to Achieve Maximum Information." *Talanta*, 66(4), 844-857.
- Fetter, C. W. (2001). "Applied Hydrogeology, 4th Edition." *Prentice Hall*, 402-405.
- Furukawa, M., and Tokunaga, S. (2004). "Extraction of Heavy Metals from a Contaminated Soil Using Citrate-Enhancing Extraction by pH Control and Ultrasound Application." *Journal of Environmental Science and Health Part a-Toxic/Hazardous Substances & Environmental Engineering*, A39, 627-638.
- Furukawa, Y., Kim, J.-w., Watkins, J., and Wilkin, R. T. (2002). "Formation of Ferrihydrite and Associated Iron Corrosion Products in Permeable Reactive

- Barriers of Zero-Valent Iron." *Environmental Science and Technology*, 36(24), 5469-5475.
- Gadd, G. M. (2005). "Microorganisms in Toxic Metal-Polluted Soils." *Soil Biology*, 3(Microorganisms in Soils), 325-356.
- Gandhi, S., Oh, B.-T., Schnoor, J. L., and Alvarez, P. J. J. (2002). "Degradation of TCE, Cr(VI), Sulfate, and Nitrate Mixtures by Granular Iron in Flow-Through Columns under Different Microbial Conditions." *Water Research*, 36(8), 1973-1982.
- Geckeler, K. E., and Volchek, K. (1996). "Removal of Hazardous Substances from Water Using Ultrafiltration in Conjunction with Soluble Polymers." *Environmental Science and Technology*, 30(3), 725-34.
- Ginder-Vogel, M., Borch, T., Mayes, M. A., Jardine, P. M., and Fendorf, S. (2005). "Chromate Reduction and Retention Processes within Arid Subsurface Environments." *Environmental Science and Technology*, 39(20), 7833-7839.
- Gould, J. P. (1982). "The Kinetics of Hexavalent Chromium Reduction by Metallic Iron." *Water Research*, 16(6), 871-877.
- Groudev, S. N., Georgiev, P. S., Spasova, I. I., Komnitsas, K., and Paspaliaris, I. (2004). "Bioremediation *In Situ* of Polluted Soil in a Uranium Deposit." *Remediation of Chlorinated and Recalcitrant Compounds--2004, Proceedings of the International Conference on Remediation of Chlorinated and Recalcitrant Compounds, 4th, Monterey, CA, United States, May 24-27, 2004*, 4C 26/1-4C 26/7.
- Groves, F. R., Jr., and White, T. (1984). "Mathematical Modeling of the Ligand Exchange Process." *AIChE Journal*, 30(3), 494-496.

- Haensler, J., and Szoka, F. C., Jr. (1993). "Polyamidoamine Cascade Polymers Mediate Efficient Transfection of Cells in Culture." *Bioconjugate Chemistry*, 4(5), 372-9.
- Han, F. X., Hargreaves, J. A., Kingery, W. L., Huggett, D. B., and Schlenk, D. K. (2001). "Accumulation, Distribution, and Toxicity of Copper in Sediments of Catfish Ponds Receiving Periodic Copper Sulfate Applications." *Journal of Environmental Quality*, 30, 912-919.
- He, F., and Zhao, D. (2005a). "Preparation and Characterization of a New Class of Starch-Stabilized Bimetallic Nanoparticles for Degradation of Chlorinated Hydrocarbons in Water." *Environmental Science and Technology*, 39(9), 3314-3320.
- He, F., and Zhao, D. (2005b). "Application of novel stabilizers for enhanced mobility and reactivity of iron-based nanoparticles for *in situ* destruction of chlorinated hydrocarbons in soils." *Abstracts of Papers, 230th ACS National Meeting, Washington, DC, United States, Aug. 28-Sept. 1, 2005*, ENVR-077.
- He, F., Zhao, D., Liu, J., and Roberts, C. B. (2006). "Stabilization of Fe/Pd Bimetallic Nanoparticles with Sodium Carboxymethyl Cellulose to Facilitate Dechlorination of Trichloroethene and Soil Transportability." *Chemical Communications*, Submitted.
- Hedden, R. C., and Bauer, B. J. (2003). "Structure and Dimensions of PAMAM/PEG Dendrimer-Star Polymers." *Macromolecules*, 36(6), 1829-1835.
- Henry, W. D., Zhao, D., SenGupta, A. K., and Lange, C. (2004). "Preparation and Characterization of a New class of Polymeric Ligand Exchangers for Selective

- Removal of Trace Contaminants from Water." *Reactive & Functional Polymers*, 60, 109-120.
- Hong, A. P., Chen, T. C., and Okey, R. W. (1993). "Chelating Extraction of Zinc from Soils Using N- (2-Acetamido) Iminodiacetic Acid (ADA)." *I & EC Special Symposium American Chemical Society*, Atlanta, GA.
- Hong, P. K. A., Li, C., Shankha Banerji, K., and Regmi, T. (1999). "Extraction, Recovery, and Biostability of EDTA for Remediation of Heavy Metal-Contaminated Soil." *Journal of Soil Contamination*, 8, 81-103.
- Hong, S., Bielinska, A. U., Mecke, A., Keszler, B., Beals, J. L., Shi, X., Balogh, L., Orr, B. G., Baker, J. R., Jr., and Holl, M. M. B. (2004). "Interaction of Poly(amidoamine) Dendrimers with Supported Lipid Bilayers and Cells: Hole Formation and the Relation to Transport." *Bioconjugate Chemistry*, 15(4), 774-782.
- Jevprasesphant, R., Penny, J., Attwood, D., McKeown, N. B., and D'Emanuele, A. (2003). "Engineering of Dendrimer Surfaces to Enhance Transepithelial Transport and Reduce Cytotoxicity." *Pharmaceutical Research*, 20(10), 1543-1550.
- Kabra, K., Chaudhary, R., and Sawhney, R. L. (2004). "Treatment of Hazardous Organic and Inorganic Compounds through Aqueous-Phase Photocatalysis: A Review." *Industrial & Engineering Chemistry Research*, 43(24), 7683-7696.
- Kantar, C., Gillow, J. B., Harper-Arabie, R., Honeyman, B. D., and Francis, A. J. (2005). "Determination of Stability constants of U(VI)-Fe(III)-Citrate Complexes." *Environmental Science and Technology*, 39, 2161-2168.

- Kavanaugh, M. C. (1994). *Alternatives for groundwater cleanup*, National Academy Press, Washington, DC.
- Kaya, A., and Yukselen, Y. (2005). "Zeta Potential of Clay Minerals and Quartz Contaminated by Heavy Metals." *Canadian Geotechnical Journal*, 42(5), 1280-1289.
- Kedziorek, M. A. M., Dupuy, A., Bourg, A. C. M., and Compere, F. (1998). "Leaching of Cd and Pb from a Polluted Soil during the Percolation of EDTA: Laboratory Column Experiments Modeled with a Non-Equilibrium Solubilization Step." *Environmental Science and Technology*, 32(11), 1609-1614.
- Khodadoust, A. P., Reddy, K. R., and Maturi, K. (2004). "Removal of Nickel and Phenanthrene from Kaolin Soil Using Different Extractants." *Environmental Engineering Science*, 21(6), 691-704.
- Khodadoust, A. P., Reddy, K. R., and Maturi, K. (2005). "Effect of Different Extraction agents on Metal and Organic Contaminant Removal from a Field Soil." *Journal of Hazardous Materials*, 117(1), 15-24.
- Kim, J.-Y., Cohen, C., and Shuler, M. L. (2000). "Use of Amphiphilic Polymer Particles for *In Situ* Extraction of Sorbed Phenanthrene from a Contaminated Aquifer Material." *Environmental Science and Technology*, 34, 4133-4139.
- Kinniburgh, D. G., van Riemsdijk, W. H., Koopal, L. K., Borkovec, M., Benedetti, M. F., and Avena, M. J. (1999). "Ion Binding to Natural Organic Matter: Competition, Heterogeneity, Stoichiometry and Thermodynamic Consistency." *Colloids and Surfaces, A: Physicochemical and Engineering Aspects*, 151(1-2), 147-166.

- Koning, M., Hupe, K., and Stegmann, R. (2005). "Soil Remediation and Disposal." *Environmental Biotechnology*, 259-274.
- Kovvali, A. S., and Sirkar, K. K. (2001). "Dendrimer Liquid Membranes: CO₂ Separation from Gas Mixtures." *Industrial & Engineering Chemistry Research*, 40(11), 2502-2511.
- Kovvali, A. S. C., H.; Sirkar, K. K. (2000). "Dendrimer membrane: A CO₂-selective Molecular Gate." *Journal of American Chemical Society*, 122, 7594-7595.
- Kriesel, J. W., and Tilley, T. D. (2001). "Carbosilane Dendrimers as Nanoscopic Building Blocks for Hybrid Organic-Inorganic Materials and Catalyst Supports." *Advanced Materials*, 13(21), 1645-1648.
- Krot, K. A., Danil de Namor, A. F., Aguilar-Cornejo, A., and Nolan, K. B. (2005). "Speciation, Stability Constants and Structures of Complexes of Copper(II), Nickel(II), Silver(I) and Mercury(II) with PAMAM Dendrimer and Related Tetraamide Ligands." *Inorganica Chimica Acta*, 358(12), 3497-3505.
- Kucharski, R., Zielonka, U., Sas-Nowosielska, A., Kuperberg, J. M., Worsztynowicz, A., and Szdzuj, J. (2005). "A Method of Mercury Removal from Topsoil Using Low-Thermal Application." *Environmental Monitoring and Assessment*, 104(1-3), 341-351.
- Kukowska-Latallo, J. F., Bielinska, A. U., Johnson, J., Spindler, R., Tomalia, D. A., and Baker, J. R., Jr. (1996). "Efficient Transfer of Genetic Material into Mammalian Cells Using Starburst Polyamidoamine Dendrimers." *Proceedings of the National Academy of Sciences of the United States of America*, 93(10), 4897-4902.

- Kunkel, A. M., Seibert, J. J., Elliott, L. J., Kelley, R. L., Katz, L. E., and Pope, G. A. (2004). "Remediation of Elemental Mercury Using *In Situ* Thermal Desorption (ISTD)." *Remediation of Chlorinated and Recalcitrant Compounds--2004, Proceedings of the International Conference on Remediation of Chlorinated and Recalcitrant Compounds, 4th, Monterey, CA, United States, May 24-27, 2004*, 4C 07/1-4C 07/8.
- Kuo, S., and Mikkelsen, D. S. (1980). "Kinetics of Zinc Desorption from Soils." *Plant and Soil*, 56(3), 355-64.
- Lasaga, A. C., Soler, J. M., Ganor, J., Burch, T. E., and Nagy, K. L. (1994). "Chemical Weathering Rate Laws and Global Geochemical Cycles." *Geochimica et Cosmochimica Acta*, 58(10), 2361-86.
- Legrand, L., El Figuigui, A., Mercier, F., and Chausse, A. (2004). "Reduction of Aqueous Chromate by Fe(II)/Fe(III) Carbonate Green Rust: Kinetic and Mechanistic Studies." *Environmental Science and Technology*, 38(17), 4587-4595.
- Leij, F. J., Dane, J. H., and Genuchten, M. T. V. (1991). "Mathematical Analysis of One-dimensional Solute Transport in a Layered Soil Profile." *Soil Science Society of America Journal*(55), 944-953.
- Leinser, D., and Imae, T. (2003). "Polyelectrolyte Behavior of an Interpolyelectrolyte Complex Formed in Aqueous Solution of a Charged Dendrimer and Sodium Poly(L-glutamate)." *Journal of Physical Chemistry B.*, 107, 13158.
- Lenhart, J. J., Cabaniss, S. E., MacCarthy, P., and Honeyman, B. D. (2000). "Uranium(VI) Complexation with Citric, Humic and Fulvic Acids." *Radiochimica Acta*, 88(6), 345-353.

- Lenhart, J. J., and Saiers, J. E. (2003). "Colloid Mobilization in Water-Saturated Porous Media under Transient Chemical Conditions." *Environmental Science and Technology*, 37(12), 2780-2787.
- Li, G., Luo, Y., and Tan, H. (2005). "PVP and G1.5 PAMAM Dendrimer Co-Mediated Synthesis of Silver Nanoparticles." *Journal of Solid State Chemistry*, 178, 1038.
- Li, Q.-L., Yuan, D.-X., and Lin, Q.-M. (2004). "Evaluation of Multi-Walled Carbon Nanotubes as an Adsorbent for Trapping Volatile Organic Compounds from Environmental Samples." *Journal of Chromatography, A*, 1026(1-2), 283-288.
- Li, Y.-H., Ding, J., Luan, Z., Di, Z., Zhu, Y., Xu, C., Wu, D., and Wei, B. (2003). "Competitive Adsorption of Pb^{2+} , Cu^{2+} and Cd^{2+} Ions from Aqueous Solutions by Multiwalled Carbon Nanotubes." *Carbon*, 41(14), 2787-2792.
- Lim, T. T., Chu, J., and Goi, M. H. (2004a). "Assessment of Heavy Metals Leachability in Clay-Amended Sewage Sludge Stabilized with Cement for Use as Fill Material." *Journal of Residuals Science and Technology*, 1(3), 157-164.
- Lim, T. T., Tay, J. H., and Wang, J. Y. (2004b). "Chelating-Agent-Enhanced Heavy Metal Extraction from a Contaminated Acidic Soil." *Journal of Environmental Engineering*, 1, 59-66.
- Lo, I. M. C., and Yang, X. Y. (1999). "EDTA Extraction of Heavy Metals from Different Soil Fractions and Synthetic Soils." *Water Air and Soil Pollution*, 109(1-4), 219-236.
- Long, R. Q., and Yang, R. T. (2001). "Carbon Nanotubes as Superior Sorbent for Dioxin Removal." *Journal of the American Chemical Society*, 123(9), 2058-2059.

- Luster, J., Blaser, P., and Magyar, B. (1994). "Equilibrium Ion Exchange Method: Methodology at Low Ionic Strength and Copper(II) Complexation by Dissolved Organic Matter in a Leaf Litter Extract." *Talanta*, 41(11), 1873-80.
- Ma, L. Q., Komar, K. M., Tu, C., Zhang, W., Cai, Y., and Kennelley, E. D. (2001). "Bioremediation: A Fern that Hyperaccumulates Arsenic." *Nature (London)*, 409(6820), 579.
- Macauley, E., and Hong, A. (1995). "Chelation Extraction of Lead from Soil Using Pyridine-2, 6-Dicarboxylic Acid." *Journal of Hazardous Materials*, 40, 257-270.
- Magdassi, S., Bassa, A., Vinetsky, Y., and Kamyshny, A. (2003). "Silver Nanoparticles as Pigments for Water-Based Ink-Jet Inks." *Chemistry of Materials*, 15(11), 2208-2217.
- Malik, N., Wiwattanapatapee, R., Klopsch, R., Lorenz, K., Frey, H., Weener, J. W., Meijer, E. W., Paulus, W., and Duncan, R. (2000). "Dendrimers: Relationship between structure and biocompatibility in vitro, and preliminary studies on the biodistribution of ¹²⁵I-labeled polyamidoamine dendrimers in vivo." *Journal of Controlled Release*, 65(1-2), 133-148.
- Manriquez, J., Juaristi, E., Munoz-Muniz, O., and Godinez, L. A. (2003). "QCM Study of the Aggregation of Starburst PAMAM Dendrimers on the Surface of Bare and Thiol-Modified Gold Electrodes." *Langmuir*, 19(18), 7315-7323.
- Martell, A. E., and Calvin, M. (1952). "Chemistry of Metal Chelate Compounds." *Prentice Hall, New York*.
- Martell, A. E., and Smith, R. M. (1974). *Critical Stability Constant*, Plenum Press.

- Masciangioli, T., and Zhang, W.-X. (2003). "Environmental Technologies at the Nanoscale." *Environmental Science and Technology*, 37(5), 102A-108A.
- Mayer, K. U., Blowes, D. W., and Frind, E. O. (2001). "Reactive Transport Modeling of an *In Situ* Reactive Barrier for the Treatment of Hexavalent Chromium and Trichloroethylene in Groundwater." *Water Resource Research*, 37(12), 3091-3103.
- Melitas, N., Chuffé-Moscoco, O., and Farrell, J. (2001). "Kinetics of Soluble Chromium Removal from Contaminated Water by Zerovalent Iron Media: Corrosion Inhibition and Passive Oxide Effects." *Environmental Science and Technology*, 35(19), 3948-3953.
- Montero, J. P., Munoz, J. F., Abeliuk, R., and Vauclin, M. (1994). "A Solute Transport Model for the Acid Leaching of Copper in Soil Columns." *Soil Science Society of America Journal*, 58(3), 678-86.
- Moreno, N., Querol, X., Ayora, C., Pereira, C. F., and Janssen-Jurkovicova, M. (2001). "Utilization of Zeolites Synthesized from Coal Fly Ash for the Purification of Acid Mine Waters." *Environmental science and technology*, 35(17), 3526-34.
- Mulligan, C. N., Yong, R. N., and Gibbs, B. F. (2001). "Remediation Technologies for Metal-Contaminated Soils and Groundwater: an Evaluation." *Engineering Geology*, 60, 193-207.
- Nabi, S. A., Sheeba, K. N., and Khan, M. A. (2005). "Chromatographic Separations of Metal Ions on Strong Acid Cation-Exchange Resin Loaded with Neutral Red." *Acta Chromatographica*, 15, 206-219.

- Neilson, J. W., Artiola, J. F., and Maier, R. M. (2003). "Characterization of Lead Removal from Contaminated Soils by Nontoxic Soil-Washing Agents." *Journal of Environmental Quality*, 32(3), 899-908.
- Niu, Y., Sun, L., and Crooks, R. M. (2003). "Determination of the Intrinsic Proton Binding Constants for Poly(amidoamine) Dendrimers via Potentiometric pH Titration." *Macromolecules*, 36(15), 5725-5731.
- Nurmi, J. T., Tratnyek, P. G., Sarathy, V., Baer, D. R., Amonette, J. E., Pecher, K., Wang, C., Linehan, J. C., Matson, D. W., Penn, R. L., and Driessen, M. D. (2005). "Characterization and Properties of Metallic Iron Nanoparticles: Spectroscopy, Electrochemistry, and Kinetics." *Environmental Science and Technology*, 39(5), 1221-1230.
- Oberdorster, G., Oberdorster, E., and Oberdorster, J. (2005). "Nanotoxicology: an emerging discipline evolving from studies of ultrafine particles." *Environmental Health Perspectives*, 113(7), 823-839.
- Ochoa-Loza, F. J., F., A. J., and Maier, R. (2001). "Stability Constant for the Complexation of Various Metals with a Rhamnolipid Biosurfactant." *Journal of Environmental Quality*, 30, 479-485.
- Ottaviani, M. F., Bossmann, S., Turro, N. J., and Tomalia, D. A. (1994). "Characterization of Starburst Dendrimers by the EPR Technique.1. Copper-Complexes in Water Solution." *Journal of the American Chemical Society*, 116(2), 661-671.

- Ottaviani, M. F., Montalti, F., Romanelli, M., Turro, N. J., and Tomalia, D. A. (1996). "Characterization of Starburst Dendrimers by EPR. 4. Mn(II) as a Probe of Interphase Properties." *Journal of Physical Chemistry*, 100, 1103-11042.
- Ottaviani, M. F., Montalti, F., Turro, N. J., and Tomalia, D. A. (1997). "Characterization of Starburst Dendrimers by the EPR technique. Copper(II) Ions Binding Full-Generation Dendrimers." *Journal of Physical Chemistry B*, 101(2), 158-166.
- Ottaviani, M. F., Valluzzi, R., and Balogh, L. (2002). "Internal Structure of Silver-Poly(amidoamine) Dendrimer Complexes and Nanocomposites." *Macromolecules*, 35(13), 5105-5115.
- Pandey, A. K., Pandey, S. D., and Misra, V. (2000). "Stability Constants of Metal-Humic Acid Complexes and its Role in Environmental Detoxification." *Ecotoxicology and Environmental Safety*, 47(2), 195-200.
- Pang, L., Close, M. E., Noonan, M. J., Flintoft, M. J., and van den Brink, P. (2005). "A laboratory study of bacteria-facilitated cadmium transport in alluvial gravel aquifer media." *Journal of Environmental Quality*, 34(1), 237-247.
- Patterson, R. R., Fendorf, S., and Fendorf, M. (1997). "Reduction of Hexavalent Chromium by Amorphous Iron Sulfide." *Environmental Science and Technology*, 31(7), 2039-2044.
- Pazos, M., Sanroman, M. A., and Cameselle, C. (2006). "Improvement in electrokinetic remediation of heavy metal spiked kaolin with the polarity exchange technique." *Chemosphere*, 62(5), 817-822.

- Peng, X., Luan, Z., Ding, J., Di, Z., Li, Y., and Tian, B. (2004). "Ceria Nanoparticles Supported on Carbon Nanotubes for the Removal of Arsenate from Water." *Materials Letters*, 59(4), 399-403.
- Peters, R. W. (1999). "Chelant Extraction of Heavy Metals from Contaminated Soils." *Journal of Hazardous Materials*, 66, 151-210.
- Peters, R. W., and Shem, L. (1992). "Adsorption/Desorption Characteristics of Lead on Various Types of Soil." *Environmental Progress*, 11(3), 234-40.
- Pettine, M., D'Ottone, L., Campanella, L., Millero, F. J., and Passino, R. (1998). "The Reduction of Chromium (VI) by Iron (II) in Aqueous Solutions." *Geochimica et Cosmochimica Acta*, 62(9), 1509-1519.
- Pickering, W. F. (1986). "Metal Ion Speciation - Soils and Sediments (A review)." *Ore Geology Reviews*, 1(1), 83-146.
- Pignatello, J. J., Ferrandino, F. J., and Huang, L. Q. (1993). "Elution of Aged and Freshly Added Herbicides from a Soil." *Environmental Science and Technology*, 27(8), 1563-71.
- Pinyerd, C. A., Odom, J. W., Long, F. L., and Dane, J. H. (1984). "Boron Movement in a Norfolk Loamy Sand." *Soil Science*, 137(6), 428-33.
- Ponder, S. M., Darab, J. G., Bucher, J., Caulder, D., Craig, I., Davis, L., Edelstein, N., Lukens, W., Nitsche, H., Rao, L., Shuh, D. K., and Mallouk, T. E. (2001). "Surface Chemistry and Electrochemistry of Supported Zerovalent Iron Nanoparticles in the Remediation of Aqueous Metal Contaminants." *Chemistry of Materials*, 13(2), 479-486.

- Ponder, S. M., Darab, J. G., and Mallouk, T. E. (2000). "Remediation of Cr(VI) and Pb(II) Aqueous Solutions Using Supported, Nanoscale Zero-valent Iron." *Environmental Science and Technology*, 34(12), 2564-2569.
- Powell, R. M., Puls, R. W., Hightower, S. K., and Sabatini, D. A. (1995). "Coupled Iron Corrosion and Chromate Reduction: Mechanisms for Subsurface Remediation." *Environmental Science and Technology*, 29(8), 1913-22.
- Pratt, A. R., Blowes, D. W., and Ptacek, C. J. (1997). "Products of Chromate Reduction on Proposed Subsurface Remediation Material." *Environmental Science and Technology*, 31(9), 2492-2498.
- Puls, R. W., Blowes, D. W., and Gillham, R. W. (1999). "Long-term performance monitoring for a permeable reactive barrier at the U.S. Coast Guard Support Center, Elizabeth City, North Carolina." *Journal of Hazardous Materials*, 68(1-2), 109-124.
- Qafoku, N. P., Zachara, J. M., Liu, C., Gassman, P. L., Qafoku, O. S., and Smith, S. C. (2005). "Kinetic Desorption and Sorption of U(VI) during Reactive Transport in a Contaminated Hanford Sediment." *Environmental Science and Technology*, 39(9), 3157-3165.
- Rai, D., and Zachara, R. J. (1986). "Geochemical Behaviour of Chromium Species." *EPRI EA4544, Electrical Power Research Institute: Palo Alto, California.*
- Rampléy, C. G., and Ogden, K. L. (1998). "Preliminary Studies for Removal of Lead from Surrogate and Real Soils Using a Water Soluble Chelator: Adsorption and Batch Extraction." *Environmental Science and Technology*, 32, 987-993.

- Reed, B. E., Carriere, P. C., and Moore, R. (1996). "Flushing of a Pb(II) Contaminated Soil Using HCl, EDTA, AND CaCl₂." *Journal of Environmental Engineering-Asce*, 122(1), 48-50.
- Rether, A., and Schuster, M. (2003). "Selective Separation and Recovery of Heavy Metal Ions Using Water-Soluble N-Benzoylthiourea Modified PAMAM Polymers." *Reactive and Functional Polymers*, 57(1), 13-21.
- Roma-Luciw, R., Sarraf, L., and Morcellet, M. (2000). "Concentration Effects during the Formation of Poly (acrylic acid)-Metal Complexes in Aqueous Solutions." *Polymer Bulletin*, 45(4-5), 411-418.
- Roy, S. B., Dzombak, D. A., and Ali, M. A. (1995). "Assessment of In-Situ Solvent-Extraction for Remediation of Coal-Tar Sites - Column Studies." *Water Environment Research*, 67(1), 4-15.
- Samani, Z., Hu, S., Hanson, A. T., and Heil, D. M. (1998). "Remediation of Lead Contaminated soil by Column Extraction with EDTA: II. Modeling." *Water Air and Soil Pollution*, 102(3-4), 221-238.
- Savage, N., and Diallo, M. S. (2005). "Nanomaterials and Water Purification: Opportunities and Challenges." *Journal of Nanoparticle Research*, 7(4-5), 331-342.
- Schlautman, M. A., and Han, I. (2001). "Effects of pH and Dissolved Oxygen on the Reduction of Hexavalent Chromium by Dissolved Ferrous Iron in Poorly Buffered Aqueous Systems." *Water Research*, 35(6), 1534-1546.

- Schnitzer, M., and Hansen, E. H. (1970). "Organo-Metallic Interactions in Soils: 8. an Evaluation of Methods for the Determination of Stability Constants of Metal-fulvic Acid Complexes." *Soil Science*, 109, 333-340.
- Schnitzer, M., and Skinner, S. I. M. (1966). "Organo-Metallic Interactions in Soils: 5. Stability Constants of Cu^{++} -, Fe^{++} -, and Zn^{++} -- Fulvic Acid Complexes." *Soil Science*, 102, 247-252.
- Schrick, B., Blough, J. L., Jones, A. D., and Mallouk, T. E. (2002). "Hydrodechlorination of Trichloroethylene to Hydrocarbons Using Bimetallic Nickel-Iron Nanoparticles." *Chemistry of Materials*, 14(12), 5140-5147.
- Schrick, B., Hydutsky, B. W., Blough, J. L., and Mallouk, T. E. (2004). "Delivery Vehicles for Zerovalent Metal Nanoparticles in Soil and Groundwater." *Chemistry of Materials*, 16(11), 2187-2193.
- Schubert, J. (1948). "The use of Ion Exchangers for the Determination of Physical-Chemical Properties of Substances, Particularly Radiotracers, in Solution. I. Theoretical." *Journal of Physical and Colloid Chemistry*, 52(No. 2), 340-350.
- Schubert, J. (1956). "Measurement of Complex Ion Stability by Use of Ion-Exchange Resins." *Methods of Biochemistry Analysis*, 3, 247-63.
- Schubert, J., and Lindenbaum, A. (1950). "Complexes of Calcium with Citric Acid and Tricarballic Acids Measured by Ion Exchange." *Nature (London, United Kingdom)*, 166, 913-914.
- Schubert, J., and Richter, J. W. (1948). "The Use of Ion Exchangers for the Determination of Physical-Chemical Properties of Substances, Particularly Radiotracers, in Solution. II. The Dissociation Constants of Strontium Citrate and

- Strontium Tartrate." *Journal of Physical and Colloid Chemistry*, 52(No. 2), 350-357.
- Schubert, J., Russell, E. R., and Myers, L. S., Jr. (1950). "Dissociation Constants of Radium-Organic Acid Complexes Measured by Ion Exchange." *Journal of Biological Chemistry*, 185, 387-98.
- Seaman, J. C., Bertsch, P. M., and Schwallie, L. (1999). "In Situ Cr(VI) Reduction within Coarse-Textured, Oxide-Coated Soil and Aquifer Systems Using Fe(II) Solutions." *Environmental Science and Technology*, 33(6), 938-944.
- Shi, Z., Di Toro, D. M., Allen, H. E., and Ponizovsky, A. A. (2005). "Modeling Kinetics of Cu and Zn Release from Soils." *Environmental Science and Technology*, 39(12), 4562-4568.
- Si, S., Kotal, A., Mandal, T. K., Giri, S., Nakamura, H., and Kohara, T. (2004). "Size-Controlled Synthesis of Magnetite Nanoparticles in the Presence of Polyelectrolytes." *Chemistry of Materials*, 16(18), 3489-3496.
- Sims, G. K., Ellsworth, T. R., and Mulvaney, R. L. (1995). "Microscale Determination of Inorganic Nitrogen in Water and Soil Extracts." *Communication of Soil Science: Plant Analysis*, 26, 303.
- Singh, I. B., and Singh, D. R. (2003). "Effects of pH on Cr-Fe Interaction during Cr(VI) Removal by Metallic Iron." *Environmental Technology*, 24(8), 1041-1047.
- Smith, D. J. T., and Harrison, R. M. (1996). "Concentrations, trends and vehicle source profile of polynuclear aromatic hydrocarbons in the U.K. atmosphere." *Atmospheric Environment*, 30(14), 2513-2525.

- Sukreeyapongse, O., Holm, P. E., Strobel, B. W., Panichsakpatana, S., Magid, J., and Hansen, H. C. B. (2002). "pH-dependent Release of Cadmium, Copper, and Lead from Natural and Sludge-Amended Soils." *Journal of Environmental Quality*, 31(6), 1901-1909.
- Sun, B., Zhao, F. J., Lombi, E., and McGrath, S. P. (2001). "Leaching of Heavy Metals from Contaminated Soils Using EDTA." *Environmental Pollution (Oxford, United Kingdom)*, 113(2), 111-120.
- Sun, L., and Crooks, R. M. (2002). "Interactions between Dendrimers and Charged Probe Molecules. 1. Theoretical Methods for Simulating Proton and Metal Ion Binding to Symmetric Polydentate Ligands." *Journal of Physical Chemistry B*, 106(23), 5864-5872.
- Tarazona-Vasquez, F., and Balbuena, P. B. (2004). "Complexation of the Lowest Generation Poly(amidoamine)-NH₂ Dendrimers with Metal Ions, Metal Atoms, and Cu(II) Hydrates: An ab Initio Study." *Journal of Physical Chemistry B*, 108(41), 15992-16001.
- TCLP. "<http://www.iwrc.org/summaries/TCLP.cfm>", accesses September 2004.
- Thayalakumaran, T., Vogeler, I., Scotter, D. R., Percival, H. J., Robinson, B. H., and Clothier, B. E. (2003). "Leaching of Copper from Contaminated Soil Following the Application of EDTA. II. Intact Core Experiments and Model Testing." *Australian Journal of Soil Research*, 41(2), 335-350.
- Tomalia, D. A. (1993). "Starburst / Cascade Dendrimers: Fundamental Building Blocks for a New Nanoscopic Chemistry Set." *Aldrichimica Acta*, 26, 91-101.

- Tomalia, D. A., Naylor, A. M., and III, W. A. G. (1990). "Starburst Dendrimers: Molecular-level Control of Size, Shape, Surface Chemistry, Topology, and Flexibility from Atoms to Macroscopic Matter." *Angewandte Chemie International Edition*, 29, 138-175.
- Tran, M. L., Gahan, L. R., and Gentle, I. R. (2004). "Structural Studies of Copper(II)-Amine Terminated Dendrimer Complexes by EXAFS." *Journal of Physical Chemistry B*, 108(52), 20130-20136.
- Tran, Y. T., Barry, D. A., and Bajracharya, K. (2002). "Cadmium Desorption in Sand." *Environment International*, 28(6), 493-502.
- Tu, C., Ma, L. Q., and Bondada, B. (2002). "Arsenic Accumulation in the Hyperaccumulator Chinese Brake and Its Utilization Potential for Phytoremediation." *Journal of Environmental Quality*, 31(5), 1671-1675.
- Van Benschoten, J. E., Reed, B. E., Matsumoto, M. R., and McGarvey, P. J. (1994). "Metal Removal by Soil Washing for an IronOxide Coated Sandy Soil." *Water Environment Research*, 66(2), 168-174.
- Van Noort, P. C. M., Cornelissen, G., ten Hulscher, T. E. M., Vrind, B. A., Rigterink, H., and Belfroid, A. (2003). "Slow and Very Slow Desorption of Organic Compounds from Sediment: Influence of Sorbate Planarity." *Water Research*, 37(10), 2317-2322.
- Wang, C.-B., and Zhang, W.-x. (1997). "Synthesizing Nanoscale Iron Particles for Rapid and Complete Dechlorination of TCE and PCBs." *Environmental Science and Technology*, 31(7), 2154-2156.

- Widdowson, M. A., Molz, F. J., and Benefield, L. D. (1988). "A Numerical Transport Model for Oxygen- and Nitrate-Based Respiration Linked to Substrate and Nutrient Availability in Porous Media." *Water Resources Research*, 24(9), 1553-65.
- Wieland, E., Wehrli, B., and Stumm, W. (1988). "The Coordination Chemistry of Weathering: III. A Generalization on the Dissolution Rates of Minerals." *Geochimica et Cosmochimica Acta*, 52(8), 1969-81.
- Wilkin, R. T., Puls, R. W., and Sewell, G. W. (2003). "Long-term Performance of Permeable Reactive Barriers Using Zero-Valent Iron: Geochemical and Microbiological Effects." *Ground Water*, 41(4), 493-503.
- Wilkin, R. T., Su, C., Ford, R. G., and Paul, C. J. (2005). "Chromium-Removal Processes during Groundwater Remediation by a Zerovalent Iron Permeable Reactive Barrier." *Environmental Science and Technology*, 39(12), 4599-4605.
- Wu, C.-H., Kuo, C.-Y., and Lo, S.-L. (2004). "Removal of Metals from Industrial Sludge by Extraction with Different Acids." *Journal of Environmental Science and Health, Part A: Toxic/Hazardous Substances & Environmental Engineering*, A39(8), 2205-2219.
- Yoo, H., Sazani, P., and Juliano, R. L. (1999). "PAMAM Dendrimers as Delivery Agents for Antisense Oligonucleotides." *Pharmaceutical Research*, 16(12), 1799-1804.
- Zeng, F., and Zimmerman, S. C. (1997). "Dendrimers in Supramolecular Chemistry: from Molecular Recognition to Self-Assembly." *Chemical Reviews (Washington, D. C.)*, 97(5), 1681-1712.

- Zhang, W.-x. (2003). "Nanoscale Iron Particles for Environmental Remediation: An Overview." *Journal of Nanoparticle Research*, 5(3-4), 323-332.
- Zhang, W., Cai, Y., Tu, C., and Ma, L. Q. (2002). "Arsenic Speciation and Distribution in an Arsenic Hyperaccumulating Plant." *Science of the Total Environment*, 300(1-3), 167-177.
- Zhao, D., and SenGupta, A. K. (2000). "Ligand Separation with a Copper(II)-Loaded Polymeric Ligand Exchanger." *Industrial and Engineering Chemistry Research*, 39(2), 455-462.
- Zhao, M., and Crooks, R. M. (1999a). "Dendrimer-Encapsulated Pt Nanoparticles. Synthesis, Characterization, and Applications to Catalysis." *Advanced Materials (Weinheim, Germany)*, 11(3), 217-220.
- Zhao, M., Sun, L., and Crooks, R. M. (1998). "Preparation of Cu Nanoclusters within Dendrimer Templates." *Journal of the American Chemical Society*, 120(19), 4877-4878.
- Zhao, M. Q., and Crooks, R. M. (1999b). "Intradendrimer Exchange of Metal Nanoparticles." *Chemistry of Materials*, 11(11), 3379-3385.
- Zhou, L., Russell, D. H., Zhao, M., and Crooks, R. M. (2001). "Characterization of Poly(amidoamine) Dendrimers and Their Complexes with Cu²⁺ by Matrix-Assisted Laser Desorption Ionization Mass Spectrometry." *Macromolecules*, 34, 3567-3573.

APPENDIX A FORTRAN CODE FOR TRACER TEST

```

C****modeling the tracer test *****
      IMPLICIT NONE
      INTEGER i,node,j,nstep,control
      Parameter (node=4/0.05+1)
      DOUBLE PRECISION Co,velocity,distance,x,time, dt,tfinal,
&          dx,a,b,c,d,alpha, PC,CC,xx, Dis,beta,Pa
      DIMENSION PC(node),CC(node),a(node),b(node),c(node),
&          d(node),XX(node),X(node)
      time=0.0
      dx=0.05
      Dis=1.15D-3
      distance=4 !column length, cm
      tfinal=2000 !injection time, second
      velocity=1.13D-2 !cm/s
      control=0 ! to control the output
      CALL ana(node,xx,dx,velocity,dis,CC)
10    FORMAT(3F10.2)
      STOP
      END
*****Create subroutine to get the analytical solution for time 20 days*****
      SUBROUTINE ana(node,xx,dx,velocity,dis,CC)
      IMPLICIT NONE
      INTEGER i,node
      DOUBLE PRECISION CC, xx,dx,erf,erfc1,erfc2,xxx,dis,velocity,
&          tt,control
      DIMENSION CC(node)
      control=0
      DO tt=1,2000 !injection time, sec
      control=control+1
      DO i=1,node
      xx=(i-1)*dx
      xxx=(xx+velocity*tt)/(2*(dis*tt)**0.5)
      CALL ERROR(xxx,erf)
      erfc1=1-erf
      xxx=(xx-velocity*tt)/(2*(dis*tt)**0.5)
      IF (xxx. LT. 0.0) THEN
      xxx=abs(xxx)
      call ERROR(xxx,erf)

```

```

    erfc2=1+erf
    ELSE
    CALL ERROR(XXX,erf)
    erfc2=1-erf
    END IF
    CC(i)=0.5*(exp(velocity*xx/dis)*erfc1+erfc2)
    END DO
    IF (control. EQ.10) THEN
    write(805,10) tt/60*0.18/(3.14*0.4230), CC(node)
    control=0
    ELSE
    END IF
    END DO
10  FORMAT(3F10.2)
    RETURN
    END
*****creat SUBROUTINE to calculate the error function*****
SUBROUTINE ERROR(xx,erf)
IMPLICIT NONE
DOUBLE PRECISION xx,erf,erfc,p,t,a1,a2,a3,a4,a5
p=0.3275911
t=1/(1+p*xx)
a1=0.254829592
a2=-0.284496736
a3=1.421413741
a4=-1.453152027
a5=1.061405429
erf=1-(a1*t+a2*t**2+a3*t**3+a4*t**4+a5*t**5)*DEXP(-xx**2)
RETURN
END

```

APPENDIX B IMPLICIT METHOD FOR ONE-SITE MODEL

C****Dendrimer-Metal complex in column using implicit method (one-site)*****

```

IMPLICIT NONE
INTEGER i,node,j,nstep,control,m
Parameter (node=4.0/0.01+1)
DOUBLE PRECISION Co,velocity,distance,x,time,dt,tfinal,Cmo,Cm,Pcm,
& dx,a1,a2,b1,b2,c1,c2,d1,d2,alpha,PC1,PC2,CC,xx, Dis,beta,Pa
DIMENSION PC1(node),PC2(node),CC(node),a1(node),a2(node),
& b1(node),b2(node),c1(node),c2(node),
& Pcm(node),d1(node),d2(node),XX(node),X(node),Cm(node)
time=0.0
! write(*,*) "input m"
! read(*,*) m
Cmo=? !initial metal concentration in mmol/L
Dis=? !D determined from tracer
dt=1
dx=0.01
distance=4.0 !column length, cm
tfinal=26*60*60!injection time, second
velocity=? ! v determined from tracer, cm/s
nstep=(tfinal-time)/dt+1
alpha=dt*dis/dx**2
beta=velocity*dt/(2*dx)
Co=(velocity*dt)/dx
Pa=(dx*velocity)/Dis
write(*,*) "Co number is"
write(*,10) Co
write(*,*) "Pa number is"
write(*,10) Pa
C****set up the parameters for tridia*****
a1(1)=0 !1+alpha+beta
a2(1)=0
b1(1)=1
b2(1)=1 !+2*alpha
c1(1)=0
c2(1)=0 !-(alpha-beta)
a1(node)=-2*beta
a2(node)=-2*beta

```

```

b1(node)=1+2*beta
b2(node)=1+2*beta
c1(node)=0
c2(node)=0
DO i=1,node
  PC1(i)=0.0
  PC2(i)=0.0
Cm(i)=Cmo
END DO
control=0 ! control the output

```

```

C*****calculate the concentration in seconds*****
write(*,*) "numerical solution"
write(901,*) time, 0, Cmo

Do i=1, 16 !assume DI water can not extract any metal from the soil
write(901,*) i, 0, Cmo
END DO

DO i=1, nstep
time=(i-1)*dt
control=control+1
DO j=1, node
  PCm(j)=Cm(j)
END DO
  CALL Extrablemetal(node,time,PC1,Cmo,Cm)
CALL para(node,alpha,beta,PC1,PC2,a1,a2,b1,b2,c1,c2,d1,d2,Pcm,Cm,m)
Call Tridia (node,a1,b1,c1,d1,CC)
DO j=1,node
  x(j)=(j-1)*dx
  PC1(j)=CC(j)
END DO
Call Tridia (node,a2,b2,c2,d2,CC)
DO j=1,node
  x(j)=(j-1)*dx
  PC2(j)=CC(j)
END DO
IF (time. LT. 500) THEN
  IF (control. EQ.60) THEN
write(901,*) time/60*0.16/3.14+16,PC2(node)*m*64,Cm(node)
10          FORMAT(5F10.3)
control=0
ELSE
END IF

```



```

ELSE IF (control. EQ.1000) THEN
  write(901,*) time/60*0.16/3.14+16,PC2(node)*m*64,Cm(node)
  control=0
  ELSE
  END IF
END DO

STOP
END

```

```

C*****Create subroutine to calculate a,d,c and PC1,PC2*****
SUBROUTINE para(node,alpha,beta,PC1,PC2,a1,a2,
&   b1,b2,c1,c2,d1,d2,Pcm,Cm,m)
  IMPLICIT NONE
  INTEGER node,i,m
  DOUBLE PRECISION a1,a2,b1,b2,c1,c2,d1,d2,PC1,PC2,alpha,beta,
&   dx,PCm,Cm,dt,n
  DIMENSION a1(node),a2(node),b1(node),b2(node),c1(node),c2(node),
&   d1(node),d2(node),PC1(node),PC2(node), Pcm(node),Cm(node)
  n=1.0/m
  DO i=2,node-1
    a1(i)=- (alpha+beta)
    a2(i)=- (alpha+beta)
    b1(i)=1+2*alpha
    b2(i)=1+2*alpha
    c1(i)=- (alpha-beta)
    c2(i)=- (alpha-beta)
    d1(i)=PC1(i)+n*(Cm(i)-PCm(i))
    d2(i)=PC2(i)-n*(Cm(i)-PCm(i))
  END DO
  d1(1)=? !initial dendrimer concentration mmol/L
  d2(1)=0 ! PC2(1)-n*(Cm(1)-PCm(1))
  d1(node)=PC1(node)+n*(Cm(node)-PCm(node))
  d2(node)=PC2(node)-n*(Cm(node)-PCm(node))
  RETURN
END

```

```

C*****Create subroutine to solve the tridiagonal matrices*****
SUBROUTINE Tridia (node,a,b,c,d,CC)
  IMPLICIT NONE
  INTEGER node,n, i,L
  PARAMETER (n=4/0.01+1)
  DOUBLE PRECISION a, b, c, d, pT,bb,dd,ff,CC
  DIMENSION bb(n), dd(n),a(node), b(node), c(node), d(node), CC(node)
  DO i= 1, node
    bb(i)=b(i)

```

```

dd(i)=d(i)
END DO
DO i=2,node
ff=a(i)/bb(i-1)
bb(i)=bb(i)-c(i-1)*ff
dd(i)=dd(i)-dd(i-1)*ff
END DO
CC(n)=dd(n)/bb(n)
DO i=1,node-1
L=node-i
CC(L)=(dd(L)-c(L)*CC(L+1))/bb(L)
END DO
RETURN
END

```

```

C*****Create subroutine to get the potentially extractable metal*****8
SUBROUTINE Extrablemetal(node,time,PC1,Cmo,Cm)
IMPLICIT NONE
integer node, i
DOUBLE PRECISION time, PC1,Cmo, Cm, K
DIMENSION Cm(node), PC1(node)
.....! Find best K based on least square of difference
DO i=1,node
Cm(i)=Cmo*Dexp(-K*PC1(i)*time/Cmo)
END DO
RETURN
END

```

APPENDIX C IMPLICIT METHOD FOR GAMMA-DISTRIBUTION MODEL

```

C****Dendrimer-Metal complex in column using implicit method (gamma)*****
  IMPLICIT NONE
  INTEGER i,node,j,nstep,control,m
  Parameter (node=4.0/0.1+1)
  DOUBLE PRECISION Co,velocity,distance,x,time,dt,tfinal,Cmo,Cm,Pcm,
& C2a,dx,a1,a2,b1,b2,c1,c2,d1,d2,alpha,PC1,PC2,CC,xx,Dis,beta,Pa,
& Cmnew, dcdt,ratio,K
  DIMENSION PC1(node),PC2(node),CC(node),a1(node),a2(node),
& b1(node),b2(node),c1(node),c2(node), C2a(node), ratio(node),
& Pcm(node),d1(node),d2(node),XX(node),X(node),Cm(node)
  time=0.0
  Cmo=? !initial metal concentration in mmol/L
  Dis=? !D determined from tracer
  dt=10
  dx=0.1
  distance=4.0 !column length, cm
  tfinal=26*60*60!injection time, second
  velocity=? ! v determined from cm/s
  nstep=(tfinal-time)/dt+1
  alpha=dt*dis/dx**2
  beta=velocity*dt/(2*dx)
  Co=(velocity*dt)/dx
  Pa=(dx*velocity)/Dis
  write(*,*) "Co number is"
  write(*,10) Co
  write(*,*) "Pa number is"
  write(*,10) Pa
C****set up the parameters for tridia*****
  a1(1)=0 !1+alpha+beta
  a2(1)=0
  b1(1)=1
  b2(1)=1 !+2*alpha
  c1(1)=0
  c2(1)=0 !-(alpha-beta)
  a1(node)=-2*beta
  a2(node)=-2*beta
  b1(node)=1+2*beta
  b2(node)=1+2*beta

```

```

c1(node)=0
c2(node)=0
DO i=1,node
  PC1(i)=0.0
  PC2(i)=0.0
  C2a(i)=0
  Cm(i)=Cmo
END DO
control=0 ! to control the output

```

C*****calculate the concentration in seconds*****

```

write(*,*) "numerical solution"
write(908,*) time, 0, Cmo

```

```

Do i=1, 16 !assume DI water can not extract any metal from the soil
write(908,*) i, 0, Cmo
END DO

```

```

DO i=1, nstep
time=(i-1)*dt
control=control+1
DO j=1, node
  PCm(j)=Cm(j)
  ratio(j)=Cm(j)/Cmo
  CALL EULER(PC1,Cm,ratio(j),dt,Cmnew,dcdt,K)
  Cm(j)=Cmnew

```

```

! write(*,*) "lucida"
END DO

```

```

CALL para(node,alpha,beta,PC1,PC2,a1,a2,b1,b2,c1,c2,d1,d2,Pcm,Cm,m)

```

```

! write(*,*) "lucida"

```

```

Call Tridia (node,a1,b1,c1,d1,CC)

```

```

! write(*,*) "lucida"

```

```

DO j=1,node
  x(j)=(j-1)*dx
  PC1(j)=CC(j)
END DO

```

```

Call Tridia (node,a2,b2,c2,d2,CC)

```

```

! write(*,*) "lucida"

```

```

DO j=1,node
  x(j)=(j-1)*dx
  PC2(j)=CC(j)
  C2a(j)=C2a(j)+PC2(j) !get the average value in 10 minutes
END DO

```

```

IF (control. EQ.60) THEN
C2(node)=C2a(node)/control

```

```

10      write(908,*) time/60*0.16/3.14+16,C2(node)*m*64, Cm(node)
          FORMAT(5F10.3)
          control=0
          DO j=1, node
            C2a(j)=0.0
          END DO
          ELSE
            END IF
          END DO

          STOP
          END

```

```

C*****Create subroutine to calculate a,d,c and PC1,PC2*****
SUBROUTINE para(node,alpha,beta,PC1,PC2,a1,a2,
&      b1,b2,c1,c2,d1,d2,Pcm,Cm,m)
IMPLICIT NONE
INTEGER node,i,m
DOUBLE PRECISION a1,a2,b1,b2,c1,c2,d1,d2,PC1,PC2,alpha,beta,
&      dx,PCm,Cm,dt,n
DIMENSION a1(node),a2(node),b1(node),b2(node),c1(node),c2(node),
&      d1(node),d2(node),PC1(node),PC2(node), Pcm(node),Cm(node)
n=1.0/m
DO i=2,node-1
a1(i)=-(alpha+beta)
a2(i)=-(alpha+beta)
b1(i)=1+2*alpha
b2(i)=1+2*alpha
c1(i)=-(alpha-beta)
c2(i)=-(alpha-beta)
d1(i)=PC1(i)+n*(Cm(i)-PCm(i))
d2(i)=PC2(i)-n*(Cm(i)-PCm(i))
END DO
d1(1)=38 !initial dendrimer concentration mmol/L
d2(1)=0 ! PC2(1)-n*(Cm(1)-PCm(1))
d1(node)=PC1(node)+n*(Cm(node)-PCm(node))
d2(node)=PC2(node)-n*(Cm(node)-PCm(node))
RETURN
END

```

```

C*****Create subroutine to solve the tridiagonal matrices*****
SUBROUTINE Tridia (node,a,b,c,d,CC)
IMPLICIT NONE
INTEGER node,n, i,L
PARAMETER (n=4/0.1+1)
DOUBLE PRECISION a, b, c, d, pT,bb,dd,ff,CC

```

```

DIMENSION bb(n), dd(n),a(node), b(node), c(node), d(node), CC(node)
DO i= 1, node
bb(i)=b(i)
dd(i)=d(i)
END DO
DO i=2,node
ff=a(i)/bb(i-1)
bb(i)=bb(i)-c(i-1)*ff
dd(i)=dd(i)-dd(i-1)*ff
END DO
CC(n)=dd(n)/bb(n)
DO i=1,node-1
L=node-i
CC(L)=(dd(L)-c(L)*CC(L+1))/bb(L)
END DO
RETURN
END

```

```

!***** Create subroutine to calculate the new Metal concentration*****
SUBROUTINE EULER(Cd,Cm,ratio,dt,Cmnew,dcdt,K)
IMPLICIT NONE
DOUBLE PRECISION Cd,Cm,ratio,Cmnew,dt,dcdt,K
CALL Derivative(Cd,ratio,dcdt,K)
Cmnew=Cm+dcdt*dt
Cm=Cmnew
RETURN
END

```

```

!***** Create subroutine to calculate the Derivative of funciton dx dy***
SUBROUTINE Derivative(Cd,ratio,dcdt,K)
IMPLICIT NONE
DOUBLE PRECISION ratio,Cd,dcdt, K
CALL Gamma(ratio,K)
dcdt=-K*Cd*ratio
RETURN
END

```

```

C****using gamma function to calculate K value*****
SUBROUTINE Gamma(K)
IMPLICIT NONE
..... !function to find best alpha and beta
RETURN
END

```

APPENDIX D IMPLICIT METHOD FOR TWO-SITE MODEL

```
C****Dendrimer-Metal complex in column using implicit method*****
IMPLICIT NONE
INTEGER i,node,j,nstep,control,m
Parameter (node=4.0/0.1+1)
DOUBLE PRECISION Co,velocity,distance,x,time,dt,tfinal,Cmo,Cm,Pcm,
& C2a,dx,a1,a2,b1,b2,c1,c2,d1,d2,alpha,PC1,PC2,CC,xx,Dis,beta,Pa,
& Cmnew,dcdt,Cm1,Cm2,dc1dt,dc2dt,f,Cmi
DIMENSION PC1(node),PC2(node),CC(node),a1(node),a2(node),
& b1(node),b2(node),c1(node),c2(node),C2a(node),Cm1(node),
& Pcm(node),d1(node),d2(node),XX(node),X(node),Cm(node),Cm2(node)
time=0.0
!write(*,*) "input m"
!read(*,*) m
Cmo=? !initial metal concentration in mmol/L
Dis=? !dispersion D determined from tracer test
dt=10
dx=0.1
distance=4.0 !column length, cm
tfinal=26*60*60!injection time, second
velocity=? ! v determined from tracer, cm/s
nstep=(tfinal-time)/dt+1
alpha=dt*dis/dx**2
beta=velocity*dt/(2*dx)
Co=(velocity*dt)/dx
Pa=(dx*velocity)/Dis
!f=? find best f: fraction for site 1
write(*,*) "Co number is"
write(*,10) Co
write(*,*) "Pa number is"
write(*,10) Pa
C****set up the parameters for tridia*****
a1(1)=0 !1+alpha+beta
a2(1)=0
b1(1)=1
b2(1)=1 !+2*alpha
c1(1)=0
c2(1)=0 !-(alpha-beta)
```

```

a1(node)=-2*beta
a2(node)=-2*beta
b1(node)=1+2*beta
b2(node)=1+2*beta
c1(node)=0
c2(node)=0
DO i=1,node
  PC1(i)=0.0
  PC2(i)=0.0
  C2a(i)=0.0
  Cm1(i)=f*Cmo
  Cm2(i)=(1-f)*Cmo
  Cm(i)=Cmo
END DO
control=0 ! to control the output

C*****calculate the concentration in seconds*****
write(*,*) "numerical solution"
write(9099,*) time, 0, Cmo

Do i=1, 16 !assume DI water can not extract any metal from the soil
write(9099,*) i, 0, Cmo
END DO

DO i=1, nstep
time=(i-1)*dt
control=control+1
DO j=1, node
  PCm(j)=Cm(j)
  CALL Derivative(PC1,Cm1,Cm2,Cmo,f,dc1dt,dc2dt)
  Cm1(j)=Cm1(j)+dc1dt*dt
  Cm2(j)=Cm2(j)+dc2dt*dt
  Cm(j)=Cm1(j)+Cm2(j)
END DO
CALL para(node,alpha,beta,PC1,PC2,a1,a2,b1,b2,c1,c2,d1,d2,Pcm,Cm)
Call Tridia (node,a1,b1,c1,d1,CC)
DO j=1,node
  x(j)=(j-1)*dx
  PC1(j)=CC(j)
END DO
Call Tridia (node,a2,b2,c2,d2,CC)
DO j=1,node
  x(j)=(j-1)*dx
  PC2(j)=CC(j)
  C2a(j)=C2a(j)+PC2(j) !get the average value in 10 minutes
END DO

```



```

      IF (control. EQ.10) THEN
      C2(node)=C2a(node)/control
      write(9099,*) time/60*0.16/3.14+16,PC2(node)*64, Cm(node)
10      FORMAT(5F10.3)
      control=0
      DO j=1, node
      C2a(j)=0.0
      END DO
      ELSE
      END IF
      END DO

      STOP
      END

C*****Create subroutine to calculate a,d,c and PC1,PC2*****
SUBROUTINE para(node,alpha,beta,PC1,PC2,a1,a2,
&      b1,b2,c1,c2,d1,d2,Pcm,Cm)
IMPLICIT NONE
INTEGER node,i,m
DOUBLE PRECISION a1,a2,b1,b2,c1,c2,d1,d2,PC1,PC2,alpha,beta,
&      dx,PCm,Cm,dt,n
DIMENSION a1(node),a2(node),b1(node),b2(node),c1(node),c2(node),
&      d1(node),d2(node),PC1(node),PC2(node), Pcm(node),Cm(node)
DO i=2,node-1
a1(i)=-(alpha+beta)
a2(i)=-(alpha+beta)
b1(i)=1+2*alpha
  b2(i)=1+2*alpha
c1(i)=-(alpha-beta)
c2(i)=-(alpha-beta)
d1(i)=PC1(i)+(Cm(i)-PCm(i))
  d2(i)=PC2(i)-(Cm(i)-PCm(i))
END DO
d1(1)=38 !initial dendrimer concentration mmol/L
d2(1)=0 ! PC2(1)-n*(Cm(1)-PCm(1))
d1(node)=PC1(node)+(Cm(node)-PCm(node))
  d2(node)=PC2(node)-(Cm(node)-PCm(node))
RETURN
END

C*****Create subroutine to solve the tridiagonal matrices*****
SUBROUTINE Tridia (node,a,b,c,d,CC)
IMPLICIT NONE
INTEGER node,n, i,L
PARAMETER (n=4/0.1+1)

```

```

DOUBLE PRECISION a, b, c, d, pT,bb,dd,ff,CC
DIMENSION bb(n), dd(n),a(node), b(node), c(node), d(node), CC(node)
DO i= 1, node
bb(i)=b(i)
dd(i)=d(i)
END DO
DO i=2,node
ff=a(i)/bb(i-1)
bb(i)=bb(i)-c(i-1)*ff
dd(i)=dd(i)-dd(i-1)*ff
END DO
CC(n)=dd(n)/bb(n)
DO i=1,node-1
L=node-i
CC(L)=(dd(L)-c(L)*CC(L+1))/bb(L)
END DO
RETURN
END

```

```

!***** Create subroutine to calculate the Derivative of funciton dcdt***
SUBROUTINE Derivative(Cd,Cm1,Cm2,Cmi,f,dc1dt,dc2dt)
IMPLICIT NONE
DOUBLE PRECISION Cm1,Cm2,Cm, Cmi,Cd,dc1dt,dc2dt, K1,K2, f
.....!function to find Ks for two sites based on least square of difference
dc1dt=-K1*Cd*Cm1/(f*Cmi)
dc2dt=-K2*Cd*Cm2/((1-f)*Cmi)
RETURN
END

```

**APPENDIX E RUNGE-KUTTA METHOD FOR BATCH METAL RELEASE
WITH TWO-SITE MODEL**

```

C**** Runge-Kutta Solution of Batch Metal Release for Two-Site Model****
  IMPLICIT NONE
  INTEGER i,n, control ! n is the steps
  DOUBLE PRECISION Cm,Cmi1,Cmi2,ti,Cd,Cdi,t,tf,Cm1new,Cm2new,
& dt,dc1dt,dc2dt,Cmnew,f,Cm1,Cm2,Cmi,K1rate,k2rate,time
  ti=0
  Cmi=? !mg/g, metal concentration in soil
  Cdi=? !initial demdrimer concentration
  dt=1
  !f=?.....!! find best f
  tf=22520
  n=(tf-ti)/dt+1
  t=ti
!initial conditions
  Cm1=Cmi*f
  Cm2=Cmi*(1-f)
  Cm1=Cmi1
  Cm2=Cmi2
  Cd=Cdi
  K1rate=4.9D-4
  K2rate=4.5D-6
  control = 0
  write (30,*) " 0 1 "

  DO i=1, n
    t=t+dt
    control=control+1
    Call Rk4(Cd,dt,t,Cmi1,Cmi2,Cm1,Cm2,K1rate,K2rate,Cm1new,Cm2new)
    Cm1=Cm1new
    Cm2=Cm2new
    Cm=Cm1+Cm2
    Cd=Cdi-(Cmi-Cm)*60*1000/64
    IF (control. EQ. 100) THEN
      write(30,*) t,Cm/Cmi
      control=0

```

```

        ELSE
        END IF
    END DO
10    FORMAT (7F10.5)
    STOP
    END

C      To calculate the K average
      SUBROUTINE Rk4(Cd,dt,t,Cmi1,Cmi2,y1,y2,Ka,Kb,y1new,y2new)
      IMPLICIT NONE
      DOUBLE PRECISION dt,t,Cd,y1new,y2new,dydt,K11,K21,y1,y2,dy1dt,
& dy2dt,K31,K41,k12,k22,k32,k42,
& y1estimate,y2estimate,Ka,Kb,Cmi1,Cmi2

          ! the maximum number of the equations is 10
C*****R-K step1-find slope at the start point(y,t)*****
      CALL Eqns(Cd,y1,y2,Cmi1,Cmi2,t,Ka,Kb,dy1dt,dy2dt)
      K11=dy1dt
      K12=dy2dt
C*****R-K step 2a-evaluate the estimates of y at the intermediate half-step point(dt/2),
      using the slope of K1
      y1estimate=y1+K11*dt/2
      y2estimate=y2+k12*dt/2
C      R-K step2b-find the slope at the intermediate point
      CALL Eqns(Cd,y1estimate,y2estimate,Cmi1,Cmi2,(t+dt/2),
&Ka,Kb,dy1dt,dy2dt)
      K21=dy1dt
      k22=dy2dt
C*****R-K step3a-refine the estimates of y at the half intermediate half-step point (dt/2),
      using K2
      y1estimate=y1+K21*dt/2
      y2estimate=y2+K22*dt/2
C      R-K step3b-find the newly refined slope at the intermediate point
      CALL Eqns(Cd,y1estimate,y2estimate,Cmi1,Cmi2,(t+dt/2),
&Ka,Kb,dy1dt,dy2dt)
      K31=dy1dt
      k32=dy2dt
C*****R-K step4a-evaluate the estimates of y at the end full-step point (dt) using the
      slope k3
      y1estimate=y1+k31*dt
      y2estimate=y2+k32*dt
C      R-K step4b-find the slope K4 at the end point using the estimated y
      CALL Eqns(Cd,y1estimate,y2estimate,Cmi1,Cmi2,(t+dt),
&Ka,Kb,dy1dt,dy2dt)

```

```

      K41=dy1dt
      K42=dy2dt
C*****Final R-K computation*****
      y1new=y1+(K11+2*K21+2*K31+k41)*dt/6.0
      y2new=y2+(K12+2*K22+2*K32+k42)*dt/6.0

      RETURN
      END
      ..... !find best Ka and Kb

C*****calculate all the K
      SUBROUTINE Eqns(Cd,Cm1,Cm2,Cmi1,Cmi2,t,Ka,Kb,dy1dt,dy2dt)
      IMPLICIT NONE
      INTEGER n
      DOUBLE PRECISION y,t,dy1dt,dy2dt,Ka,Kb,Cd,Cmi1,Cmi2,Cm1,Cm2
!      DIMENSION y(n), dydt(n)
      dy1dt=-Ka*Cd*Cm1/Cmi1/60/1000*64
      dy2dt=-Kb*Cd*Cm2/Cmi2/60/1000*64
      RETURN
      END

```